องค์ประกอบทางเคมีและฤทธิ์ทางชีวภาพของเมล็ดตะบูนดำ *Xylocarpus moluccensis* Roem. จากจังหวัดภูเก็ต

นางสาววารินทร์ ระวังภัย

วิทยานิพนธ์นี้เป็นส่วนหนึ่งของการศึกษาตามหลักสูตรปริญญาวิทยาศาสตรมหาบัณฑิต
สาขา วิชาเคมี ภาควิชาเคมี
คณะวิทยาศาสตร์ จุฬาลงกรณ์มหาวิทยาลัย
ปีการศึกษา 2553

CHEMICAL CONSTITUENTS AND BIOLOGICAL ACTIVITY OF *Xylocarpus moluccensis* Roem. SEEDS FROM PHUKET PROVINCE

Miss Warin Ravangpai

A Thesis Submitted in Partial Fulfillment of the Requirements
for the Degree of Master of Science Program in Chemistry
Department of Chemistry
Faculty of Science
Chulalongkorn University
Academic Year 2010

Thesis Title	CHEMICAL CONSTITUENTS AND BIOLOGICAL ACTIVITY OF *Xylocarpus moluccensis* Roem. SEEDS FROM PHUKET PROVINCE
By	Miss Warin Ravangpai
Field of Study	Chemistry
Thesis Advisor	Associate Professor Somchai Pengprecha, Ph.D.
Thesis Co-advisor	Assistant Professor Khanitha Pudhom, Ph.D.

Accepted by the Faculty of Science, Chulalongkorn University in Partial Fulfillment of the Requirements for the Master's Degree

S. Hannongbua ..... Dean of the Faculty of Science

(Professor Supot Hannongbua, Dr.rer.nat.)

THESIS COMMITTEE

Warinthorn Chavasiri ..... Chairman

(Assistant Professor Warinthorn Chavasiri, Ph.D.)

Somchai Pengprecha ..... Thesis Advisor

(Associate Professor Somchai Pengprecha, Ph.D.)

Khanitha Pudhom ..... Thesis Co-advisor

(Assistant Professor Khanitha Pudhom, Ph.D.)

P. Phuwapraisirisan ..... Examiner

(Assistant Professor Preecha Phuwapraisirisan, Ph.D.)

N. Muangsin ..... Examiner

(Associate Professor Nongnuj Muangsin, Ph.D.)

Damrong Sommit ..... External Examiner

(Damrong Sommit, Ph.D.)

วารินทร์ ระวังภัย : องค์ประกอบทางเคมีและฤทธิ์ทางชีวภาพของเมล็ดตะบูนดำ *Xylocarpus moluccensis* Roem. จากจังหวัดภูเก็ต. (CHEMICAL CONSTITUENTS AND BIOLOGICAL ACTIVITY OF *Xylocarpus moluccensis* Roem. SEEDS FROM PHUKET PROVINCE) อ. ที่ปรึกษาวิทยานิพนธ์หลัก : รศ.ดร. สมใจ เพ็งปรีชา, อ. ที่ปรึกษาวิทยานิพนธ์ร่วม: ผศ.ดร. ขนิษฐา พุดหอม, 132 หน้า.

จากการนำส่วนสกัดเอธิลอะซิเตทของเมล็ดตะบูนดำ (*Xylocarpus moluccensis* Roem) จากจังหวัดภูเก็ตมาทำการแยกให้บริสุทธิ์ด้วยเทคนิคทางโครมาโทรกราฟี สามารถแยกสารลิโมนอยด์ ได้ 11 ชนิด เป็นสารใหม่ 3 ชนิด ซึ่งเป็นลิโมนอยด์ประเภท andirobin 1 ชนิดคือ xylomoluccensin A (**9**) และลิโมนอยด์ประเภท phragmalin อีก 2 ชนิดคือ xylomoluccensin B-C (**10-11**) และเป็นสารที่มีรายงานมาก่อนอีก 8 ชนิด ได้แก่ mexicanolide (**1**), 3β-deacetylfissinolide (**2**), 2-hydroxyfissinolide (**3**), 7-deacetylgedunin (**4**), 7-oxo-7-deacetoxygedunin (**5**), moluccensin H (**6**), moluccensin I (**7**) และ xyloccensin E (**8**) การพิสูจน์ทราบโครงสร้างทางเคมีของสารที่แยกได้ทำโดยอาศัยวิธีทางสเปกโทรสโกปี ร่วมกับเทคนิค single-crystal x-ray diffraction สำหรับสาร 7-deacetylgedunin (**4**) และ xylomoluccensin A (**9**) เมื่อนำสารบริสุทธิ์ที่แยกได้มาทดสอบฤทธิ์ต้านการอักเสบ พบว่าสารลิโมนอยด์ประเภท gedunin 2 ชนิดคือ 7-deacetylgedunin (**4**) และ 7-oxo-7-deacetoxygedunin (**5**) แสดงฤทธิ์ต้านการอักเสบได้ดีที่สุด อีกทั้งยังมีความเป็นพิษค่อนข้างต่ำ

ภาควิชา.....เคมี.....ลายมือชื่อนิสิต.....วารินทร์ ระวังภัย.....
สาขาวิชา.....เคมี.....ลายมือชื่อ อ.ที่ปรึกษาวิทยานิพนธ์หลัก.....
ปีการศึกษา.....2553.....ลายมือชื่อ อ.ที่ปรึกษาวิทยานิพนธ์ร่วม.....

5272530723 : MAJOR CHEMISTRY

KEYWORDS : limonoides / *Xylocarpus moluccensis* / anti-inflammatory

WARIN RAVANGPAI : CHEMICAL CONSTITUENTS AND BIOLOGICAL ACTIVITY OF *Xylocarpus moluccensis* Roem. SEEDS FROM PHUKET PROVINCE. ADVISOR : ASSOC. PROF. SOMCHAI PENGPRECHA, Ph.D., CO-ADVISOR : ASST. PROF. KHANITHA PUDHOM, Ph.D., 132 pp.

A new andirobin, xylomoluccensin A (**9**), and two new phragmalin-type limonoids, xylomoluccensins B (**10**) and C (**11**), were isolated from EtOAc extract of seeds of a Thai mangrove plant, *Xylocarpus moluccensis* Roem. collected form Phuket province, together with eight known limonoids, including mexicanolide (**1**), 3β-deacetylfissinolide (**2**), 2-hydroxyfissinolide (**3**), 7-deacetylgedunin (**4**), 7-oxo-7-deacetoxygedunin (**5**), moluccensin H (**6**), moluccensin I (**7**) and xyloccensin E (**8**). The structures of isolated compounds were established by analysis of spectroscopic data and by comparison with data in the literature for known compounds. In the case of 7-deacetylgedunin (**4**) and xylomoluccensin A (**9**), their structures and relative configuration were also confirmed by means of single-crystal X-ray diffraction analysis. Only gedunin-type limonoids, 7-oxo-7-deacetoxygedunin (**6**) and 7-deacetylgedunin (**7**), exhibited significant inhibitory activity against nitric oxide production from activated macrophages at a concentration of 10 μg/mL, suggesting that the compounds have anti-inflammatory activity. More importantly, they displayed less toxicity.

Department : Chemistry	Student's Signature Warin Ravangpai
Field of Study : Chemistry	Advisor's Signature Somch. Pengpreed
Academic Year : 2010	Co-advisor's Signature Khanitha Pudhom

ACKNOWLEDGEMENTS

I wish to express my deep gratitude to my advisor, Associate Professor Dr. Somchai Pengprecha, and co-advisor, Assistant Professor Dr. Khanitha Pudhom, for their generous assistance, benevolent guidance and encouragement throughout the course of this research.

Many thanks to the thesis committees, Assistant Professor Dr. Warinthorn Chavasiri, Assistant Professor Dr. Preecha Phuwapraisirsan, Associate Professor Dr. Nongnuj Muangsin, Department of chemistry, Faculty of science, Chulalongkorn University and Dr. Damrong sommit, Mahanakorn University of Technology, For their invaluable discussion and suggestion.

I am grateful to Associate Professor Dr. Nongnuj Muangsin and Mr. Thapong Teerawatananond, Department of Chemistry, Faculty of Science, Chulalongkorn University who kindly preformed the X-ray Crystallographic analysis. I wish to thank Assistant Professor Dr. Tanapat Palaga for anti-inflammatory activity.

I would like to acknowledge the grant and funding supports provided by Center for Petroleum, Petrochemicals, and Advanced Materials. I wish to thank The 100th Chemistry of Chulalongkorn University for supporting scholarship.

I wish to thank all member of laboratory room 1528/1 and 1532 for their help and kind friendship, especially Mr. Thanesuan Nuanyai, for his valuable suggestions.

Finally, I am deeply grateful to my family for their love and encouragement throughout my M.Sc. Study.

CONTENTS

Page

Page

LIST OF TABLES

LIST OF FIGURES

Page

Page

Page

Page

LIST OF SCHEMES

LIST OF ABBREVIATIONS

J	Coupling constant
δ	Chemical shift
δ_H	Chemical shift of proton
δ_C	Chemical shift of carbon
s	Singlet (for NMR spectra)
d	Doublet (for NMR spectra)
dd	Doublet of doublet (for NMR spectra)
t	Triplet (for NMR spectra)
m	Multiplet (for NMR spectra)
q	Quartet (for NMR spectra)
brs	Broad singlet (for NMR spectra)
qC	Quaternary carbon
calcd.	Calculated
^{1}H NMR	Proton nuclear magnetic resonance
^{13}C NMR	Carbon-13 nuclear magnetic resonance
2D NMR	Two dimensional nuclear magnetic resonance
^{1}H-^{1}H COSY	Homonuclear (proton-proton) correlation spectroscopy
NOESY	Nuclear overhauser effect spectroscopy
HSQC	Heteronuclear single quantum coherence
HMBC	Heteronuclear multiple bond correlation
ORTEP	Oak ridge thermal ellipsoid plot
HRESIMS	Hight resolution electrospray ionization mass spectrometry
CC	Column chromatography
IC_{50}	Half maximal inhibitory concentration

$CDCl_3$	Deuterated chloroform
MeOH	Methanol
EtOH	Ethanol
CH_2Cl_2	Dichloromethane
EtOAc	Ethyl acetate
KBr	Potassium bromide
SiO_2	Silicon dioxide
g	Gram (s)
mg	Milligram (s)
mL	Milliliter (s)
μg	Microgram (s)
μL	Microliter (s)
L	Liter (s)
h	Hour
nm	Nanometer
Hz	Hertz
MHz	Megahertz
cm^{-1}	Reciprocal centimeter (unit of wave number)
ppm	part per million
NMR	Nuclear magnetic resonance
MS	Mass spectrometry
IR	Infared
UV	Ultraviolet
m.p.	Melting point
α	Alpha
β	Beta

Δ	Delta
m/z	Mass to charge ratio
$[M+H]^+$	Protonated molecule
$[M+Na]^+$	Pseudomolecular ion
$[\alpha]_D^{20}$	Specific rotation at 20 ˚C and sodium D line (589 nm)
λ_{max}	Wavelength of maximum absorption
c	Concentration
ε	Molar extinction coefficient
Å	Angstrom
˚C	Degree celcius
deg.	Degree
sp.	Species

CHAPTER I

INTRODUCTION

1.1 Drug discovery from natural sources

For thousands of years, natural products have played an important role throughout the world in treating and preventing human diseases. Natural product medicines have come from various source materials including terrestrial plants, terrestrial microorganisms, marine organisms, and terrestrial vertebrates and invertebrates [1]. The importance of natural products in modern medicine has been discussed in recent reviews and reports. The value of natural products in this regard can be assessed using 3 criteria: (1) the rate of introduction of new chemical entities of wide structural diversity, including serving as templates for semi-synthetic and total synthetic modification, (2) the number of diseases treated or prevented by these substances, and (3) their frequency of use in the treatment of disease [2].

An analysis of the origin of the drugs developed between 1981 and 2002 showed that natural products or natural product derived drugs comprised 28% of all new chemical entities (NCEs) launched onto the market [2]. In addition, 24% of these NCEs were synthetic or natural mimic compounds, based on the study of pharmacophores related to natural products [1]. This combined percentage (52% of all NCEs) suggests that natural products are important sources for new drugs and are also good lead compounds suitable for further modification during drug development. The large proportion of natural products in drug discovery has stemmed from the diverse structures and the intricate carbon skeletons of natural products. Since secondary metabolites from natural sources have been elaborated within living systems, they are often perceived as showing more “drug-likeness and biological friendliness than totally synthetic molecules” [3], making them good candidates for further drug development [4, 5].

Scrutiny of medical indications by source of compounds has demonstrated that natural products and related drugs are used to treat 87% of all categorized human diseases (48/55), including as antibacterial, anticancer, anticoagulant, antiparasitic, and immunosuppressant agents, among others. There was

no introduction of any natural products or related drugs for 7 drug categories (anesthetic, antianginal, antihistamine, anxiolytic, chelator and antidote, diuretic, and hypnotic) during 1981 to 2002. In the case of antibacterial agents, natural products have made significant contributions as either direct treatments or templates for synthetic modification. Of the 90 drugs of that type that became commercially available in the United States or were approved worldwide from 1982 to 2002, ~79% can be traced to a natural product origin [2].

Frequency of use of natural products in the treatment and/or prevention of disease can be measured by the number and/or economic value of prescriptions, from which the extent of preference and/or effectiveness of drugs can be estimated indirectly. According to a study by Grifo and colleagues, [6] 84 of a representative 150 prescription drugs in the United States fell into the category of natural products and related drugs. They were prescribed predominantly as anti-allergy/pulmonary/respiratory agents, analgesics, cardiovascular drugs, and for infectious diseases. Another study found that natural products or related substances accounted for 40%, 24%, and 26%, respectively, of the top 35 worldwide ethical drug sales from 2000, 2001, and 2002 [7]. Of these natural product-based drugs, paclitaxel (ranked at 25 in 2000), a plant-derived anticancer drug, had sales of $1.6 billion in 2000. The sales of 2 categories of plant-derived cancer chemotherapeutic agents were responsible for approximately one third of the total anticancer drug sales worldwide, or just under $3 billion dollars in 2002; namely, the taxanes, paclitaxel and docetaxel, and the camptothecin derivatives, irinotecan and topotecan [8, 9].

1.1.1 Drug discovery from terrestrial plants

Terrestrial plants, especially higher plants, have a long history of use in the treatment of human diseases. Several well-known species, including licorice (*Glycyrrhiza glabra*), myrrh (*Commiphora* species), and poppy capsule latex (*Papaver somniferum*), were referred to by the first known written record on clay tablets from Mesopotamia in 2600 BC, and these plants are still in use today for the treatment of various diseases as ingredients of official drugs or herbal preparations used in systems of traditional medicine [1]. Furthermore, morphine, codeine, noscapine (narcotine), and papaverine isolated from *P. somniferum* were developed as

single chemical drugs and are still clinically used. Hemisuccinate carbenoxolone sodium, a semi-synthetic derivative of glycyrrhetic acid found in licorice, is prescribed for the treatment of gastric and duodenal ulcers in various countries [10].

Historical experiences with plants as therapeutic tools have helped to introduce single chemical entities in modern medicine. Plants, especially those with ethnopharmacological uses, have been the primary sources of medicines for early drug discovery. In fact, a recent analysis by Fabricant and Farnsworth showed that the uses of 80% of 122 plant derived drugs were related to their original ethnopharmacological purposes [11]. Current drug discovery from terrestrial plants has mainly relied on bioactivity-guided isolation methods, which, for example, have led to discoveries of the important anticancer agents, paclitaxel from *Taxus brevifolia* and camptothecin from *Camptotheca acuminate* [12].

1.1.2 Examples of plant-derived compounds currently in clinical trials

From terrestrial plant-derived secondary metabolites, several new chemical entities (Figure 1.1) are undergoing clinical trials including four that are derivatives of known anticancer drugs (camptothecin, paclitaxel, epipodophyllotoxin and vinblastine) [13]. In addition, combretastatin A4, isolated from the South African medicinal tree, *Combretum caffrum* (Combretaceae), was derivatized to combretastatin A4 phosphate and AVE-8062 [14, 15]. These analogs bind to tubulin leading to morphological changes and then disrupt tumor vasculature, and are in phase II trials [16, 17]. Homoharringtonine, a cephalotaxus alkaloid from the tree, *Cephalotaxus harringtonia* found in mainland China [18], is an inhibitor of protein synthesis and is reported to have activity against hematologic malignancies [19]. Ingenol 3-*O*-angelate, an analog of the polyhydroxy diterpenoid, ingenol, which was originally obtained from *Euphorbiapeplus* (known as “petty spurge” in England or “radium weed” in Australia), is a potential topical chemotherapeutic agent for skin cancer and exhibits its action through activation of protein kinase C [20, 21]. Phenoxodiol, a synthetic analog of daidzein, a well known isoflavone from soybean (*Glycine max*), is being developed as a therapy for cervical, ovarian, prostate, renal, and vaginal cancers, and induces apoptosis through inhibition of anti-apoptotic

proteins including XIAP and FLIP [22]. Phenoxodiol is currently undergoing clinical studies in the United States and Australia [23]. Protopanaxadiol, a derivative of a triterpene aglycone of several saponins from ginseng (*Panax ginseng*), exhibits its apoptotic effects on cancer cells through various signaling pathways, and is also reported to be cytotoxic against multidrug resistant tumors [24, 25]. Triptolide, a diterpene triepoxide, was isolated from *Tripterygium wilfordii* , and has been used for autoimmune and inflammatory diseases in the People 's Republic of China [26]. PG490 – 88 (PG490 – 88, 14-succinyl triptolide sodium salt), a semi-synthetic analog of triptolide, exerts antiproliferative and proapoptotic activities on primary human prostatic epithelial cells as well as tumor regression of colon and lung xenografts [27].

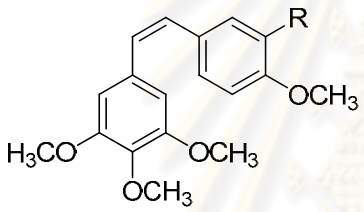

R= OPO_3Na_2 Combretastatin A4 phosphate

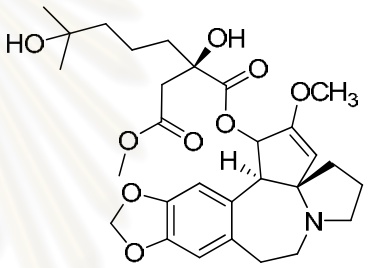

Homoharringtonine

R= AVE-8062

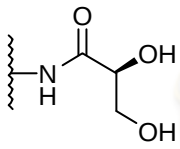

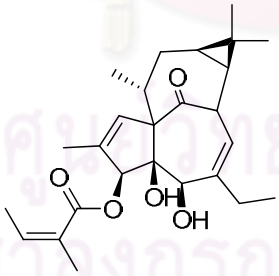

Ingenol 3-*O*-angelate

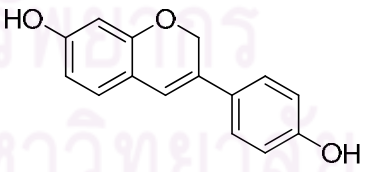

Phenoxodiol

Figure 1.1 Plant-derived drug candidates

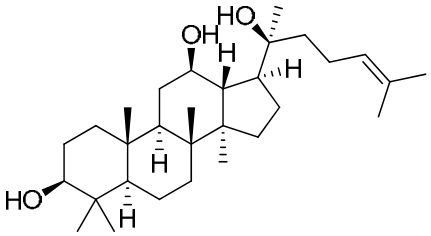

Protopanaxadiol

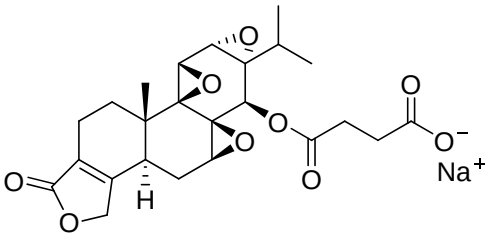

PG490 – 88

Figure 1.1 Plant-derived drug candidates (continued)

1.2 Mangrove plants, a potential source of bioactive metabolites

Mangroves are salt tolerant forest ecosystems found mainly in the tropical and subtropical intertidal regions of the world largely confined to the region between 30° north and south of the equator [28]. Approximately, 25% of the world's coastline is dominated by mangroves distributed in 112 countries and territories encompassing an area of 181,000 sq km worldwide [29]. These mangroves are among the most productive habitats which proliferate luxuriantly in the coastal areas and river estuaries and back water areas as a muddy substratum of varying depth and consistency is necessary for their growth. They occupy low laying areas where regular tidal inundation takes place. In total, there are 84 mangrove plant species in the world, out of which 70 species are true mangroves and 14 species are semi-mangroves [30]. Mangrove plants are usually categorized into two groups, true mangrove and semi-mangrove plants. The true mangrove plants are restricted to the typical intertidal mangrove habitats whereas semi-mangrove plants grow on the landward fringe mangrove habitat or in terrestrial marginal zones subjected to irregular high tides. On the other hand, there is a third group called mangrove associated plants which are salt tolerant terrestrial plants occasionally found in landward edge of mangrove habitat and are irregularly flushed by high tides [30].

Several mangrove species are used in traditional medicine or have found application as insecticides and pesticides and have recently attracted attention for pharmaceutical and other industries. These plants represent a great resource for detection of unique secondary metabolites which can supply information about the wide range of phytochemicals in nature and give knowledge about biological

activities of plant compounds as antimicrobial, anticancer, antioxidant and other agents [28, 31-33]. This information might also lead to development of new medicinally useful constituents as therapeutics against certain diseases. However, the scientific information about the biological effects of mangrove plants and active substances is scarce and poorly documented. The present review contributes to increase the knowledge about chemical composition and biological activities of medicinal mangrove plants and their uses in pharmaceutical industry and traditional health care system as well.

1.2.1 Traditional uses of mangroves

Traditionally, the mangroves have been exploited for construction of dwellings, furniture, rafts, boats, fences, fishing gear, paddles, and production of tannins for dying and leather production [28]. The mangrove wood with high content of tannin is used as timber for its durability. Stems of *Avicennia marina*, *Bruguiera cylindrica*, *Bruguiera parviflora*, *Xylocarpus granatum*, and *Sonneratia apetala* are used for construction of houses. The pneumatophores are used to make bottle stoppers and floats. Grasses and palm leaves are used to make door mats, and mats for sails, to thatch walls and roofs [34, 35]. *Rhizophora mangle* has uses in textile industry [28]. Due to high calorific values, mangrove twigs are used for making charcoal and firewood. One ton of mangrove firewood is equivalent to 5 tons of Indian coal, and it burns producing high heat without generating smoke. Some of the mangrove plant parts are used for food purposes. Fruits of *Bruguiera gymnorhiza*, *Phoenix paludosa*, *Sonneratia alba*, *Sonneratia caseolaris*, and *Terminalia catappa* are used as vegetables [28, 35]. The mangrove leaves are useful contributors to the nutrient system of the mangrove environment. It is known that mangrove leaves contain sufficient amounts of minerals, vitamins and amino acids, which are essential for the growth and nourishment of marine organisms and livestock [28, 31]. The indirect use in the form of important ecological functions such as control of coastal erosion, protection of coastal land, stabilization of sediments etc. and the economic importance of mangrove plants and mangrove forests for prawn fisheries, crabs, shrimp, oysters, lobsters and fish cultivation etc.

Apart from the above uses, mangrove plants are known to possess medicinal values and have been used traditionally for ailment of various diseases by local inhabitants (Table 1.1). The rural people fully or partially depend upon the plants surrounded by them for curing various diseases. Some of these examples include treatment of headache and various type of inflammation including jelly fish sting dermatitis by extracts of *Ipomoea pescaprae*, Cigarettes prepared from the chopped stem bark of I. *pescaprae* are smoked to relieve the pain of sinusitis and in Indo-china, the leaves and young shoots are crushed, mixed with alcohol, and applied in the back in cases of lumbago and are also used to relieve rheumatic pains and in baths to treat scabies [28]. The fruit of *Xylocarpus moluccensis* is used in folk medicine in East Africa. The fruits are used as aphrodisiacs and the young fruits tasted bitter [30]. In recent, much is studied about the terrestrial medicinal plants but a little report is available regarding mangroves and mangrove associated plants.

Table 1.1 Some of the mangrove plants, their ethnomedicinal uses and biological activities

Botanical name	**Plant parts and their ethnomedicinal uses**	**Bioactivity test**	**Reference**
Acanthus ilicifolius	Leaves, bark, total plant-Blood purifier, diuretic, diabetes, leprosy, paralysis, skin disease, snake bite, hepatitis, stomach pain, rheumatism	Anti-inflammatory, antiviral, analgesic, anticancer	[28, 31, 35-40]
Acrostichum aureum	Leaves-boils, wound	Biotoxicity on fingerlings of fish	[28,36]
Aegiceras corniculatum	Leaves-boil-earache; flowershoney, seeds and barks-cure for asthma, diabetes, rheumatism	Antiviral, toxicity to fish	[28, 36, 41]

Table 1.1 Some of the mangrove plants, their ethnomedicinal uses and biological activities (continued)

Botanical name	Plant parts and their ethnomedicinal uses	Bioactivity test	Reference
Amoora cuculata	Bark, seeds-dysentry	Cytotoxicity, antibacterial activity	[28, 42]
Avicennia officinalis	Seed, root, bark-cure for boils, small pox, leprosy, diuretic	Antiviral, Biotoxicity on fingerlings of fish, diuretic, leprosy	[28, 35-36, 41, 43-44]
Avicennia marina	Leaves-cure for Ulcers	Antimicrobial activity, antitumor	[36, 40, 45-48]
Bruguiera gymnorrhiza	Bark-astringent; malaria; fruit-astringent, treatment of eye disease, Fish posion	Growth hormone tests on plants	[36, 44, 49]
Bruguiera parviflora	Bark-constipation, antitumor agent	Antitumor	[36]
Bruguiera sexangula	Bark-anticancer; root and leavesin burns	-	[36, 43, 48]
Cerbera manghas	Bark-purgative; fruit-narcotic, poisonous; seeds-illuminant, treatment for rheumatism		[28]
Ceriops decandra	Root, Bark-cure for ulcers, hepatitis, stop hemorrhage	Antiviral, antiulcer, antibacterial	[28, 41, 50]
Cynometra iripa	Seed-oil-skin disease	-	[28]

Table 1.1 Some of the mangrove plants, their ethnomedicinal uses and biological activities (continued)

Botanical name	Plant parts and their ethnomedicinal uses	Bioactivity test	Reference
Derris trifoliate	Total plant, bark-stimulant, antiseptic, fish poisoning, rheumatism, laxative, pesticide, spasmodic and counter irritant	Toxicity to fish	[28]
Excoecaria agallocha	Leaves-epilepsy, ulcers; roothand and feet swelling, leprosy, toothache, uterotonic, purgative, conjunctivitis , dermatitis, fish poison	Antiviral, antioxidant, antimicrobial, antifilarial, anti-HIV	[51-54]
Heritiera fomes	Bark-healing wound and cuts; seeds-edible	-	[28, 31, 35, 49]
Heritiera littoralis	Seeds-diarrhea, dysentery, fish toxicant	Antifungal, antifeedant	[36]
Hibiscus tiliaceus	Leaves-for treating fever, to soothe coughs, dysentery and ear infections	-	[55]
Kandelia candel	Bark-diabetes	-	[45]
Lumnitzera racemosa	Stem-itches and herpes, asthma, diabetes, snake bite	Antiviral	[36, 41, 44-45, 48]

Table 1.1 Some of the mangrove plants, their ethnomedicinal uses and biological activities (continued)

Botanical name	Plant parts and their ethnomedicinal uses	Bioactivity test	Reference
Phoenix paludosa	Leaves, root-stomach disorder, cardiac trouble, rheumatism	-	[31, 35]
Rhizophora apiculata	Bark-diarrhea, nausea, vomiting, typhoid, hepatitis, antiseptic, insecticide	Antiviral, larvicidal, antifungal, antifeedant, antimicrobial, anti-HIV, antioxidant	[44, 52]
Rhizophora mucronata	Bark-diabetes, hemorrhage, hepatitis, ulcer	Antiviral, anti-HIV, growth hormone tests on plants	[56]
Salicornia brachiata	Treat hepatitis	Antiviral activity	[28]
Sonneratia alba	Hemorrhages, piles	Toxicity against mosquito larvae	[45]
Thespesia populnea	All parts-skin diseases, dysentery, mirgraine, urethritis, gonorohoea, heart disease	Antibacterial, antifertility, cytotoxic	[57]
Xylocarpus granatum	Bark-astringent, dysentery, diarrhea, febrifuge, malaria, cholera	Antifungal, insect antifeedant, antibacterial	[36]
Xylocarpus mekongensis	Bark-astringent, dysentery, fever, malaria	Antifeedant	[36]

1.2.2 Bioactivity of mangrove plants

The development of pharmaceuticals begins with the identification of active principles, detailed biological assays and dosage formulations, followed by clinical studies to establish safety, efficacy and pharmacokinetic profile of the new drug. The same follows for mangrove plant therapeutic agents. The mangrove plants possess a number of biological activities such as antibacterial, antioxidant, anticancer, cytotoxic, antiproliferative, insecticidal, antimalarial, antifungal, antifeedant, antidiarrheal, central nervous system depressant, antimitotic, antileukemic and anti-plasmodial activities (Table 1.1). Informations of the biological activities of the mangrove plants have been provided by a number of review and research articles [28, 30, 32, 35, 38, 41, 44].

1.2.3 Metabolites and novel chemicals from mangroves

Traditionally used medicinal mangrove plants have recently attracted the attention of the pharmaceutical and scientific communities. This has involved the isolation and identification of secondary metabolites produced by plants and their use as active principles in medicinal preparations [58]. Many of the mangrove plant secondary metabolites are constitutive, existing in healthy plants in their biologically active forms, but others occur as inactive precursors and are activated in response to tissue damage or pathogen attack [59]. Metabolites, with some novel chemical structures and which belong to a diversity of chemical classes have been characterized from mangroves and mangal associates. According to a review, about 349 metabolites have been isolated from mangrove species out of which 200 metabolites are reported exclusively from true mangrove plants [30]. Aliphatic alcohols and acids, alkaloids, carotenoids, amino acids, hydrocarbons, lipids, pheromones, phorbol esters, phenolics and related compounds, steroids, triterpenes, tannins, other terpenes and related compounds are some of the important chemical classes. Chemicals such as amino acids, carbohydrates and proteins are the products of primary metabolism and are vital for the maintenance of life processes, while others likephenolics, steroids, alkaloids, terpenoids are the products of secondary metabolism and have toxicological, pharmacological and ecological importance [31].

In 1913, for the first time Bournot characterized lapachol from the wood of the Indian and West African *Avicennia lomentosa*. Then in 1959, Rao and Bose isolated a triterpene named genin-A from the bark of the Indian *Aegiceras corniculatum*. In 1965, Taylor obtained a limonoid named gedunin from the timber of African *X. granatum*. Recently, the antifungal property of gedunin was found by Sundarasiva Rao and his coworkers. Similarly, the anti-allergic activity of gedunin has also been reported [30].

From 1970 to 2000, Australian, Indian and Japanese scientists investigated novel compounds from some mangrove plants like *Acanthus ilicifolius, Bruguiera gymnorrhiza, Heritiera littoralis* and *Excoecaria agallocha* [30, 60-61], the details of which are discussed subsequently. All parts of the plant *Pongamia pinnata*, a mangrove associate, are used as a crude drug for the treatment of tumors, piles, skin diseases, wounds and ulcers. It is a rich source of flavonoids and related compounds [28, 44]. *Sesuvium portulacastrum*, a salt marsh halophyte, is a rich source of amino acids. The fruit of *Sonneratia acida* is used as poultice in swelling and sprains [28].

Researchers have isolated a variety of other mangrove compounds including taraxerol, careaborin and taraxeryl *cis-p*-hydroxycinnamate from leaves of *Rhizophora apiculata* [44, 48]; 2-nitro-4-(2′-nitroethenyl phenol) from leaves of *S. acida*; alkanes (46.7–97.9% wax) and triterpenoids (53.3% wax) from leaves of *Rhizophora* species; and iridoid glycosides from leaves of *Avicennia officinalis* and *A. germinans* [41, 44]. Metabolites belong to diterpenoids such as seven labdanes, viz. rhizophorin-A, *ent*-(13*S*)-2,3-*seco*-14-labden-2,8-olide-3-oic acid, ribenone, *ent*-16-hydroxy-3-oxo-13-epi-manoyl oxide, *ent*-15-hydroxy-labda-8,13*E*-dien-3-one, *ent*-3a,15 dihydroxylabda-8,13*E*-diene, excoecarin A, and an *ent*-beyerane, rhizophorin-B were identified from the roots of the Indian *A. officinalis*. A number of compounds such as a flavonone, a monoterpene, a sterol glucoside, two phenolic acids, three alkaloids, five protolimonoids, and 83 limonoids, have been reported from the stem bark, timber, fruits, and seeds of *X. moluccensis* and *X. granatum*. Three limonoids of the gedunin group, gedunin, 7-oxogedunin and 1a-hydroxy-1,2-dihydrogedunin, were isolated from the genus *Xylocarpus*. Gymnorrhizol, a potent proteintyrosinephosphatase 1B inhibitor, was identified from the stems and leaves of

B. gymnorrhiza. Fifteen naphthoquinones were reported from *A. marina, A. alba* and *A. officinalis*. They possess strong antiproliferative activity against L-929 mouse fibroblast. Xylogranatins F, G and R, limonoids identified from the seeds of *X. granatum*, exhibited marked antifeedant activity against the third instar larvae of *Mythimna separata* (Walker), a pest to wheat in the north of China [30].

1.2.4 Drug discovery and potential application of mangrove plants

Research in drug discovery from plant species involves a multifaceted approach combining botanical, phytochemical, biological and molecular techniques. Medicinal drug discovery continues to provide new and important leads against various pharmacological targets including microbial infections, cancer, HIV etc. The first major step in the development of a phytomedicine is to prepare a therapeutically valuable extracts. Then, the extracts are fractionated by sequential solvent extraction and column chromatography techniques to obtain an active fraction. The active fractions are then tested for their bioactivity and the structure elucidation of the compounds showing promising results are done by liquid chromatography and mass spectroscopy (LCMS), nuclear magnetic resonance spectroscopy (NMR) techniques etc. The isolated compounds are tested using animal models to find out their efficacy and then these novel compounds are subjected to clinical trials (Phase 1, 2, and 3) using human models leading to the development of a new drug [62].

Mangroves are biochemically unique, producing a wide array of novel natural products. They are the rich source of phytochemicals and possess various biological activities which lead to discovery of herbal drugs and semi-synthetic drugs. Many of the compounds isolated from mangrove plants show pharmacological activities and are helpful for the invention and discovery of drugs, primarily for deadly diseases like cancer, acquired immuno-deficiency syndrome (AIDS), arthritis, etc., while other compounds have been developed as analgesics or to treat inflammation, etc. Many of the bioactive compounds with novel chemical structures are isolated from mangrove plants; however, a few of them with novel isolated compounds have been tested for drug discovery with clinical trials. *Rhizophora mangla* has clinical use in the control of diabetes [28]. Many clinical trials have been carried out on *E. agallocha* plant extracts and some of its isolated compounds showed

potent as anti-HIV, anticancer and antiviral agents [53]. Some of the mangrove species such as *B. sexangula*, *A. Africana* etc. have been tested for curing cancer and tumors [37].

Mangroves with unique biochemicals like polyphenols, flavonoids and tannins have potential commercial applications. For example, mangrove extracts kill larvae of the mosquitos viz. *Anopheles stephensi*, *Culex tritaeniorhynchus*, *Aedes aegypti*, and *Culex quinquefasciatus*. A pyrethrin-like compound in stilt roots of *R. apiculata* shows strong mosquito larvicidal activity. Smoke from burned extracts repels and kills both *A. aegypti* and *C. quinquefasciatus* and extracts can also be applied directly on human skin to repel adult *A. aegypti*. Phenols and flavonoids in mangrove leaves serve as UV-screening compounds. Hence, mangroves tolerate solar-UV radiation and create a UV-free, under-canopy environment [53].

1.3 Limonoids

Limonoids are of moderate polarity, insoluble in water and hexane but soluble in hydrocarbons, alcohol and ketone; they are mostly bitter in taste and account for the scent of fresh peels of citrus fruits. Limonoids are present in neutral (noncarboxylated/aglycone) as well as acidic (carboxylated/glucoside) forms, the former are insoluble and bitter while latter are soluble and tasteless. Chemically they are highly oxygenated triterpenes, classed as tetranorterpenoids. They present, perhaps the most extreme examples of oxidation of triterpenes in nature [63].

Although hundreds of limonoids have been isolated from various plants but, their occurrence in the plant kingdom is confined to only plant families of order Rutales and that too more abundantly in Meliaceae and Rutaceae, and less frequently in Cneoraceae and *Harrisonia* sp. of Simaroubaceae. The limonoids occurring in Meliaceae are also known as meliacins. Out of over 300 limonoids known today, about one-third is accounted by neem (*Azadirachta indica*) and Chinaberry (*Melia azedarach*) alone [63].

Citrus fruits and its closely related genera contain about 36 limonoid aglycones and 17 limonoid glucosides. Citrus limonoids and their glucosides, the water-soluble triterpenoid compounds that occur naturally in citrus fruit and citrus

juice in amounts comparable to vitamin C, can be reclaimed from citrus processing and citrus seeds as by-products in large quantities. Limonin glucoside is the most abundant of the limonoid glucosides in citrus. *Azadirachta indica* (Neem tree) a species of meliaceae family is a storehouse of limonoids containing more than hundred different limonoids and their derivatives in its different plant parts. Other important sources of limonoids in meliaceae family are *Cedrela* sp., *Khaya* sp., *Melia azedarach, Sandoricum koetjape, Swietenia mahogany, Trichilia* sp. and. *Xylocarpus granatum* [63].

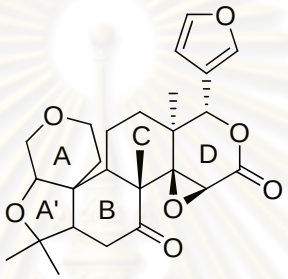

Limonin

Figure 1.2 Citrus limonoid (limonin)

1.3.1 Chemistry and biosynthesis of limonoids

Limonoids, which have been found only plants of the order Rutales, are triterpene derivatives from a precursor with a 4,4,8-trimetyl-17-furanylsteroid skeleton. All naturally occurring limonoids contain a furan ring attached to the D-ring, at C-17, as well as oxygen containing function group at C-3, C-4, C-16 and C-17 [64].

The biosynthesis of limonoids shows that limonoids are synthesized via terpenoid biosynthetic pathway, starting with cyclization of squalene (Figure 1.3), which result into a tetracyclic ion, euphane and tirullane (Figure 1.4), two chemically corresponding compounds may be the ultimate biogenetic precursors. Oxidative degradation at the C-17 side chain of either of these nucleus result in loss of four carbon atoms and formation of β-substitued furan, further oxidation and skeletal rearrangements in one or more of the four rings, which are designated as A, B, C and D (Figure 1.2), give rise to different groups of limonoids as shown in Figure 1.5. However, the oxidations are either epoxidations of double or Baeyer Villiger attacks

on ketones and all of the type to be expected from a biological peracid equivalent, presumably a peroxidase [65].

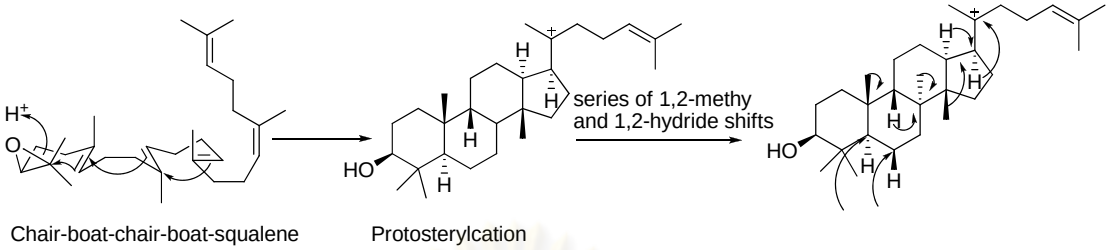

Figure 1.3 Squalene epoxide leading to different intermediate triterpene cations

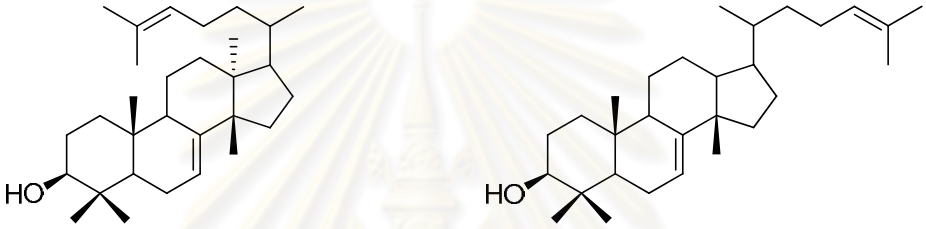

Euphane Tirucallane

Figure 1.4 Proposed precursors of limonoids

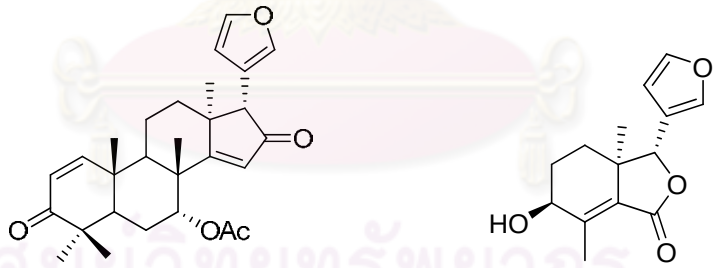

Intact limonoid Degraded limonoid

Figure 1.5 Example of limonoids showing different degree of oxidation and skeleton arrangement

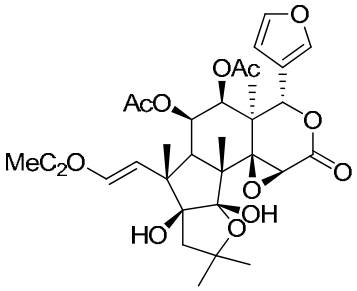

Highly modified limonoid

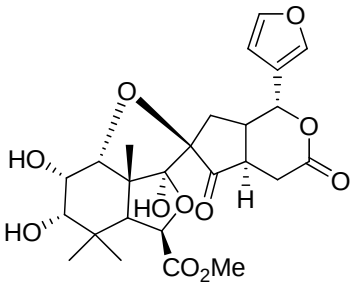

Highly cleaved limonoid

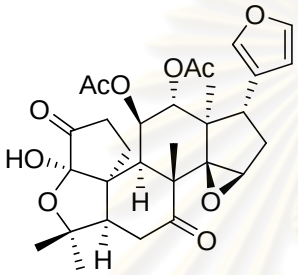

Ring A-*seco* limonoid

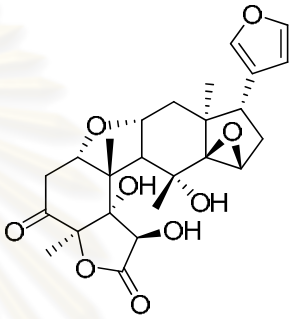

Ring-A,C,D-intact-ring-B-*seco* limonoid

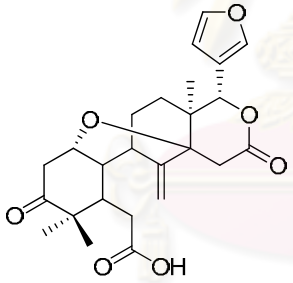

Ring-B,D-*seco* limonoid

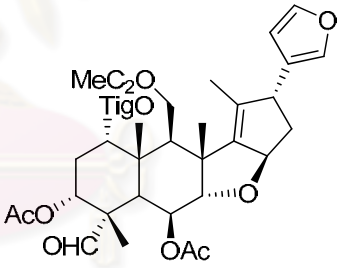

Ring-C-*seco* limonoid

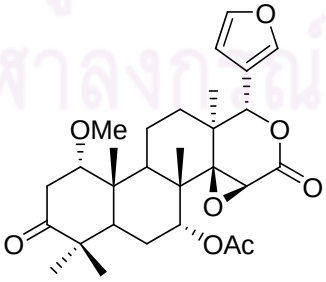

Ring-D-lactone-limonoid

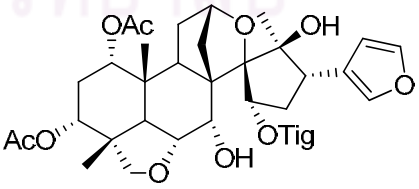

Ring-C-*seco* limonoid

Figure 1.5 Example of limonoids showing different degree of oxidation and skeleton arrangement (continued)

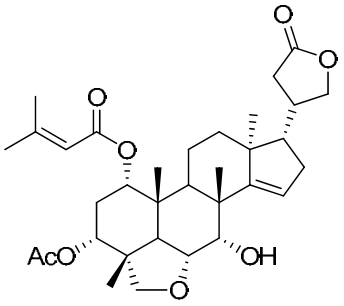

Gamma-lactone side chain limonoid

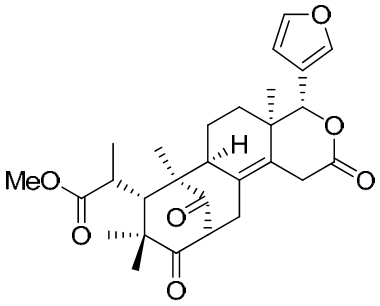

Mexicanolide

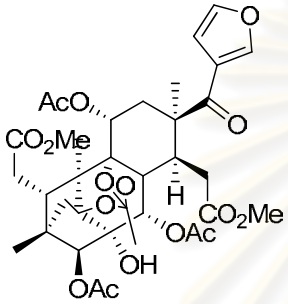

Phragmalin

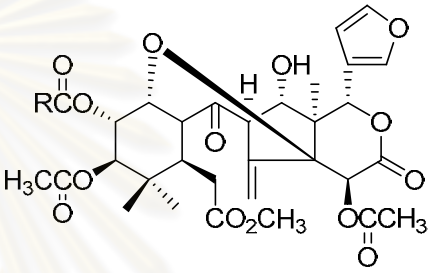

Trijugin-type-limonoid

Figure 1.5 Example of limonoids showing different degree of oxidation and skeleton arrangement (continued)

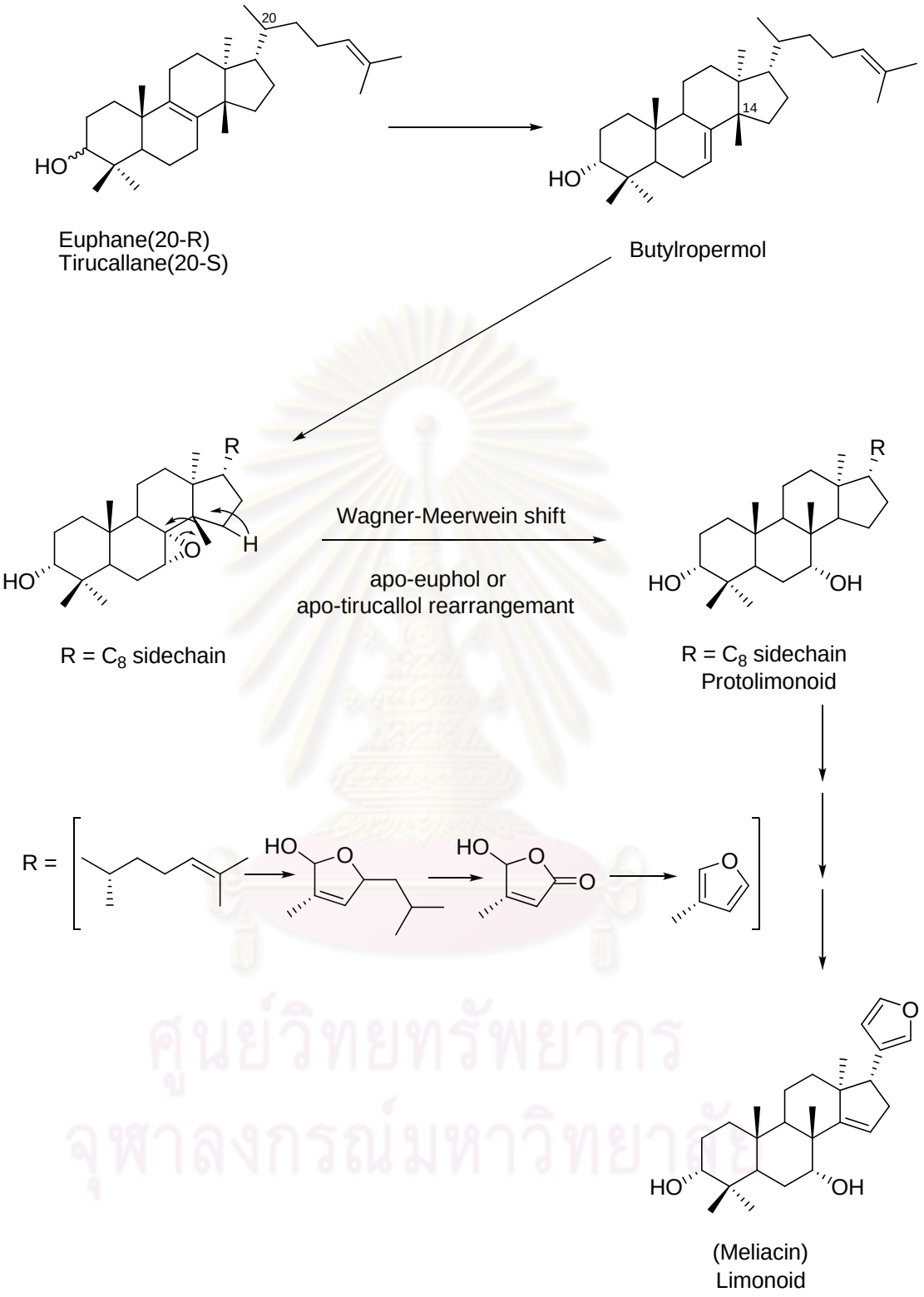

Scheme 1.1 Biosynthetic pathway leading to the formation of a simple limonoid [66]

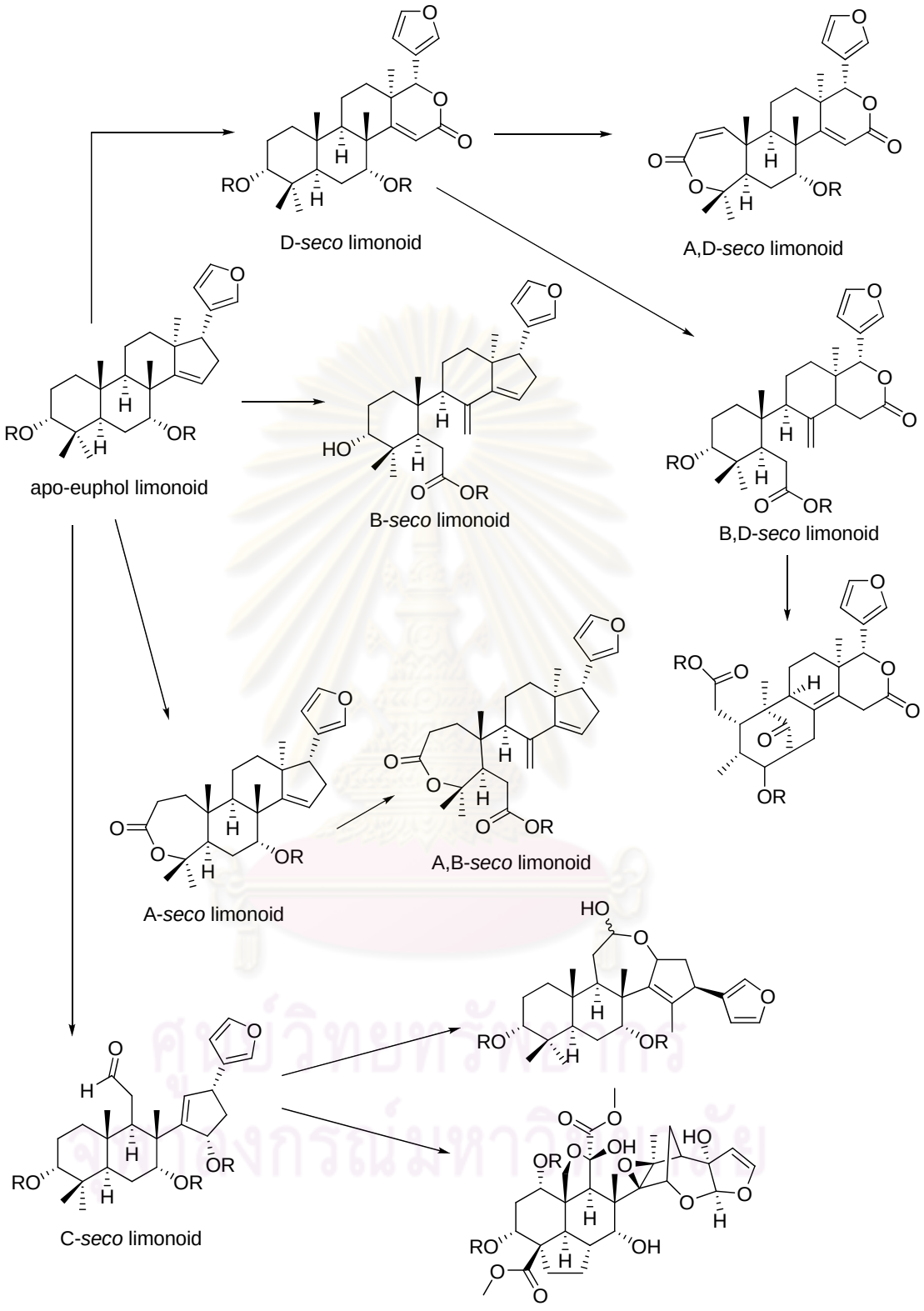

Scheme 1.2 Major biosynthetic routes of limonoids [66]

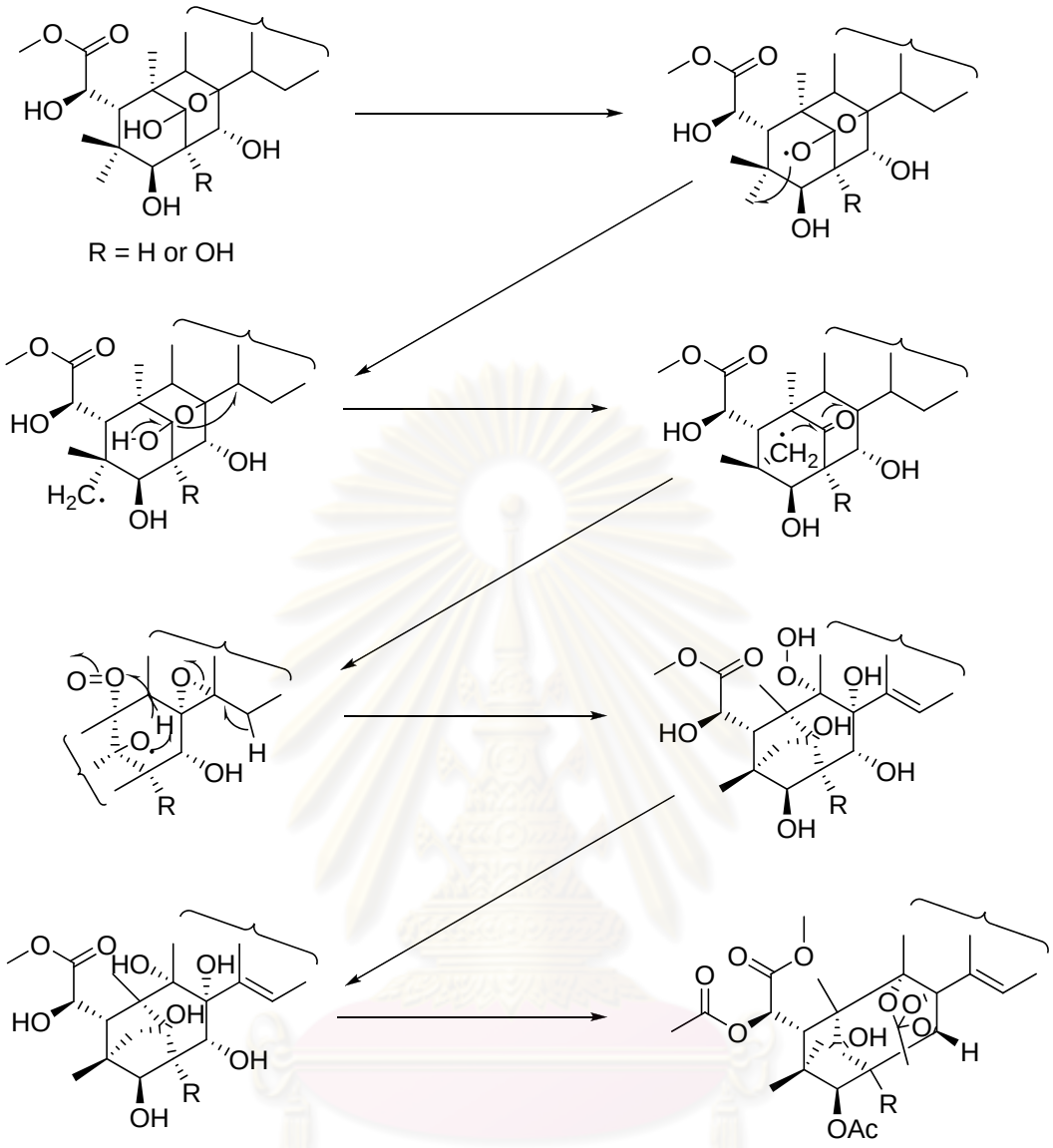

Scheme 1.3 Proposal biosynthethic pathway to 8,9,30-phragmalin ortho esters from mexicarnolide [67]

1.3.2 Pharmacolgical activities of limonoids

Anti-cancer Activity. Many experimental evidences have revealed that limonoids present in citrus fruits and their juice have cancer chemopreventive property, have been shown to inhibit the growth of estrogen receptor- negative and positive human breast cancer cells in culture, and have been found to target and stop neuroblastoma cells [68]. Hesperidin, other flavonoids, limonin, 17β-D-glucopyranoside, and other limonoid glucosides are potential chemopreventive agents in orange juice that could account for the decreased colon tumor-genesis associated with feeding orange juice. Significant cytotoxic activity has also been exhibited by limonoids isolated from *Melia azedarach* [69], *Melia toosendan* and azadirachtin A [70].

The citrus limonoids, obacunone, limonin, nomilin and their glucosides, and some aglycones inhibit chemically induced carcinogenesis and a series of human cancer cell lines, with remarkable cytotoxicity against lung, colon, oral and skin cancer in animal test system and human breast cancer cells. Obacunone was found to enhance the cytotoxicity of vincristine against L1210 cells by approximately 10-fold. Further, it was found that the cytotoxicity of other microtubule inhibitors such as vinblastine and taxol in drugsensitive KB-3-1 cells as well as in multidrug-resistant KB-V1 cells was enhanced greatly in the presence of obacunone [71]. Pure limonin glucoside and limonin, its water insoluble relative lacking glucose, have been found to possess significant anti-tumor properties in animal tests and with human cells [72]. All these studies have reported the lack of toxicity of the limonoids in mammals and also have presented their modifying effect on the development of aberrant crypt foci, as well as ability of these compounds to induce specific carcinogen-metabolizing enzymes, glutathione Stransferace and quinine reductase in the liver and mucosa of the small intestine to detoxify chemical carcinogenesis. Studies show that the activity of phase II enzyme glutathione-Stransferase in the liver of the rats, fed diets containing limonin and nomilin, increased significantly in dose dependent manner. While simultaneously the limonoids, nomilin and limonin, were found to have no significant affect on the phase I enzyme Cytochrome P450. A dose dependent increase in small intestinal GST activity was also observed in nomilin fed animals, whereas some citrus limonoids were able to inhibit the development of 7,12-

dimethylbenz[*a*]anthracene-induced oral tumors. The data from these studies have suggested that certain rings in the limonoid nucleus may be critical to antineoplastic activity. Nutritional research on health benefits of chemicals present in plant foods advocate that citrus limonoids possess substantial anticancer activity and they are also free of any toxic effects in animal models [68].

Anti-malarial Activity. Gedunin, nimbin, nimbolide and many more limonoids isolated from *Azadirachta indica, Cedrela odorata, Guarea mltiflora* and *Khaya grandifoliola* have been identified for their *in-vitro* antimalarial activity on *Plasmodium falciparum* [73]. Gedunin was found to be most effective, against *P. falciperum,* out of several limonoids isolated from *Khaya grandifoliola* and it also exhibited additive effect in combination with chloroquine [74]. Furthermore, novel antimalarial limonoids were isolated following a veterinary and self-medicative behavioral survey of wild chimpanzees in Uganda, from leaves of *Trichilia rubescens* [75].

Anti-microbial Activity. Germano *et al*., 2005 have recently reported the presence of limonoids in Trichilia *emetica,* which can be considered responsible for activity against many clinically, isolated bacterial strains. Limonoids obtained from some *Khaya* species, showed good antibacterial and antifungal activity [76]. In another study limonoids from several plants belonging to meliaceae as well as rutaceae family were reported to have significant antifungal activity [77].

Anti-HIV Activity. Limonin and nomilin have shown to inhibit the replication of HIV-1 in a number of cellular systems. A novel limonoid isolated from *Clausena excavate* have also shown HIV-1 inhibitory activity [78].

1.4 Plants belonging to the genus *Xylocarpus*

The genus *Xylocarpus* belongs to the order Geraniales of the family Meliaceae [79]. The family meliaceae comprises of the 50 genera including *Xylocarpus* and 1400 other species distributed all over the world [80]. Plants in the genus *Xylocarpus* are distributed in the coastal regions of India, Ceylon, Burma and Malaya [81]. It was reported that the genus of mangrove *Xylocarpus* has six species, *X. gangeticus*, *X. granatum*, *X. mekongensis*, *X. minor*, *X. moluccensis*, and *X.*

parvifolius. However, *X. gangeticus*, *X. mekongensis* and *X. moluccensis* may be the same species, though they were given three different names. The taxonomy and nomenclature of these species still need to be clarified in the future. In addition, the genus *Xylocarpus* is reported to contain a special class of bitter substances termed as "Limonoids".

Genus *Xylocarpus* is reported to have compounds belonging to some of the above-mentioned groups of limonoids from its different species. The classes of limonoids which have been isolated from this genus are as follows:

Gedunin group (Ring D opened)

Andirobin group (ring B and D opened)

Mexicanolide group (modified ring B opened and recyclised)

Phragmalin group (modified, ring B opened and recyclised)

Obacunol group (Rings A and D opened)

1.4.1 Medicinal uses of genus *Xylocarpus*

All the species of *Xylocarpus* have similar medicinal uses. All parts are used as astringent [79], but the bark and root are more widely used. The bark is also used in dysentery, diarrhoea, and other abdominal troubles and febrifuge [81]. Seed ash is mixed with sulphur and coconut oil and applied as ointment for itch [81]. The root is used to treat cholera, from Burma to Phillipines. Traditionally, the bark pressings of *X. granatum* are used in the treatment of cholera, fever and malaria and that of *X. moluccensis* is used in cholera and fever [31]. The fruits of *X. moluccensis* are also used as an aphrodisiac [31]. The kernels are used in tonics and in relieving colic. The seeds or peels of the fruits are utilized to poultice swellings and ash of the seeds is applied to itch. In addition, fruits are used as a cure for swellings of the breast and in elephantiasis.

Various biological activities of the extracts and compounds from the genus *Xylocarpus* have been reported. Antidiarrhoeal activity of methanol extract of the barks of *X. moluccensis* in castor oil and magnesium sulphate have been studied in 2005 [82], and antibacterial activity of the extract of *X. granatum* has also been reported in the same year by Choudhary and coworkers [83]. The extract is reported to inhibit the growth of six virulent strains of bacteria pathogenic to fish including

Edwradsiella tarda, *Vibrio alginolyticus*, *Pseudomonas fluorescens*, *Pseudomonas aeruginosa* and *Acromonas hydrophila*. Gedunin, a limonoid from *X. granatum* showed significant *in vitro* antimalarial activity but poor *in vivo* activity. Another compound from *X. granatum*, *N*-Methylflindersine displayed antifeedant, insect repellant, antimicrobial, antiyeast and antifungal activities. Xyloccensins Q-V from *X. granatum* have also been reported to have antifeedant activity [84].

1.4.2 General characteristics of *Xylocarpus moluccensis* Roem.

Taxonomy of *Xylocarpus moluccensis* Roem. is categorized as

Kingdom : Plantae
Division : Tracheophyta
Class : Magnoliopsida
Order : Rutales
Family : Meliaceae
Genus : *Xylocarpus*
Species : *Xylocarpus moluccensis* Roem.

Medium-sized crooked much-branched evergreen tree up to 10 m. tall (taller elsewhere); bark smooth and yellowish, or brown and green and flaking; surface roots laterally compressed and forming a spreading network of ribbon-like pneumatophores with the upper edges protruding above the mud and suggesting a mass of snakes. Leaves paripinnate, drying orange-brown; petiole and rhachis up to 8·5 cm. long, glabrous; leaflets up to 12 × 5 cm., usually much smaller, opposite, 1–2 (3)-jugate, elliptic, oblong-elliptic or obovate-elliptic, apex usually rounded, rarely obtuse or emarginate, base narrowly or broadly cuneate, glabrous, coriaceous, venation prominent on both sides; petiolules 2–5 mm. long. Flowers whitish or pale pink, in lax racemes of (2) 3-flowered cymes; peduncle plus rhachis 4–7 cm. long; bracts minute, usually caducous. Calyx about 3 mm. long, glabrous, lobed to the middle, lobes rounded. Petals 5–6·5 × 2·5 mm., glabrous. Staminal tube 4–5 mm. long, glabrous. Ovary less than 1 mm. in diam.; style 1·5 mm. long; disk fused to the lower half of the ovary. Fruit large, up to 20 cm. in diam., obscurely 4-sulcate. Seeds 4–8 cm. long. The picture of *X. moluccensis* is shown in Figure 1.6. [85]

Figure 1.6 The picture of *X. moluccensis*

1.4.3 Previous study of limonoids of *Xylocarpus moluccensis* Roem.

In 1983, Taylor and coworkers reported three new limonoids, xyloccensins G-I, isolated from the timber of the *X. moluccensis* [86].

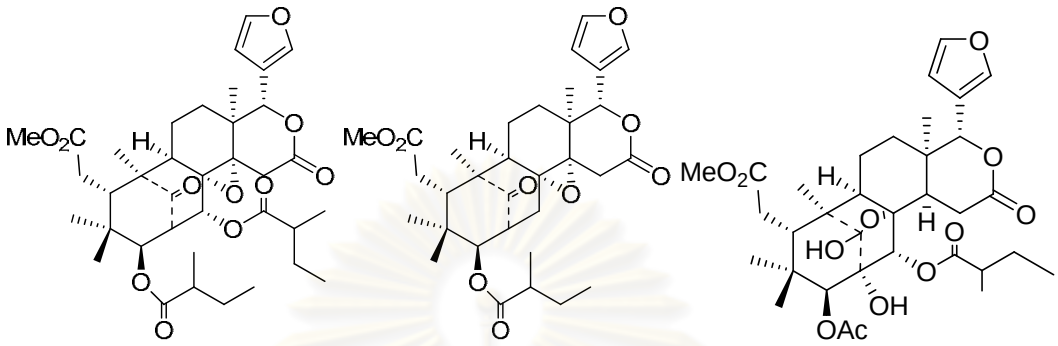

Xyloccensin G Xyloccensin H Xyloccensin I

Figure 1.7 Structures of xyloccensins G-I

In 2009, Li and coworkers isolated seven new phragmalins, named moluccensins A-G, from the seeds of an Indian mangrove, *X. moluccensis* [87].

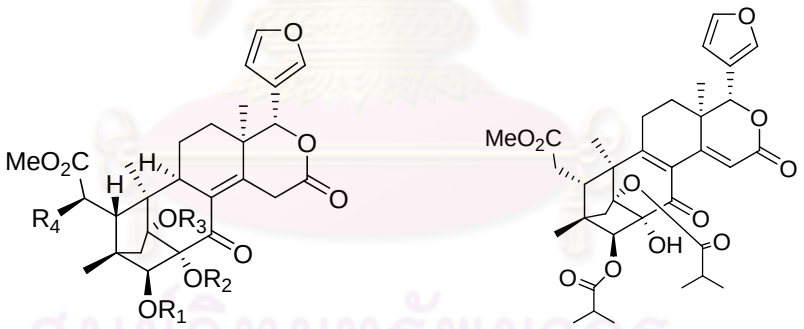

Moluccensin G

Moluccensin A R^1 = isobutyryl R^2 = H R^3 = isobutyryl R^4 = H

Moluccensin B R^1 = 2*S*-methylbutyryl R^2 = H R^3 = isobutyryl R^4 =H

Moluccensin C R^1 = isobutyryl R^2 = H R^3 = 2*S*-methylbutyryl R^4 =H

Moluccensin D R^1 = 2*S*-methylbutylryl R^2 = H R^3 = isobutyryl R^4 =OH

Moluccensin E R^1 = isobutyryl R^2 = H R^3 = 2*S*-methylbutyryl R^4 = OH

Moluccensin H R^1 = isobutyryl R^2 = isobutyryl R^3 = H R^4 = H

Figure 1.8 Structures of moluccensins A-G

In 2010, Pudhom and coworkers reported three new phragmalin limonoids, moluccensins H-J, obtained from seed kernels of the cedar mangrove, *X. Moluccensis*. Moluccensin I displayed weak antibacterial activity against *Staphylococcus hominis* and *Enterococcus faecalis* [88].

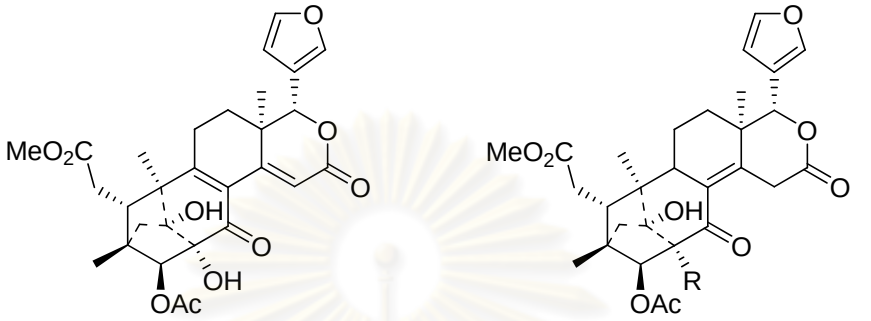

Moluccensin H

Moluccensin I R = OMe

Moluccensin J R = H

Figure 1.9 Structures of moluccensins H-J

In 2010, Wu and coworkers found six new phragmalins, moluccensins H-M, two new andirobin-type limonoids, moluccensins N and O, and two new tirucallane derivatives, moluccensins P and Q, from seeds of an Indian mangrove, *X. Moluccensis*. Moluccensins H and I showed moderate insecticidal activity against the fifth instar larvae of *Brontispa longissima* (Gestro) at a concentration of 100 mg/L [89].

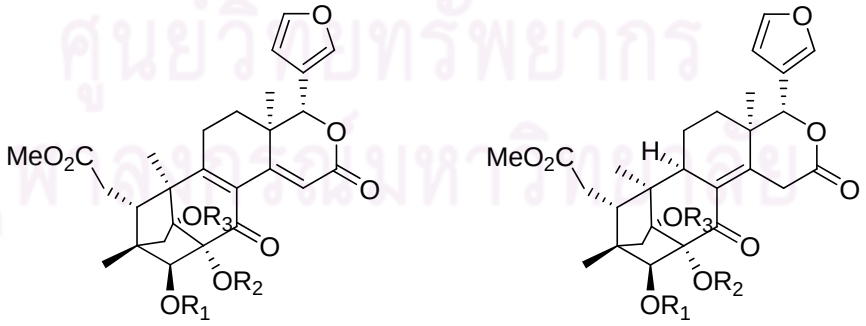

Moluccensin H R^1 = A R^2 = H R^3 = B

Moluccensin I R^1 = B R^2 = H R^3 = A

Moluccensin K R^1= A R^2 = B R^3 = H

Moluccensin L R^1 = B R^2 = H R^3 = B

Figure 1.10 Structures of moluccensins H-Q

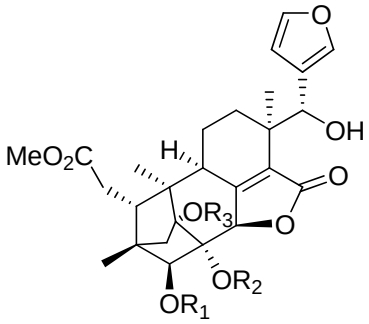

Moluccensin N R^1= B R^3 = H R^3 = A

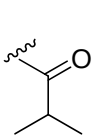

A

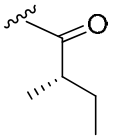

B

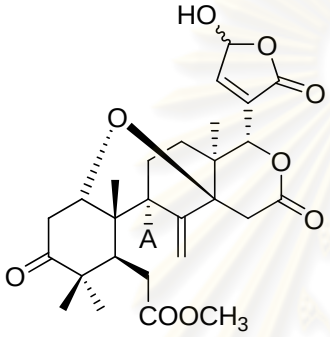

Moluccensin N

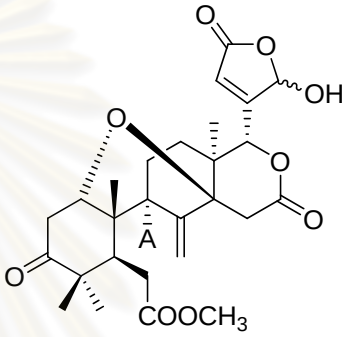

Moluccensin O

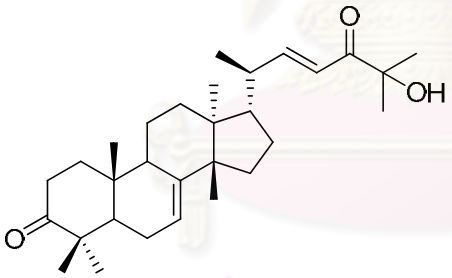

Moluccensin P

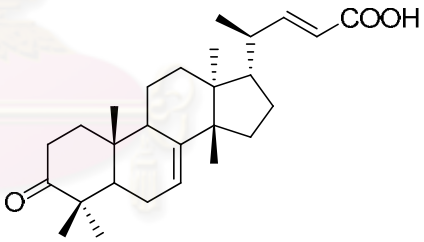

Moluccensin Q

Figure 1.10 Structures of moluccensins H-Q (continued)

In 2010 Zhang and coworkers reported two new mexicanolides, named xylomexicanolides A and B, isolated from the seeds of an Indian mangrove, *X. moluccensis*, together with four known limonoids, Khayasin, angolensic acid methyl ester, Khayasin T, and 2′*S*-methylbutanoylproceranolide. Khayasin was found to exhibit marked insecticidal activity against the fifth instar larvae of *Brontispa longissima* (Gestro) at a concentration of 10 mg/L [90].

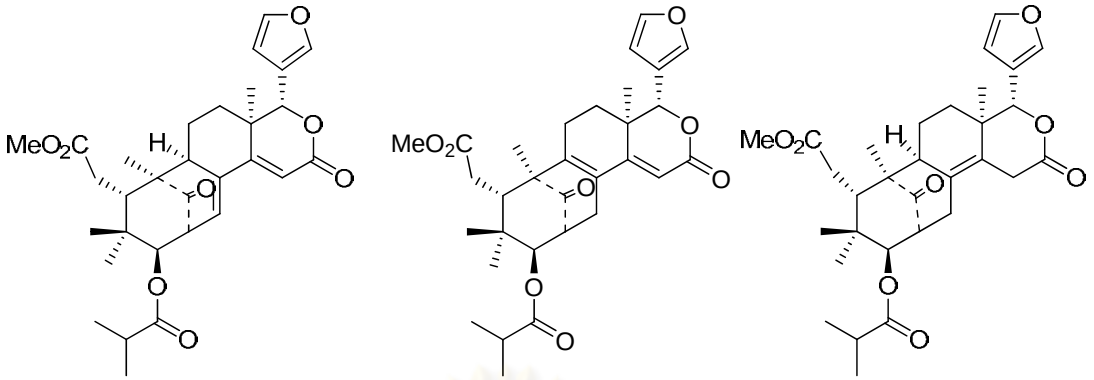

Xylomexicanolide A Xylomexicanolide B Khayasin

Figure 1.11 Structures of xylomexicanolides A-B and khayasin

According to the study on limonoid constituents of *X. moluccensis* collected from various areas, it was found that the ecological system in each area has much effect on structures of limonoids found in this plant. This prompted us to investigate limonoids of the seed kernels of *X. moluccensis* collected from a mangrove area in Phuket province. It is because there are very few reports of limonoids from Thai *Xylocarpus* sp., particularly *X. moluccensis* in southern area. Moreover, biological activity of isolated limonoids would be evaluated.

1. To extract, isolate and purify limonoid constituents of the seed kernels of *X. moluccensis* collected from Phuket province.
2. To identify the structures of the isolated limonoids by spectroscopic techniques.
3. To study biological activity of pure compounds such as anti-inflammatory, antibacterial and anticancer activities.

CHAPTER II

EXPERIMENTS

2.1 General experimental Procedures

2.1.1 Fourier transform infrared spectrophotometer (FT-IR)

The FT-IR spectra were recorded on a Perkin-Elmer Model 1760X Fourier Transform Infrared Spectrophotometer. Each solid sample was formally examined by incorporating sample with potassium bromide (KBr) to form a pellet.

2.1.2 Mass spectrometer (MS)

HRESIMS spectra were obtained with a Bruker micrOTOF

2.1.3 Nuclear magnetic resonance spectrometer

The NMR spectra were recorded in chloroform-*d* ($CDCl_3$) using a Bruker AV400 spectrometer at 400 MHz for ^{1}H NMR and at 100 MHz for ^{13}C NMR using TMS (tetramethylsilane) as internal standard.

2.1.4 Optical rotation

Optical rotations were measured on a Perkin-Elmer 341 polarimeter at 589 nm.

2.1.5 Single-crystal X-ray crystallography

A colorless crystal of compounds **4** and **9** were obtained in EtOAc-n-hexane. Crystals data were obtained on a Bruker APEX II system diffractometer with graphite-monochromated Mo Kα radiation (λ = 0.71073 Å) and operating in the ω scan mode. The structure was solved by direct methods (SHELXS-97) and refined using full-matrix least-squares difference Fourier techniques. All non-hydrogen atoms were refined anisotropically, and all hydrogen atoms were placed in idealized positions and refined as riding atoms with the relative isotropic parameters. Crystallographic data for compounds **4** and **9** have been deposited with the Cambridge

Crystallographic Data Centre with the deposition number CCDC 743509. Copies of the data can be obtained, free of charge, on application to the Director, CCDC, 12 Union Road, Cambridge CB2 1EZ, UK [fax: +44(0)-1233-336033 or e-mail: deposit@ccdc.cam.ac.uk].

2.1.6 Ultraviolet-visible spectrophotometer (UV-Vis)

UV data were recorded on a CARY 50 Probe UV-visble spectrophotometer.

2.1.7 Melting point

Melting points were recorded on a Fisher-Johns melting point apparatus.

2.2 Chemicals

All commercial grade solvents used for extraction and isolation were distilled prior to use. Deuterated chloroform ($CDCl_3$) was utilized as a solvent for NMR experiments.

Merck's silica gel 60 No. 7734 and No.9385 were used as adsorbents for open column chromatography.

Merck's Thin layer chromatography (TLC) aluminum and glass sheets, silica gel 60 F_{254} precoated 25 sheets, 20×20 layer thickness 0.2 mm were used for TLC analysis. Detection was visualized under ultraviolet light at wavelengths of 254 and 356 nm and dipped with $(NH_4)_6Mo_7O_{24}$ solution in 5% H_2SO_4/EtOH.

2.3 Plant material

Fruits of *X. moluccensis* were collected from Phuket Province, Thailand, in December 2009. Plant materials were identified by Royal Forest Department, Bangkok, Thailand.

2.4 Extraction and Isolation

Air-dried powdered seed kernels of *X. moluccensis* (3 kg) were extracted with MeOH (5L× 2 each for three days). The extract was concentrated under

reduced pressure, followed by suspension in water and extraction with EtOAc. Then, the solvent was removed under reduced pressure to yield EtOAc crude extract (235g). The extraction procedure is depicted in Scheme 2.1.

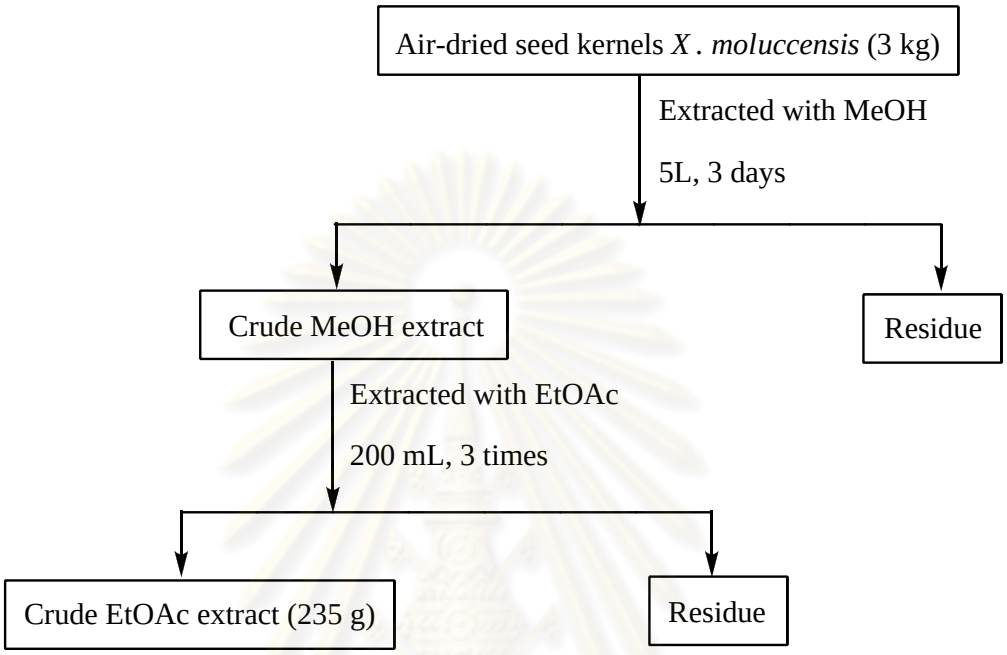

Scheme 2.1 The extraction procedure of *X. moluccensis* seed kernels.

The resulting EtOAc crude extract was chromatographed on a silica gel column eluted with a gradient of acetone-n-hexane (10-100%) to yield 12 fractions (A-L). Fraction G (2.8 g) was then applied to a silica gel column and eluted with a gradient of acetone-n-hexane (20-50%) to afford 12 subfractions (G1-G12). Subfraction (G4) was further purified by silica gel column chromatography (acetone-n-hexane, 20%) and recrystallized from EtOAc-n-hexane (1:1) to afford compound **4**, 15 mg. Subfraction G8 (800 mg) was then subjected to silica gel column eluted with a gradient of acetone-CH_2Cl_2 (20-70%) to yield compound **8** (20 mg), compound **5** (40 mg) and additional five fractions, G8.1-G8.5. Fraction G8.3 (148 mg) was separated on a silica gel column using a 1:99 mixture of MeOH-CH_2Cl_2 as an eluent to furnish compound **2** (17.2 mg) and compound **9** (5.3 mg). The isolation of Fraction G is described in Scheme 2.2.

As shown in Scheme 2.3, Fraction H (57 g) was subjected to silica gel column chromatography eluted with a gradient of MeOH-CH_2Cl_2 (2.5-5%) to afford

13 subfractions, H1-H13. Subfraction H2 (10 g) was rechromatographed on a silica gel column, eluted with a gradient of MeOH-CH_2Cl_2 (1-5%), to obtain nine fractions (H2.1-H2.9). Fraction H2.3 (345 mg) was then subjected to silica gel column chromatography using the same solvent system (MeOH-CH_2Cl_2, 1-5%) to yield compound **1** (18.8 mg) and compound **3** (35 mg), while Fraction H2.5 (547 mg) gave compound **10** (5.7 mg) after purification on a silica gel column utilizing acetone-n-hexane (1:9) as an eluent. Fraction H2.8 (40 mg) was rechromatographed on a silica gel column, eluted with a 1:9 mixture of acetone-CH_2Cl_2 to afford compound **11** (7.6 mg). Subsequently, Fraction H8 (850 mg) was subjected to silica gel column chromatography eluted with acetone-n-hexane (1:9) to give compound **6** (12.7 mg) and compound **7** (4.8 mg).

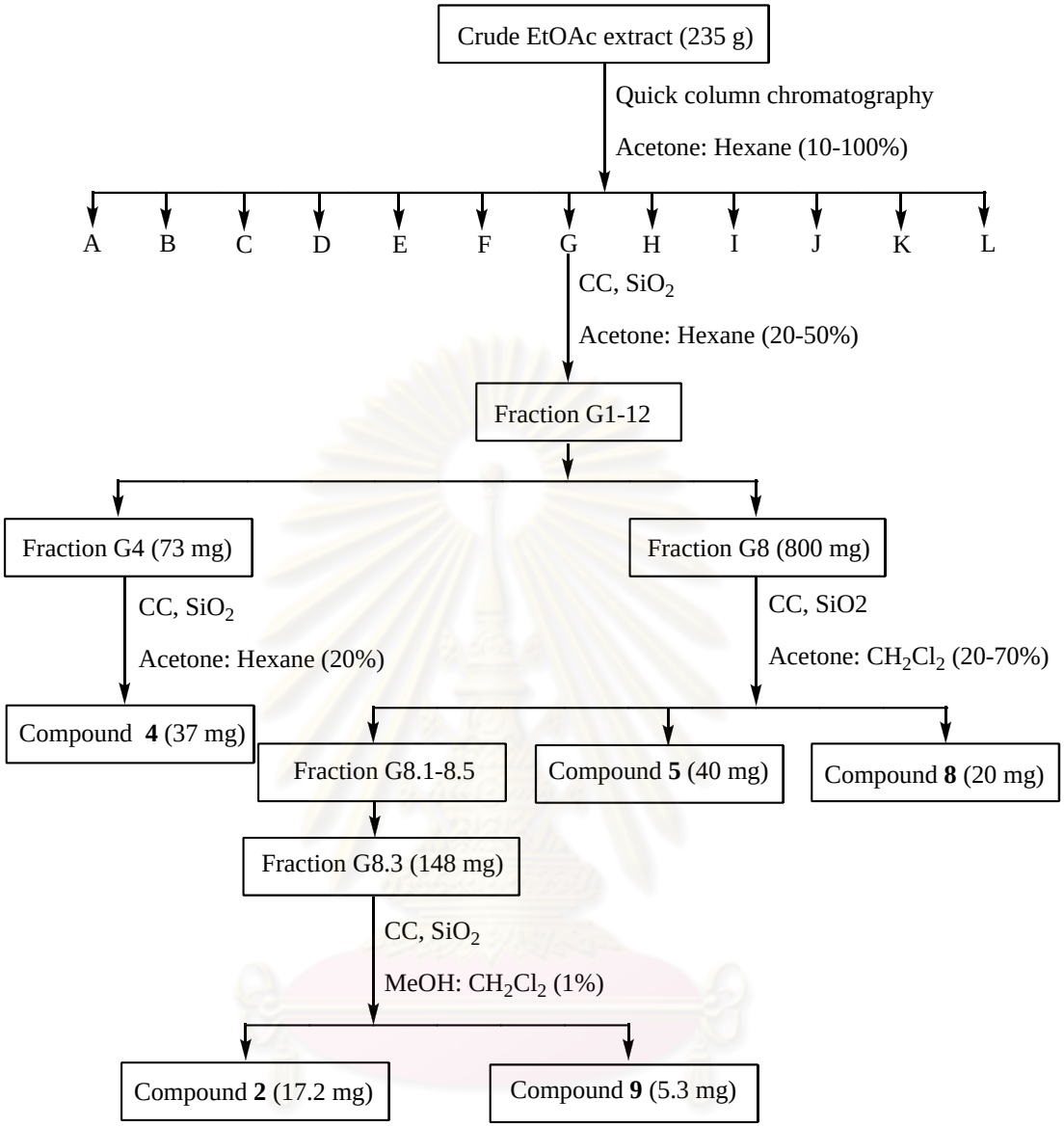

Scheme 2.2 The isolation from fraction G of EtOAc extract of *X.moluccensis* seed kernels.

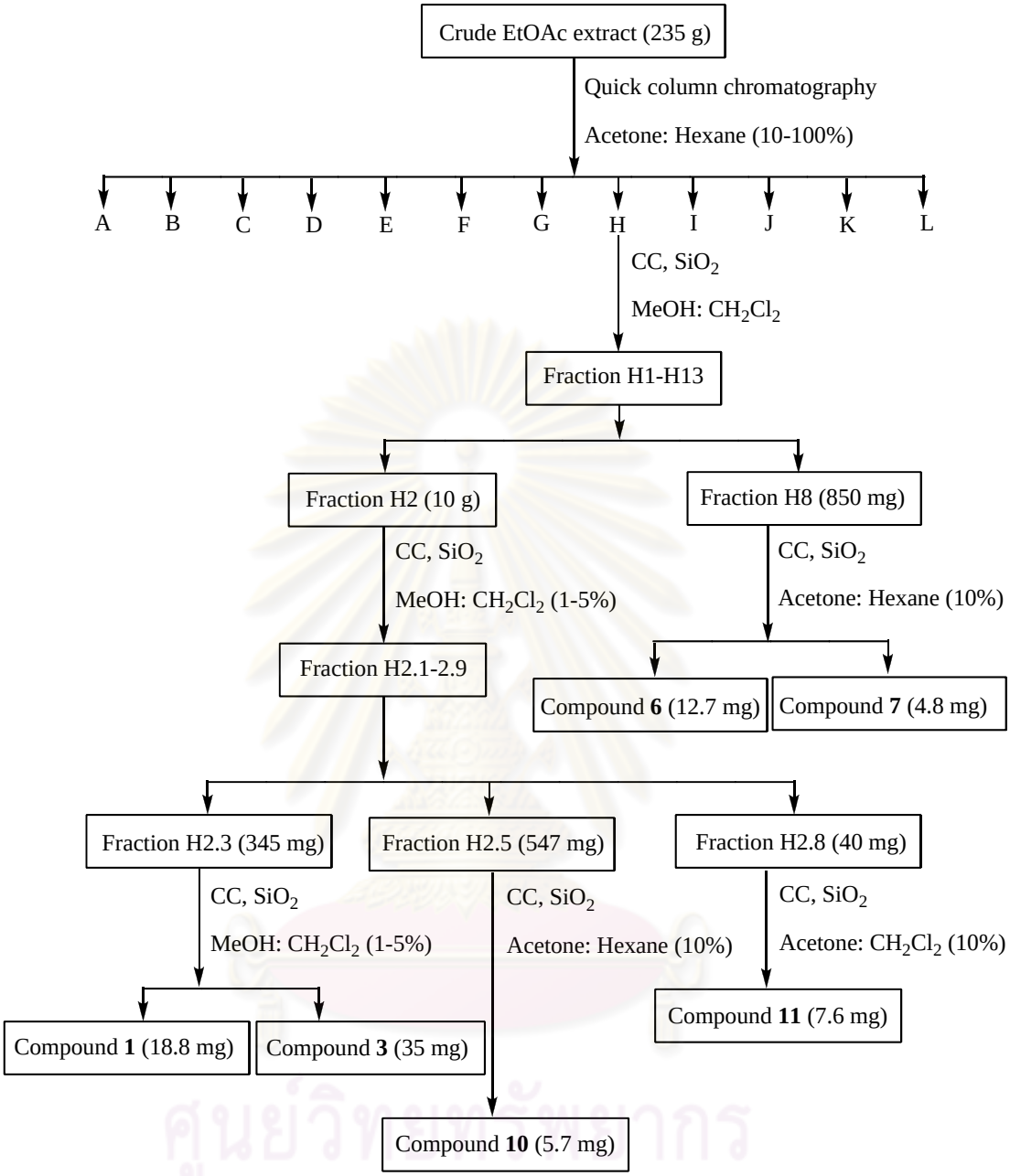

Scheme 2.3 The isolation from fraction H of EtOAc extract of *X.moluccensis* seed kernels.

2.5 Evaluation of biological activity

2.5.1 Nitric oxide inhibitory assay

Macrophage cell line RAW264.7 (ATCC TIB-71) were pretreated with compounds or vehicle control (DMSO) for 1 h before addition of lipopolysaccharide from *Escherichia coli* (100 ng/mL) and recombinant interferon gamma (10 ng/mL) to stimulate marophage. Cells were incubated further for 24 h and the culture supernants were collected. To determine the amount of nitric oxide produced, Griess reaction assay was performed. Percent of inhibition of nitric oxide production was calculated using data obtained from Griess reaction.

2.5.2 Toxicity assay

RAW264.7 cells were treated with various concentrations of tested compounds or vehicle control (DMSO) for 20 h. MTT were added to each well and cells were further incubated for another 4 h. Isopropanol was added to dissolve formazan crystal and the absorbance was measured at 540 nm. Cells incubated with DMSO were used as positive control.

CHAPTER III

RESULTS AND DISCUSSION

3.1 Isolated compounds from the seed kernels of *X. moluccensis* Roem.

In the present study, two new phragmalin-type limonoids, xylomoluccensin B (**10**) and xylomoluccesin C (**11**), and a new andirobin-type limonoid, xylomoluccensin A (**9**), were isolated from the EtOAc extract of the seed kernels of *X.moluccensis*, along with eight known compounds. Known limonoids were determined to be mexicanolide (**1**), 3*β*-deacetylfissinolide (**2**), 2-hydroxyfissinolide (**3**), 7-deacetylgedunin (**4**), 7-oxo-7-deacetoxygedunin (**5**), moluccensin H (**6**), moluccensin I (**7**) and xyloccensin E (**8**) by analysis of NMR spectroscopic data and by comparison of their data with those reported in literature. In the case of novel compounds (**9**-**11**), their structures were established on the basis of spectroscopic methods, particularly NMR and MS, as well as single-crystal X-ray diffraction analysis. The structures of isolated compounds are shown in Figure 3.1.

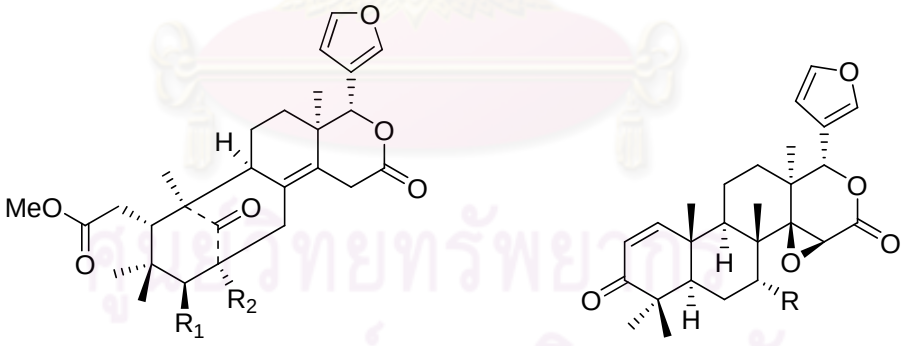

1: R^1= =O, R^2= H

2: R^1= OH, R^2= H

3: R^1= OAc, R^2= OH

4: R= OH

5: R= =O

Figure 3.1 The chemical structures of isolated compounds from *X. moluccensis*

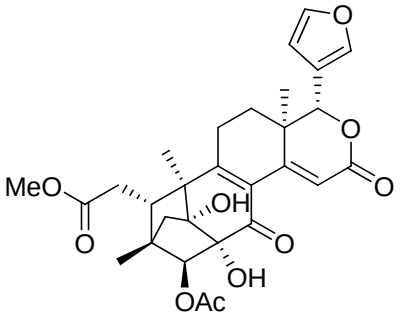

6

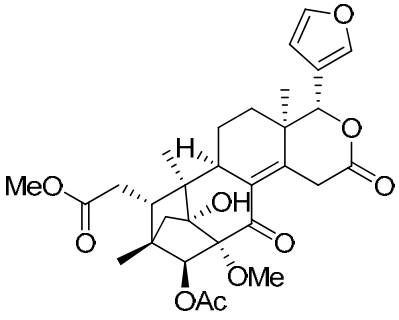

7

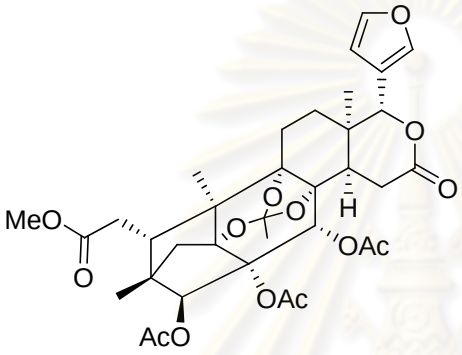

8

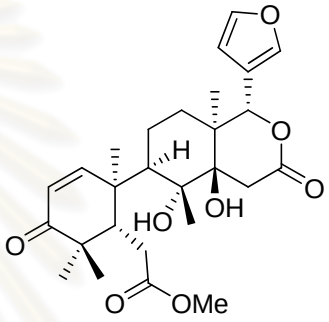

9

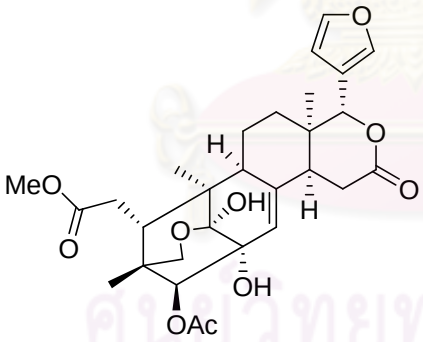

10

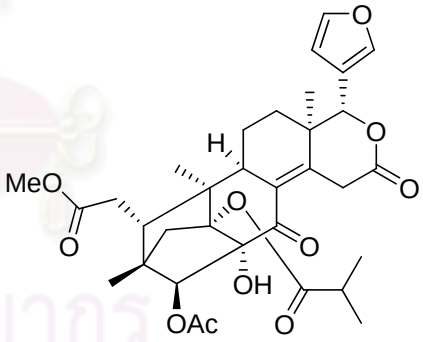

11

Figure 3.1 The chemical structures of isolated compounds from *X. moluccensis* (continued)

3.2 Structure elucidation of isolated compounds

3.2.1 Structure elucidation of compound 1

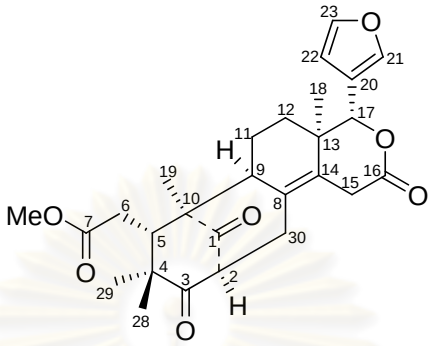

Figure 3.2 Compound **1**

Molecular formula	$C_{27}H_{32}O_7$
Appearance	White amorphous solid
m.p.	210-212 °C
$[\alpha]_D^{20}$	-62 (*c* 0.1, MeOH)
UV (MeOH) λ_{max} (logε)	285 nm (2.71)
IR (KBr)	3443, 3143, 2969, 1734, 1704, 1465, 1382, 1304, 1247, 1182, 1130 and 1021 cm^{-1}
^1H and ^{13}C NMR ($CDCl_3$)	See Table 3.1

Compound **1** was isolated as a white amorphous solid, with molecular formula $C_{27}H_{32}O_7$, indicating 12 degrees of unsaturation. The ^1H NMR spectrum (Table 3.1) displayed typical signals for a β-substituted furanyl ring (δ_H 6.49, 7.40 and 7.57), four tertiary methyls (δ_H 0.87, 0.99, 1.00 and 1.24), and one methoxy group (δ_H 3.72). In the ^{13}C NMR spectrum, 27 nonequivalent carbon resonances were observed, indicating four carbonyl carbons (δ_C 168.9, 173.6 211.0 and 212.9), six olefinic carbons (δ_C 109.9, 120.4, 125.3, 133.9, 141.6 and 142.8) and five methyl carbons (δ_C 17.4, 17.9, 18.0, 21.9 and 52.2). The remaining carbons were assigned to five methylenes, four methines, and three quaternary carbons, based on the results of an HSQC experiment. These NMR data indicated that seven of the 12 units of

unsaturation come from three carbon-carbon double bonds and four carbonyls. Therefore, the remaining five degrees required **1** to comprise a tetracyclic core. The data from decouplings and the subsequent 2D NMR studies (HMBC and HSQC) suggested that **1** was a mexicanolide-type limonoid.

Analysis of the 2D NMR spectra, especially the HMBC data, confirmed **1** being a mexicanolide-type limonoid and allowed the assignment of most of the function groups. In the HMBC spectrum (Figure 3.3), the key correlations between OMe/C-7, H_2-6/C-7 and H-5/C-6 enabled the methoxy group to be placed at C-7 and a typical C-6–C-7 appendage of a mexicanolide-type limonoid to be linked at C-5. The HMBC correlations from H_3-28, H_3-29, H-5 and H_2 to C-3 supported the location of a ketone group at C-3, and observed correlations from H-2 and H_3-19 to C-1 indicated the presence of an additional ketone group at C-1. The presence of $\Delta^{8,14}$ double bond was indicated by the HMBC correlations from H_2-30 to C-2, C-8, C-9 and C-14, as well as from methylene proton, H_2-15 to C-14 and C-16. Thus, the structure of compound **1** was elucidated as shown and assigned as mexicanolide. This could also be confirmed by comparison of ^{13}C NMR data of **1** with those reported of mexicanolide as shown in Table 3.1 [91].

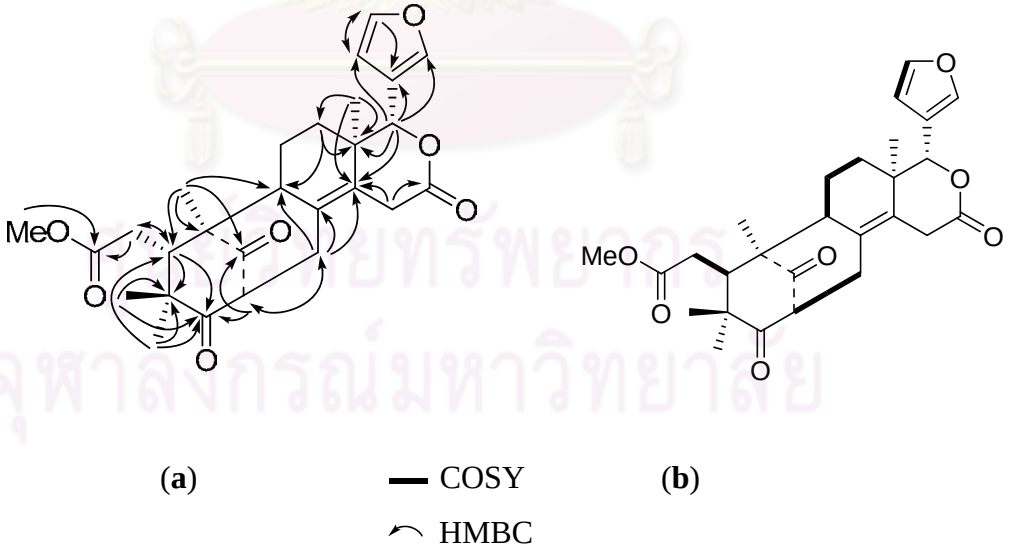

Figure 3.3 Key HMBC (**a**) and COSY (**b**) correlations of compound **1**

Table 3.1 The NMR data of compound **1** and mexicanolide

	Mexicanolide	Compound **1**	
Positions	δ_C	δ_H (mult, *J* in Hz)	δ_C
1	212.7		212.9
2	58.0	3.24 (m, 1H)	58.0
3	210.9		211.0
4	49.4		49.4
5*	50.5	2.75 (m, 1H)	40.2
6	32.3	2.49 (m, 2H)	32.3
7	173.5		173.6
8*	133.8		125.3
9*	40.2	2.10 (m, 1H)	50.5
10	54.3		54.3
11	18.6	1.87 (m, 2H)	18.6
12	28.8	1.86 (m, 1H)	28.8
		1.33 (m, 1H)	
13	37.8		38.0
14*	125.3		133.9
15	32.9	3.53 (d, *J*= 21.2 Hz, 1H)	33.0
		3.48(d, *J*= 21.1 Hz, 1H)	
16	169.7		169.8
17	80.6	5.26 (s, 1H)	80.7
18	17.8	1.00 (s, 3H)	17.4
19	17.8	1.24 (s, 3H)	17.9
20	120.7		120.4
21	142.7	7.57 (s, 1H)	141.6
22	109.8	6.49 (s, 1H)	109.9
23	141.5	7.40 (s, 1H)	142.8
28	21.9	0.99 (s, 3H)	21.9
29	17.4	0.87 (s, 3H)	18.0
30	36.4	3.20 (m, 1H)	36.5
		2.30 (m, 1H)	
3-OH			
7-OMe	52.1	3.72 (s, 3H)	52.2

*****revised data based on HMBC correlations

3.2.2 Structure elucidation of compound 2

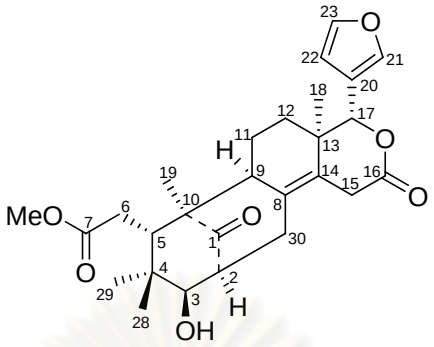

Figure 3.4 Compound **2**

Molecular formula	$C_{27}H_{34}O_7$
Appearance	White amorphous solid
m.p.	238-242 ˚C
$[\alpha]_D^{20}$	-53 (*c* 0.1, MeOH)
UV (MeOH) λ_{max} (log ε)	283 nm (2.39)
IR (KBr)	3456, 3134, 2943, 2878, 1726, 1460, 1378, 1252 and 1169 cm^{-1}
^1H and ^{13}C NMR ($CDCl_3$)	See Table 3.2

Compound **2**, obtained as a white amorphous solid, displayed a molecular formula of $C_{27}H_{34}O_7$. The IR absorptions at 3456 and 1726 cm^{-1} were indicative of the presence of hydroxyl and carbonyl groups, respectively. The NMR data of **2** (Table 3.2) also displayed characteristic signals associated with a mexicanolide limonoid, including a *β*-furanyl ring [δ_H 6.48 s, 7.37 s, 7.55 s; δ_C 110.0 CH, 120.7 qC, 141.7 CH, 142.6 CH], a methoxycarbonyl group [δ_H 3.68 s; δ_C 52.0 CH_3, 174.3 qC], and four tertiary methyls [δ_H 0.71 s, 0.79, s, 1.01 s, 1.11 s; δ_C 20.1, 23.8, 17.5, 16.9]. Moreover, the NMR data of **2** was closely related to those of **1**, with the only difference being the presence of a hydroxyl group at C-3 in **2** instead of the ketone group of **1**. This was confirmed by ^1H-^1H COSY correlation of –CH-3–CH-2–CH_2-30– fragment and HMBC correlations of H-3/C-2, H-3/C-4, H_3-29/C-3 and H-3/C-28 as shown in Figure 3.5. Therefore, the structure of **2** was elucidated as 3*β*-deacetylfissinolide which has been reported by Kadota *et al* in 1990 [92]. Comparison

of ^{13}C NMR data between both compounds (Table 3.2) also clarified that compound **2** is 3β-deacetylfissinolide.

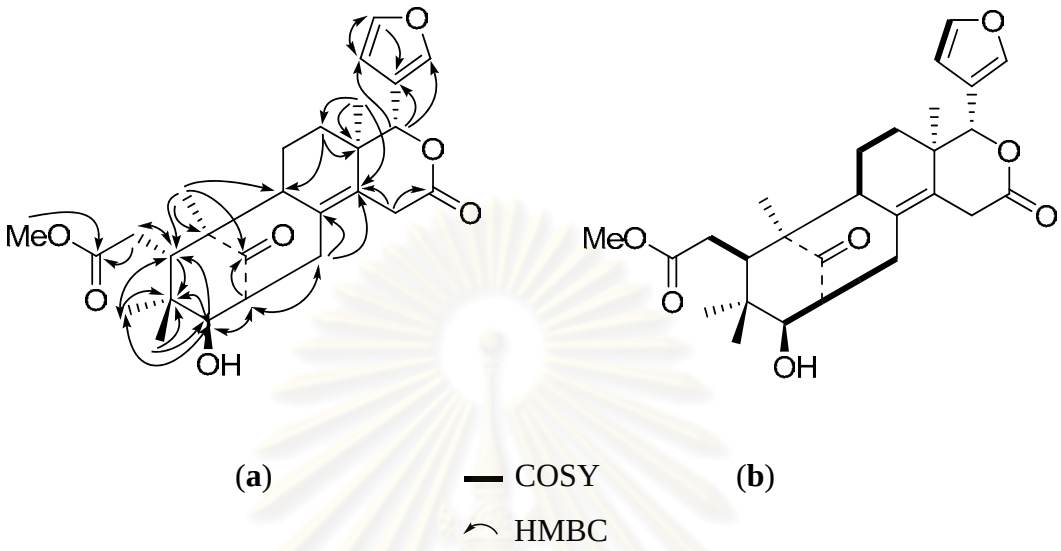

Figure 3.5 Key HMBC (**a**) and COSY (**b**) correlations of compound **2**

Table 3.2 The NMR data of compound **2** and 3β-deacetylfissinolide

	3β-deacetylfissinolide	Compound **2**	
Positions	δ_C	δ_H (mult, *J* in Hz)	δ_C
1	220.0		220.1
2	50.1	3.04 (m, 1H)	50.1
3	77.2	5.00 (s, 1H)	77.1
4	39.3		39.3
5	39.3	3.23 (dd, *J*= 2.8, 10.4 Hz,1H)	39.2
6	33.5	2.35 (m, 2H)	33.5
7	174.3		174.3
8	128.2		128.2
9	51.7	1.96 (m, 1H)	51.7
10	53.6		53.6
11	18.7	1.76 (m, 2H)	18.7
12	28.5	1.78 (m, 1H)	28.5
		1.01 (m, 1H)	
13	37.8		37.8
14	131.2		131.1
15	33.0	4.07 (d, *J*= 21.2 Hz, 1H)	33.0
		3.46 (d, *J*= 21.2 Hz, 1H)	
16	171.7		171.7
17	80.2	5.58 (s, 1H)	80.2
18	17.5	1.01 (s, 3H)	17.5
19	16.9	1.11 (s, 3H)	16.9
20	120.7		120.7
21	141.7	7.55 (s, 1H)	141.7
22	110.0	6.48 (s, 1H)	110.0
23	142.6	7.37 (s, 1H)	142.6
28	20.1	0.71 (s, 3H)	20.1
29	23.9	0.79 (s, 3H)	23.8
30	33.3	1.96 (m, 2H)	33.3
3-OH			
7-OMe	53.4	3.68 (s, 3H)	52.0

3.2.3 Structure elucidation of compound 3

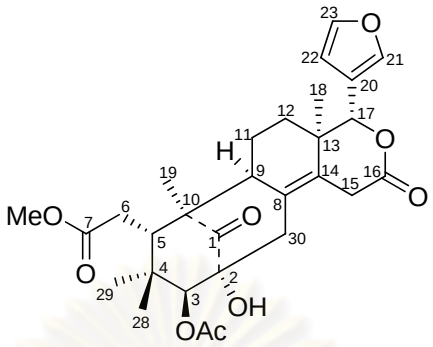

Figure 3.6 Compound **3**

Molecular formula	$C_{29}H_{36}O_9$
Appearance	White amorphous solid
m.p.	196-198 $^{\circ}$C
$[\alpha]_D^{20}$	-74 (*c* 0.1, MeOH)
UV (MeOH) λ_{max} (logε)	296 nm (2.02)
IR (KBr)	3469, 3134, 2956, 1734, 1443, 1373, 1226, 1056 and 1021 cm^{-1}
^{1}H and ^{13}C NMR ($CDCl_3$)	See Table 3.3

Compound **3**, a white, amorphous solid, showed a molecular formula $C_{29}H_{36}O_9$. An analysis of the NMR data of **3** (Table 3.3) revealed its structure to be closely related to that of **2**. The obvious difference was the appearance of the acetoxy signals (δ_H 2.14, 3H, s; δ_C 169.5 qC, 21.0 CH_3) and an additional oxygenated quaternary carbon at δ_C 77.9. Observed HMBC correlation between H-3 at δ_H 5.00 and carbonyl carbon of acetyl group at δ_C 169.5 gave evidence of acetoxy group being attached at C-3, whereas oxygenated quaternary carbon at δ_C 77.9, showing HMBC cross-peaks with H-3 and H-30, was assigned to be C-2 (Figure 3.7). Compound **3** was thus determined as 2-hydroxyfissinolide [91]. Also, it was confirmed by comparing the NMR data of **3** with those reported of 2-hydroxyfissinolide as shown in Table 3.3.

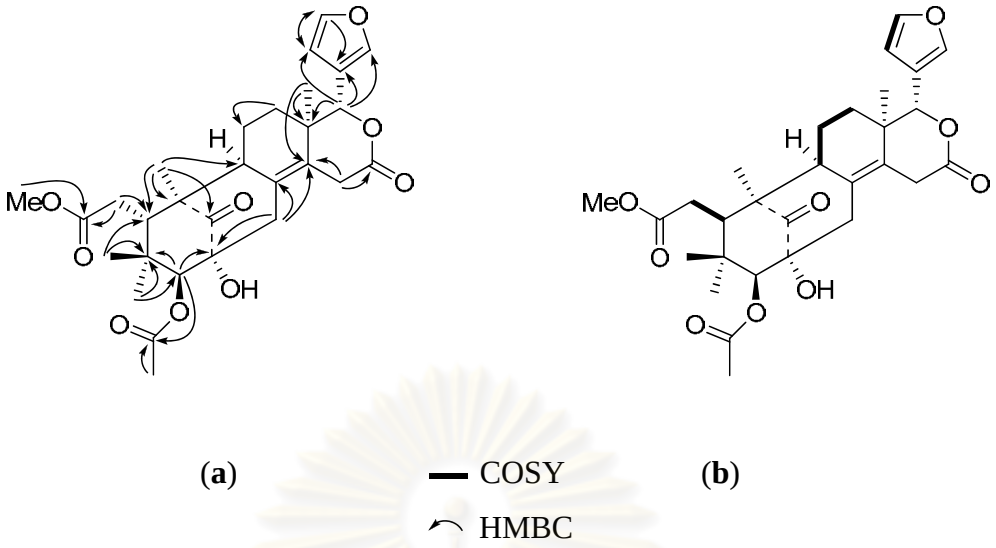

Figure 3.7 Key HMBC (**a**) and COSY (**b**) correlations of compound **3**

Table 3.3 The NMR data of compound **3** and 2-hydroxyfissinolide

	2-hydroxyfissinolide	Compound **3**	
Positions	δ_C	δ_H (mult, *J* in Hz)	δ_C
1	217.4		217.9
2	78.0		77.9
3	85.7	5.00 (s, 1H)	85.4
4	39.0		38.7
5*	52.2	3.05 (m, 1H)	40.6
6	33.3	2.31 (m, 1H)	33.0
		2.30 (m, 1H)	
7	174.0		173.9
8*	133.0		125.6
9*	40.9	1.97 (m, 1H)	51.9
10	52.2		51.8
11	18.8	1.95 (m, 1H)	18.5
		1.73 (m, 1H)	
12	29.2	1.71 (m, 1H)	28.9
		1.07 (m, 1H)	
13	38.3		38.0
14*	125.7		132.8
15	33.5	3.79 (d, *J*= 20.8 Hz, 1H)	33.2
		3.43 (d, *J*= 19.6 Hz, 1H)	
16	169.9		169.8
17	80.6	5.61 (s, 1H)	80.4
18	18.1	1.01 (s, 3H)	17.7
19	16.8	1.18 (s, 3H)	16.6
20	120.5		120.4
21	141.8	7.49 (s, 1H)	141.5
22	109.8	6.40 (s, 1H)	109.7
23	141.8	7.43 (s, 1H)	142.7
28	22.7	0.63 (s, 3H)	22.5
29	19.9	0.70 (s, 3H)	19.6
30	44.2	3.18 (d, *J*= 14.4 Hz, 1H)	43.9
		1.71 (m, 1H)	
3-OAc	169.6		169.5
	21.2	2.14 (s, 3H)	21.0
2-OH			
7-OMe	52.2	3.65 (s, 3H)	52.0

*****revised data based on HMBC correlations

3.2.4 Structure elucidation of compound 4

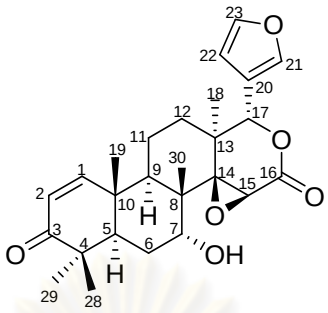

Figure 3.8 Compound **4**

Molecular formula	$C_{26}H_{32}O_6$
Appearance	Colorless prisms
m.p.	246-247 °C
$[\alpha]_D^{20}$	+72 (*c* 0.1, MeOH)
UV (MeOH) λ_{max} (log ε)	341 nm (1.89)
IR (KBr)	3530, 3486, 3121, 2956, 2865, 1734, 1656, 1465, 1391, 1260, 1169, 1021 and 921 cm^{-1}
^1H and ^{13}C NMR ($CDCl_3$)	See Table 3.4

Compoud **4** was isolated as colorless prisms. Its molecular formula was determined to be $C_{26}H_{32}O_6$. Its NMR data (Table 3.4) generally resembled those of gedunin [91], suggesting that **4** has a gedunin-type limonoid skeleton. The ^1H NMR spectrum of **4** showed the presence of five tertiary methyl groups (δ_H 1.00, 1.09, 1.14, 1.19 and 1.23), three oxymethine protons (δ_H 3.57, 3.90 and 5.60), and a β-substituted furan ring (δ_H 6.35, 7.40 and 7.41, 1H each). The ^{13}C NMR and HSQC data indicated the presence of five methyls, three methylenes, ten methines, and eight quaternary carbons, of which two at δ_C 168.3 and 204.6 were assigned to an ester and a ketone carbonyl carbon, respectively. An oxygenated methine carbon at δ_C 70.0 was assigned to as C-7 due to its HMBC correlations with H-6, H_3-30 and H-5. The ^{13}C NMR signals of C-1 (δ_C 157.8), C-2 (δ_C 125.7), and C-3 (δ_C 204.6) and the ^1H NMR signals of a pair of AB doublet at δ_H 5.84 and 7.10 (J = 10.5 Hz) suggested that the A-

ring of **4** possesses a 1-en-3-one system. The cross-peaks between H-15/C-14, H-15/C-16, H-17/C-13 and H-17/C-14 in the HMBC spectrum suggested the presence of a δ-lactone group with a 14,15-epoxide in the D-ring. From the above observations, compound **4** was determined to be 7-deacetylgedunin [93]. The structure and relative configuration of **4** were also confirmed by single-crystal X-ray crystallographic analysis as shown in Figure 3.10 and its crystal data are described in Table 3.5. Moreover, this is the first report for the complete assignment of NMR data and the crystal and molecular structure of 7-deacetylgedunin.

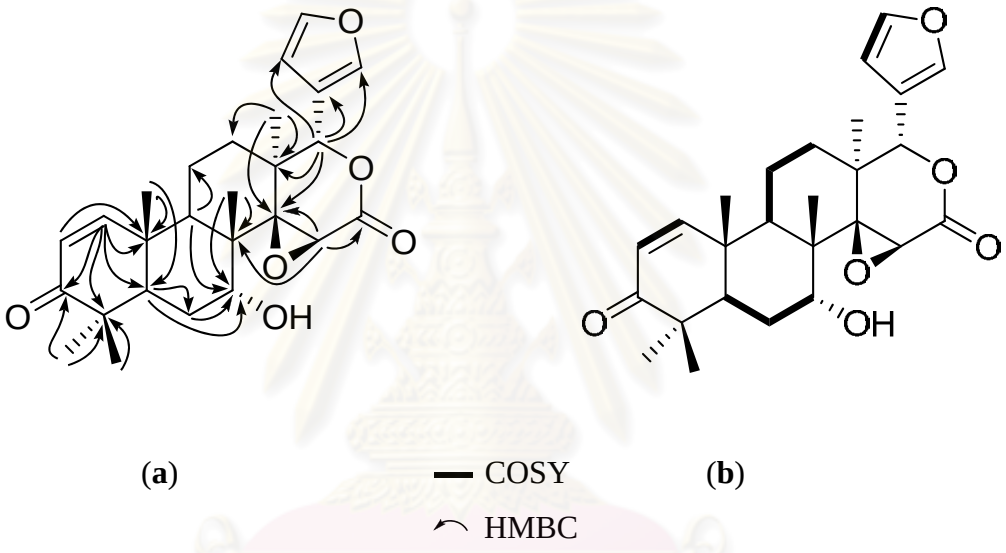

Figure 3.9 Key HMBC (**a**) and COSY (**b**) correlations of compound **4**

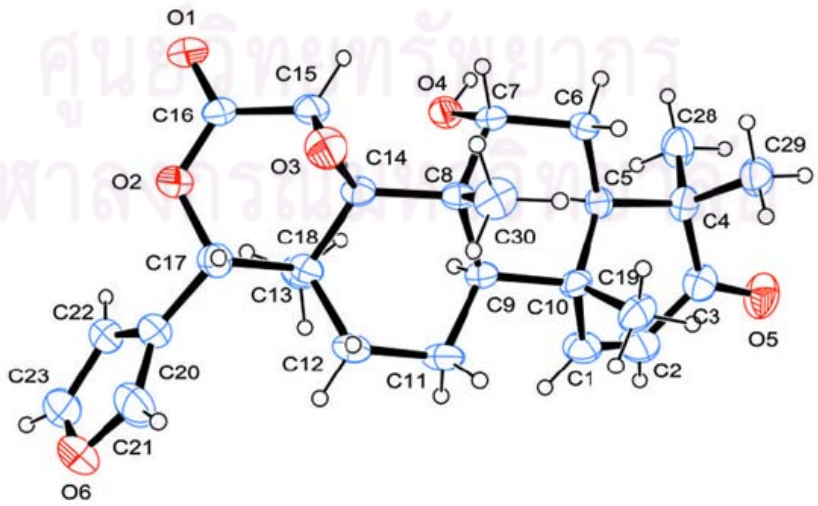

Figure 3.10 ORTEP diagram of compound **4**

Table 3.4 The NMR data of compound **4** and 7-deacetylgedunin

	7-deacetylgedunin	Compound **4**	
Positions	δ_H (mult, *J* in Hz)	δ_H (mult, *J* in Hz)	δ_C
1	7.11 (d, *J*= 10.2 Hz, 1H)	7.10 (d, *J*= 10.4 Hz, 1H)	157.8
2	5.85 (d, *J*= 10.2 Hz, 1H)	5.84 (d, *J*= 10.4 Hz, 1H)	125.7
3			204.6
4			44.2
5	2.49 (dd, *J*= 13.4, 2.4 Hz, 1H)	2.49 (m, 1H)	44.6
6	1.92 (m, 1H)	1.89 (m, 1H)	27.3
	1.83 (m, 1H)	1.69 (m, 1H)	
7	3.58 (s, 1H)	3.57 (s, 1H)	69.7
8			43.7
9	2.58 (m, 1H)	2.52 (m, 1H)	38.0
10			40.7
11	2.00 (m, 1H)	1.95 (m, 1H)	15.0
	1.81 (m, 1H)	1.80 (m, 1H)	
12	1.70 (m, 1H)	1.71 (m, 1H)	26.4
	1.57 (m, 1H)	1.54 (m, 1H)	
13			38.3
14			70.0
15	3.91 (s, 1H)	3.90 (s, 1H)	57.8
16			168.3
17	5.60 (s, 1H)	5.60 (s, 1H)	78.5
18	1.24 (s, 3H)	1.23 (s, 3H)	17.8
19	1.20 (s, 3H)	1.19 (s, 3H)	19.9
20			120.6
21	7.41 (m, 1H)	7.41 (s, 1H)	141.2
22	6.35 (m, 1H)	6.35 (s, 1H)	110.0
23	7.41 (m, 1H)	7.40 (s, 1H)	143.0
28	1.09 (s, 3H)	1.14 (s, 3H)	27.2
29	1.10 (s, 3H)	1.09 (s, 3H)	21.5
30	1.15 (s, 3H)	1.00 (s, 3H)	18.7

Table 3.5 Crystal data and structure refinement for compound **4**

Formula	$C_{26}H_{32}O_6$
Molecular weight	440.52
Crystal size (mm)	0.48× 0.40 × 0.20
Crystal system	Orthorhombic
Space group	$P2_12_12_1$
***a* (Å)**	12.2642 (4)
***b* (Å)**	12.8445 (5)
***c* (Å)**	43.5584 (15)
***V* (Å^3)**	6917.6 (4)
Z	12
D_{calc} (g/cm^{-3})	1.269
μ (mm^{-1})	0.09
***F*(000)**	2832
Independent reflections/ Observed reflections [I> 4б(I)], R_{int}	9382/ 6530, 0.059
R_1	0.068
wR_2 [I> 2б(I)]	0.212

3.2.5 Structure elucidation of compound 5

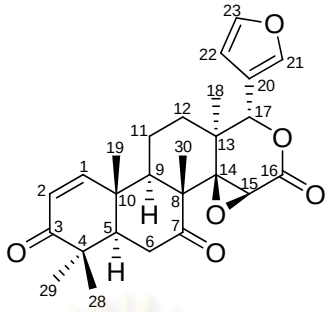

Figure 3.11 Compound **5**

Molecular formula	$C_{26}H_{30}O_6$
Appearance	Colorless prisms
m.p.	251-253 °C
$[\alpha]_D^{20}$	-47 (*c* 0.1, MeOH)
UV (MeOH) λ_{max} (log ε)	296 nm (1.73)
IR (KBr)	3452, 3121, 2966, 1739, 1708, 1665, 1456, 1391, 1347, 1286, 1165, 1065 and 1034 cm^{-1}
^1H and ^{13}C NMR ($CDCl_3$)	See Table 3.6

Compound **5** was isolated as colorless prisms. Its molecular formula was determined to be $C_{26}H_{30}O_6$. It was revealed that the ^1H and ^{13}C NMR data (Table 3.6) of **5** were virtually identical to those of **4**, implying that both compounds are of the same basic structure. The absence of an oxygenated methine carbon, along with the appearance of the ketone resonance at δ_C 208.1, suggested that methine carbon has been replaced by a ketone group at C-7. This was confirmed by HMBC correlations from H-5, H-9, H_2-6 and H_3-30 to this carbonyl carbon as shown in Figure 3.12. Thus, compound **5** was determined as 7-oxo-deactoxygedunin [91].

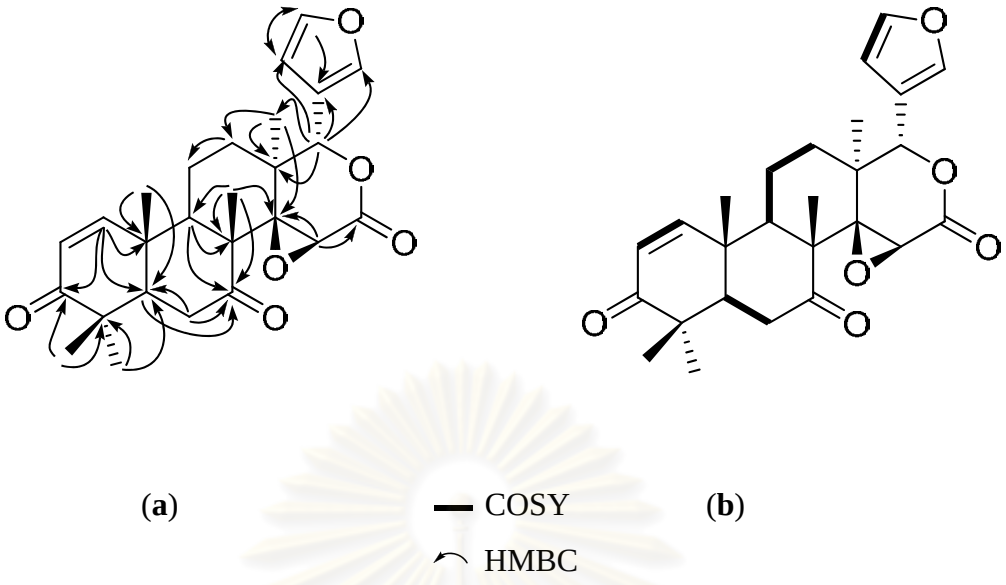

Figure 3.12 Key HMBC (**a**) and COSY (**b**) correlations of compound **5**

Table 3.6 The NMR data of compound **5** and 7-oxo-7-deacetoxygedunin

	7-oxo-7-deacetoxygedunin	Compound **5**	
Positions	δ_C	δ_H (mult, *J* in Hz)	δ_C
1	156.0	7.09 (d, *J*= 10.4 Hz, 1H)	155.9
2	126.3	5.93 (d, *J*= 10.4 Hz, 1H)	126.4
3	203.2		203.1
4	45.2		45.2
5	47.6	2. 19 (t, 1H)	47.6
6	36.7	2.93 (t, 1H)	36.7
		2.40 (dd, *J*= 2.4, 13.6 Hz, 1H)	
7	208.3		208.1
8	53.4		53.4
9	53.7	2.19 (t, 1H)	54.5
10	40.0		39.5
11	17.1	2.00 (m, 1H)	17.1
		1.79 (m, 1H)	
12	32.1	1.85 (m, 1H)	32.1
		1.46 (m, 1H)	
13	37.7		37.7
14	65.7		65.6
15	54.5	3.87 (s, 1H)	53.6
16	166.9		166.8
17	78.0	5.46 (s, 1H)	77.9
18	20.7	1.13 (s, 3H)	20.6
19	19.7	1.35 (s, 3H)	19.8
20	120.3		120.4
21	143.1	7.41 (s, 1H)	141.0
22	109.8	6.35 (s, 1H)	109.8
23	141.0	7.38 (s, 1H)	143.1
28	20.9	1.14 (s, 3H)	20.9
29	27.0	1.15 (s, 3H)	26.9
30	17.4	1.21 (s, 3H)	17.4

3.2.6 Structure elucidation of compound 6

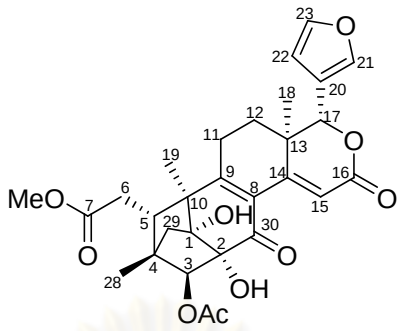

Figure 3.13 Compound **6**

Molecular formula	$C_{29}H_{32}O_{10}$
Appearance	Colorless gum
$[\alpha]_D^{20}$	+140 (*c* 0.1, MeOH)
UV (MeOH) λ_{max} (logε)	265 nm (4.16)
IR (KBr)	3434, 2952, 1730, 1600, 1469, 1382, 1260, 1226 and 1165 cm^{-1}
^1H and ^{13}C NMR ($CDCl_3$)	See Table 3.7

Compound **6** was isolated as a colorless gum, with molecular formula $C_{29}H_{32}O_{10}$, indicating 14 degrees of unsaturation. The IR absorptions at 3434, 1730, and 1600 cm^{-1} implied hydroxy and ester groups. The ^1H NMR spectrum (Table 3.7) displayed resonances of a *β*-substituted furanyl ring (δ_H 6.47, 7.44, and 7.50), an olefinic proton (δ_H 7.02), three tertiary methyl (δ_H 0.98, 1.01 and 1.24), an *O*-methyl (δ_H 3.71), and an *O*-acetyl (δ_H 1.97) group. In the ^{13}C NMR spectrum, 29 nonequivalent carbon resonances were observed, including four carbonyl carbons (δ_C 165.2, 169.4, 173.8 and 194.6), eight olefinic carbons (δ_C 109.8, 115.3, 119.9, 121.8, 141.1, 143.0, 152.2 and 169.4), and five methyl carbons (δ_C 15.8, 16.1, 16.6, 20.5, 52.2). The remaining carbons were assigned to four methylenes, three methines, and five quaternary carbons, based on the results of an HSQC experiment. These NMR data indicated that eight of the 14 units of unsaturation come from four carbon-carbon double bonds and four carbonyls. Therefore, the remaining six degrees required **6** to

comprise a hexacyclic core. The data from decouplings and the subsequent 2D NMR studies (HMBC and HSQC) suggested that **6** was a phragmalin limonoid. Two protons at δ_H 1.95 and 1.88 correlating in the HSQC spectrum to a methylene signal at δ_C 41.8 were indicative of the H-29 protons of the characteristic 4,29,1-ring bridge of phragmalin limonoids. This was confirmed by the HMBC correlations (Figure 3.14a) observed from the H-29 protons to the tertiary carbon at δ_C 43.5 (C-5) and to the quaternary carbons at δ_C 86.5 (C-1), 45.1 (C-4), and 48.3 (C-10). The HMBC correlations between C-7 (δ_C 173.8) and H_2-6 (δ_H 2.44 and 2.53) and the *O*-methyl protons at δ_H 3.71 also confirmed the typical C-6-C-7 appendage of phragmalins. A proton singlet at δ_H 5.04 was assignable to H-17 by correlations with the furanyl carbon at δ_C 119.9 (C-20) and the C-18 methyl carbon at δ_C 15.8. A δ-lactone ring was corroborated by the HMBC cross-peaks from H-17 to both bridgehead carbons, C-13 (δ_C 36.4) and C-14 (δ_C 152.2), and the carbonyl carbon at δ_C 165.2. The vinylic proton at δ_H 7.02 assigned to H-15 also exhibited significant HMBC correlation to C-13 and C-14 and the lactone carbonyl carbon (δ_C 165.2). Further, this α,β-unsaturated δ-lactone was conjugated to the $\Delta^{8,9}$ double bond to form a conjugated diene lactone system, which was confirmed by the HMBC correlation of H-15/C-8 and Me-19/C-9. The $\Delta^{8,9}$ double bond was also conjugated to the C-30 ketone carbonyl carbon, responsible for the high field carbon signal at δ_C 194.6. The above analyses, and other 1D and 2D NMR information, led us to suggest the gross structure of **6** (Figure 3.13) with a characteristic diene lactone-conjugated ketone moiety at C-30.

The relative configuration of **6** was elucidated by NOESY data (Figure 3.14c). Limonoids are stereochemically homogeneous compounds since they have a prototypical structure that either contains or is derived from a precursor with a 4,4,8-trimethyl-17-furanylsteroid skeleton. The orientation of H-17 had been found to be exclusively β in all known phragmalins. Thus, the cross-peaks in the NOESY spectrum from H-17 and H-5 to H-12β and from H-5 to Me-28 indicated a β-orientation of these protons. NOESY correlations of Me-18 with H-12α, 1-OH with Me-19, and H-3 with H-29 and 2-OH all suggested that Me-18, Me-19, H-3, H_2-29, 1-OH, and 2-OH were α-oriented. Thus, compound **6** was assigned as moluccensin H. [88]

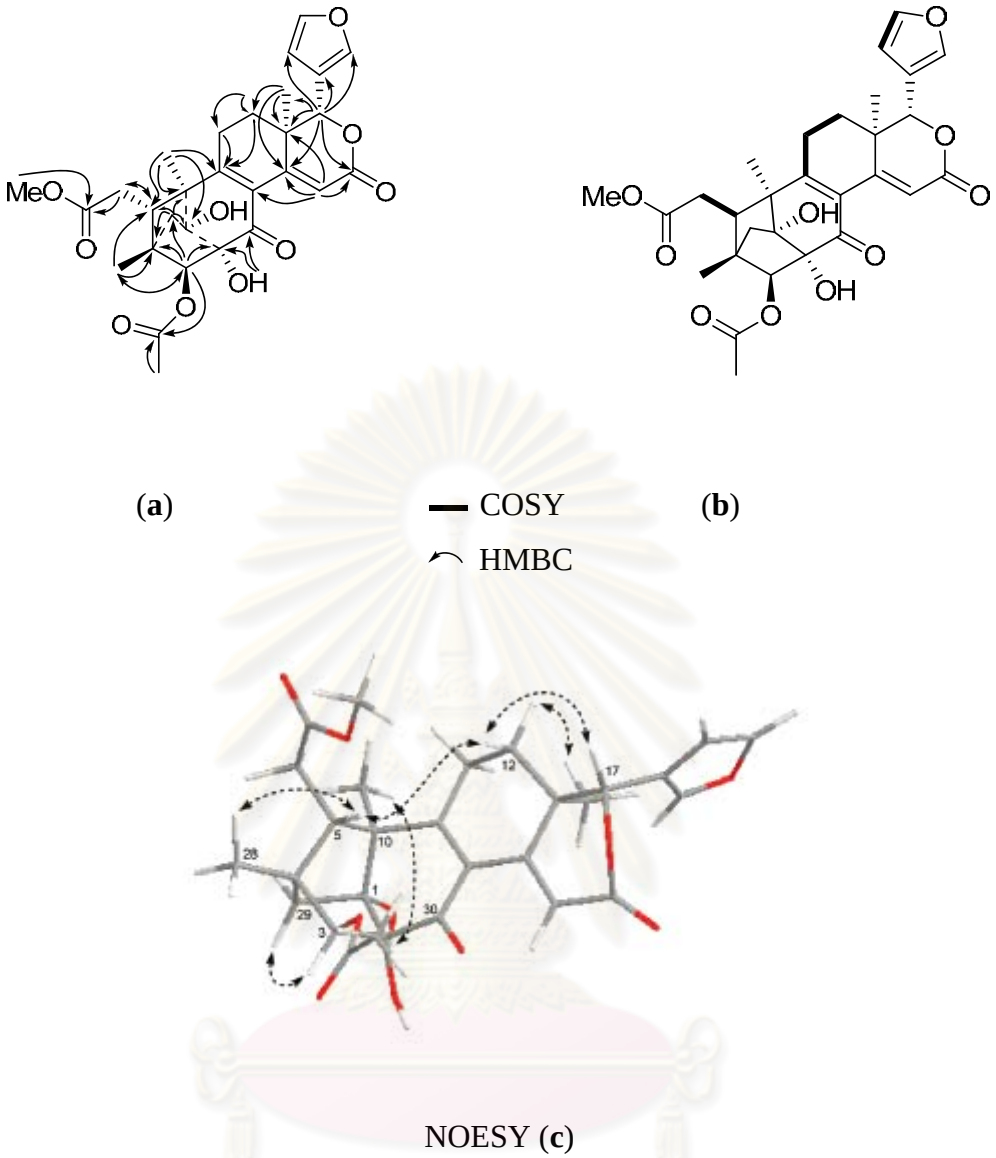

Figure 3.14 Key HMBC (**a**), COSY (**b**) and NOESY (**c**) correlations of compound **6**

Table 3.7 The NMR data of compound **6** and moluccensin H

Positions	Moluccesin H		Compound **6**	
	δ_H (mult, *J* in Hz)	δ_C	δ_H (mult, *J* in Hz)	δ_C
1		86.6		86.5
2		80.6		80.6
3	4.90 (s, 1H)	87.6	4.92 (s, 1H)	86.8
4		45.1		45.1
5	2.79 (m, 1H)	43.5	2.81 (m, 1H)	43.5
6	2.40 (m, 1H)	33.1	2.44 (m, 1H)	33.0
	2.52 (dd, *J*= 5.6, 17.2 Hz, 1H)		2.53 (dd, *J*= 5.6, 16.8 Hz, 1H)	
7		173.4		173.8
8		121.8		121.8
9		168.9		169.4
10		48.4		48.3
11	2.43 (m, 2H)	25.2	2.44 (m, 2H)	25.3
12	1.49 (m, 1H)	30.5	1.49 (m, 1H)	30.5
	1.67 (m, 1H)		1.69 (m, 1H)	
13		36.4		36.4
14		152.3		152.2
15	7.00 (s, 1H)	115.2	7.02 (s, 1H)	115.3
16		165.5		165.2
17	5.02 (s, 1H)	80.4	5.04 (s, 1H)	80.4
18	0.99 (s, 3H)	15.7	1.01 (s, 3H)	15.8
19	1.22 (s, 3H)	16.1	1.24 (s, 3H)	16.1
20		119.9		119.9
21	7.49 (s, 1H)	141.3	7.50 (s, 1H)	141.1
22	6.45 (s, 1H)	110.0	6.47 (s, 1H)	109.8
23	7.44 (s, 1H)	143.1	7.44 (s, 1H)	143.0
28	0.97 (s, 3H)	16.7	0.98 (s, 3H)	16.6
29	1.94 (d, *J*= 11.2 Hz, 1H)	41.7	1.95 (d, *J*= 10.8 Hz, 1H)	41.8
	1.87 (dd, *J*= 2.0, 11.2 Hz, 1H)		1.88 (dd, *J*= 2.0, 11.2 Hz, 1H)	
30		194.6		194.6
3-OAc		169.5		169.4
	1.96 (s, 3H)	20.6	1.97 (s, 3H)	20.5
1-OH	2.88 (s, 1H)		2.14 (s, 1H)	
2-OH	4.95 (s, 1H)		4.95 (s, 1H)	
7-OMe	3.70 (s, 3H)	52.2	3.71 (s, 3H)	52.2

3.2.7 Structure elucidation of compound 7

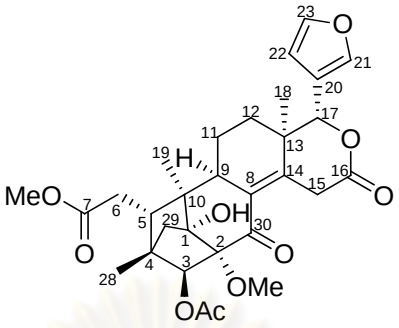

Figure 3.15 Compound **7**

Molecular formula	$C_{30}H_{36}O_{10}$
Appearance	Light yellow gum
$[\alpha]_D^{20}$	-12.0 (*c* 0.1, MeOH)
UV (MeOH) λ_{max} (logε)	215 nm (4.12)
IR (KBr)	3478, 3143, 2939, 1743, 1504, 1456, 1373, 1282, 1230, 1160, 1113 and 1026 cm^{-1}
^1H and ^{13}C NMR ($CDCl_3$)	See Table 3.8

Compound **7** was isolated as a light yellow gum with molecular formula $C_{30}H_{36}O_{10}$, implying 13 degrees of unsaturations. The ^1H and ^{13}C NMR (Table 3.8), as well as the 2D NMR data, suggested that **7** is also a 30-ketophragmalin limonoid with the same basic skeleton as **6**. The obvious difference was the absence of the olefinic proton at C-15 in **6** and the presence of only one double bond between C-8 and C-14, confirmed by the HMBC correlations of Me-18/C-14, H_2-15/C-8, and H_2-11/C-8 (Figure 3.16a). Without the extended conjugative effect as in **6**, the ketone carbonyl at C-30 of **7** was significantly shifted downfield to δ_C 203.4. Furthermore, analysis of NMR data revealed the presence of a methoxy group (δ_H 3.43 and δ_C 55.2) at C-2 in place of the hydroxy group of **6**, which was confirmed by HMBC cross-peak from the methoxy protons to C-2. The similar NOESY correlations between **7** (Figure 3.16c) and **6** indicated the same stereochemistry for the core skeleton of **7**. Compound

7 was thus determined to be moluccensin I, which has been reported by our group in 2010 (Pudhom *et al*., 2010)[88].

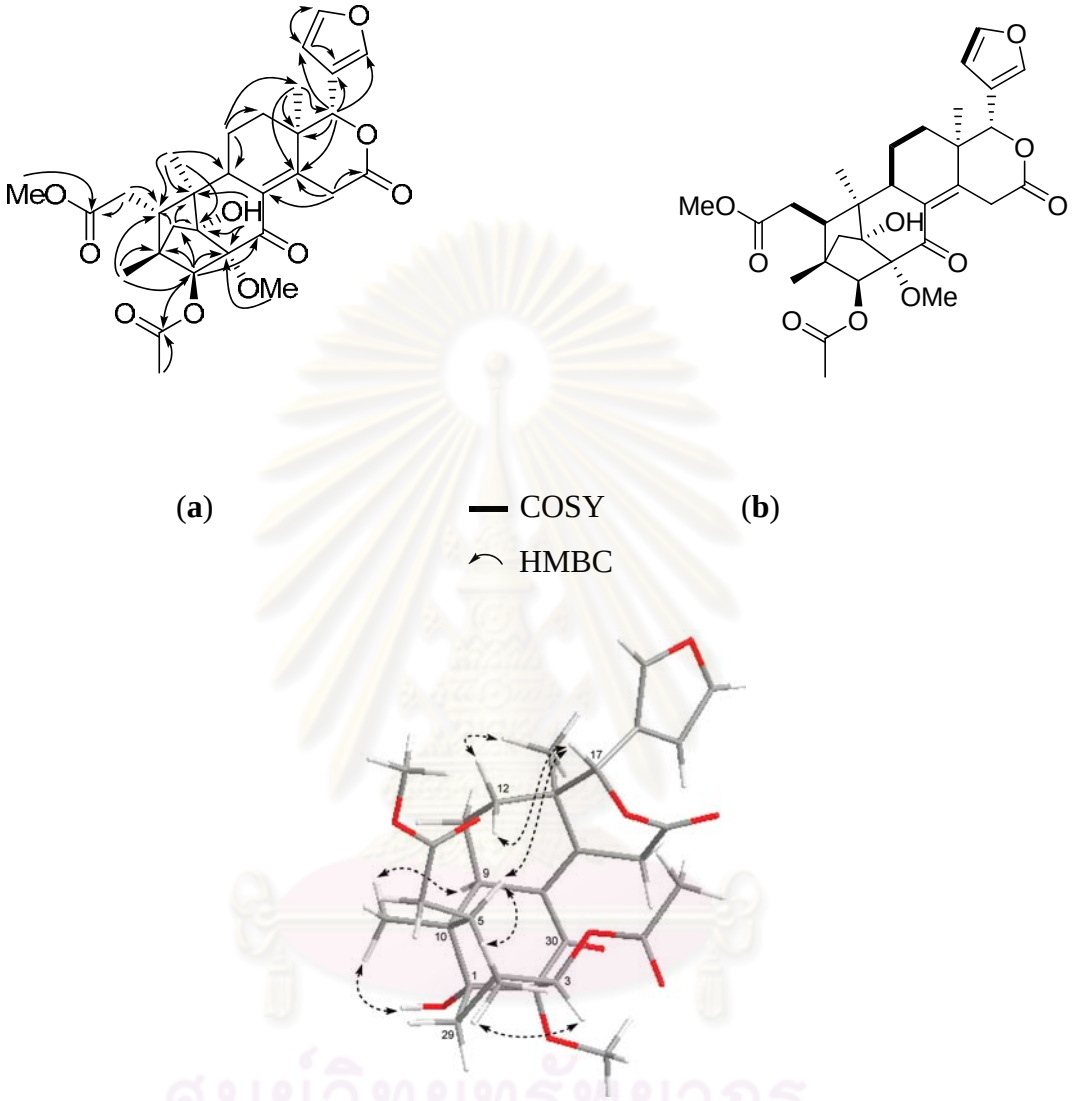

Figure 3.16 Key HMBC (**a**), COSY (**b**) and NOESY (**c**) correlations of compound **7**

Table 3.8. The NMR data of compound **7** and moluccensin I

	Moluccesin I		Compound **7**	
Positions	δ_H (mult, *J* in Hz)	δ_C	δ_H (mult, *J* in Hz)	δ_C
1		84.7		84.7
2		92.2		92.2
3	4.92 (s, 1H)	82.8	4.94 (s, 1H)	82.8
4		40.1		40.2
5	2.37 (d, *J*= 10.0 Hz, 1H)	39.6	2.39 (d, *J*= 8.4 Hz, 1H)	39.6
6	2.25 (d, *J*= 12.0 Hz, 1H)	34.2	2.29 (d, *J*= 14.8 Hz, 1H)	34.3
	2.43 (m, 1H)		2.45 (m, 1H)	
7		172.9		172.9
8		133.9		133.9
9	2.46 (m, 1H)	46.9	2.47 (m, 1H)	46.9
10		55.4		55.4
11	1.43 (m, 1H)	18.7	1.44 (m, 2H)	18.8
	1.74 (m, 1H)			
12	1.41 (m, 1H)	31.4	1.41(m, 1H)	31.5
	1.49 (m, 1H)		1.53 (m, 1H)	
13		40.8		40.8
14		139.2		139.3
15	3.75 (m, 2H)	33.0	3.77 (m, 2H)	33.0
16		169.9		169.8
17	5.17 (s, 1H)	80.2	5.19 (s, 1H)	80.2
18	1.00 (s, 3H)	17.1	1.02 (s, 3H)	17.1
19	1.03 (s, 3H)	15.1	1.05 (s, 3H)	15.1
20		120.4		120.5
21	7.45 (s, 1H)	141.2	7.46 (s, 1H)	141.2
22	6.40 (s, 1H)	110.0	6.42 (s, 1H)	110.1
23	7.40 (s, 1H)	143.0	7.41 (s, 1H)	142.9
28	0.96 (s, 3H)	19.7	0.98 (s, 3H)	19.7
29	1.72 (m, 1H)	43.7	1.75 (m, 1H)	43.8
	2.20 (d, *J*= 13.2 Hz, 1H)		2.22 (d, *J*= 13.2 Hz, 1H)	
30		203.5		203.4
1′		170.1		170.1
2′	2.15 (s, 3H)	20.5	2.17 (s, 3H)	20.6
1-OH	2.93 (brs,1H)		2.90 (brs, 1H)	
2-OMe	3.40 (s, 3H)	55.1	3.43 (s, 3H)	55.2
7-OMe	3.65 (s, 3H)	51.8	3.66 (s, 3H)	51.7

3.2.8 Structure elucidation of compound 8

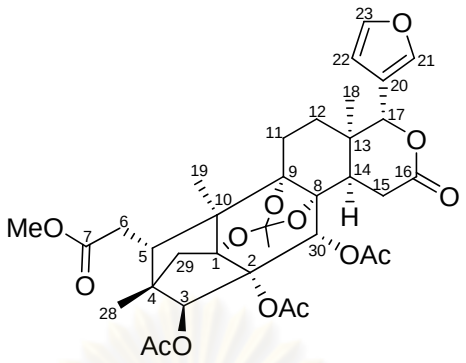

Figure 3.17 Compound **8**

Molecular formula	$C_{35}H_{42}O_{14}$
Appearance	Colorless crystals
m.p.	141.5-143.5 ° C
$[\alpha]_D^{20}$	-50.0 (*c* 0.1, $CHCl_3$)
UV ($CHCl_3$) λ_{max} (logε)	239 nm (2.70)
IR (KBr)	3447, 3139, 2966, 1739, 1634, 1452, 1369, 1239 and 1086 cm^{-1}
^1H and ^{13}C NMR ($CDCl_3$)	See Table 3.9

Compound **8**, colorless crystals, had molecular formula $C_{35}H_{42}O_{14}$. The ^1H,^{13}C and 2D NMR data (Table 3.9) of **8** indicated the presence of the following function groups; a carbomethoxy (δ_H 3.69 s, δ_C 52.1 CH_3, 172.1 qC), three oxygenated methines (δ_H 5.11 s, 6.31 s, 5.54 s; δ_C 81.1 CH, 69.3 CH, 78.6 CH), an orthoacetate (δ_H 1.67 s; δ_C 21.0 CH_3, 119.0 qC), two sp^3 methines (δ_H 2.98 (d, *J*= 9.6 Hz), 2.06 m; δ_C 35.5, 43.2), ten sp^3 methylenes (δ_H 2.47 m, 2.24 m, 2.06 m, 1.67 m, 1.54 m, 1.30 m, 3.29 m (d, *J*= 20.4 Hz), 2.70 m, 1.97 m, 1.67 m; δ_C 33.3, 25.4, 29.1, 26.5, 40.2), three methyls (δ_H 1.07 s, 1.14 s, 0.89 s; 19.6, 16.5, 14.6), three acetyls (δ_H 1.95 s, 2.15 s, 2.25 s; δ_C 21.5 CH_3, 168.5 qC; 21.7 CH_3, 170.3 qC; 21.3 CH_3, 170.0 qC). The NMR data of **8** were characteristic of a phragmalin type limonoid. The quaternary carbon at δ_C 119.0 (C-31) showing a strong HMBC correlation (Figure 3.18a) to H-32 suggested the presence of an orthoacetate group. In addition, the nature of oxygenated

carbons assigned for C-1 (δ_C 86.8), C-8 (δ_C 85.9) and C-9 (δ_C 85.3) was comparable to xyloccensin E. This suggested the position of the orthoacetate at C-1, C-8 and C-9. Three acetoxy groups were assigned to locate at C-2, C-3 and C-30 according to HMBC correlations of H-3 and H-30 to both acetyl carbonyls and its molecular formula. [94]

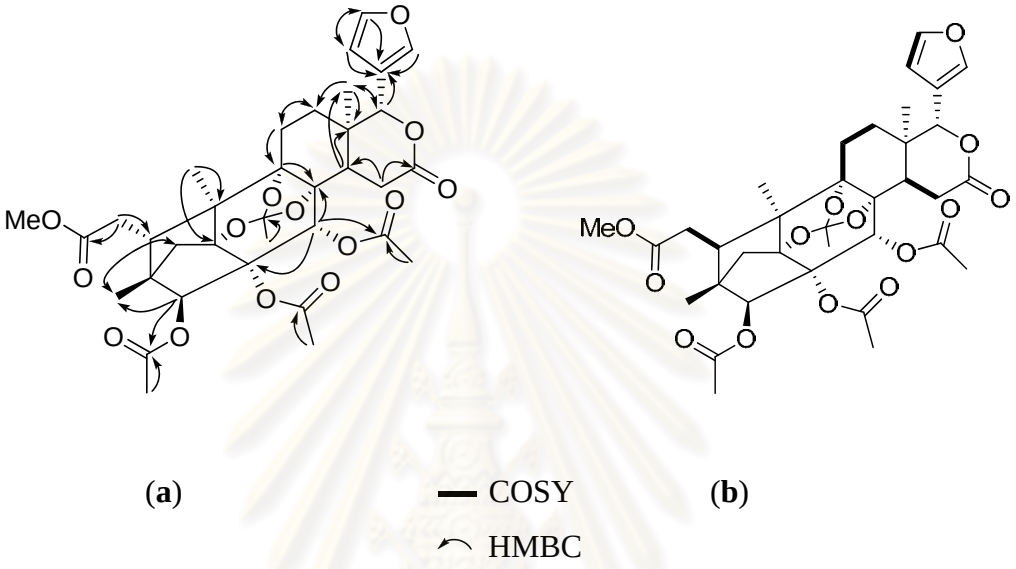

Figure 3.18 Key HMBC and COSY correlations of compound **8**

Table 3.9 The NMR data of compound **8** and Xyloccensin

	Xyloccensin E		Compound **8**	
Positions	δ_H (mult, *J* in Hz)	δ_C	δ_H (mult, *J* in Hz)	δ_C
1		86.8		86.8
2		85.2		85.2
3	5.10 (s, 1H)	81.1	5.11 (s, 1H)	81.1
4		46.2		46.2
5	2.96 (d, *J*= 8.5 Hz, 1H)	35.5	2.98 (d, *J*= 9.6 Hz, 1H)	35.5
6	2.47 (m, 1H)	33.3	2.47 (m, 1H)	33.3
	2.24 (m, 1H)		2.24 (m, 1H)	
7		172.7		172.6
8		85.9		85.9
9		85.3		85.3
10		45.7		45.7
11	2.07 (m, 1H)	25.4	2.06 (m, 1H)	25.4
	1.66 (m, 1H)		1.67 (m, 1H)	
12	1.54 (m, 1H	29.1	1.54 (m, 1H)	29.1
	1.30 (m, 1H)		1.30 (m, 1H)	
13		34.3		34.4
14	2.06 (m, 1H)	43.1	2.06 (m, 1H)	43.2
15	3.28 (d, *J*= 20.3 Hz, 1H)	26.5	3.29 (d, *J*= 20.4 Hz, 1H)	26.5
	2.70 (m, 1H)		2.70 (m, 1H)	
16		170.4		170.4
17	5.54 (s, 1H)	78.6	5.54 (s, 1H)	78.6
18	1.06 (s, 3H)	19.9	1.07 (s, 1H)	19.6
19	1.14 (s, 3H)	16.5	1.14 (s, 1H)	16.5
20		121.1		121.1
21	7.51 (s, 1H)	140.8	7.52 (s, 1H)	140.7
22	6.44 (s, 3H)	109.7	6.45 (s, 1H)	109.7
23	7.40 (s, 1H)	143.0	7.41 (s, 1H)	143.0
28	0.89 (s, 3H)	14.6	0.89 (s, 1H)	14.6
29	1.98 (m, 1H)	40.2	1.97 (m, 1H)	40.2
	1.67 (m, 1H)		1.67 (m, 1H)	
30	6.30 (s, 1H)	69.3	6.31 (s, 1H)	69.3
31		119.0		119.0
32	1.66 (s, 3H)	21.0	1.67 (s, 3H)	21.0
2-OAc	2.25 (s, 3H)	21.1	2.25 (s, 3H)	21.1
		170.2		170.3
3-OAc	2.15 (s, 3H)	21.7	2.15 (s, 3H)	21.7
		170.2		170.3
30-OAc	1.94 (s, 3H)	21.6	1.95 (s, 3H)	21.5
		168.6		168.5
7-OMe	3.69 (s, 3H)	52.1	3.69 (s, 3H)	52.1

3.2.9 Structure elucidation of compound 9

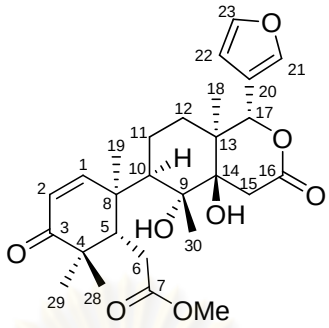

Figure 3.19 Compound **9**

Molecular formula	$C_{27}H_{36}O_8$
Appearance	Colorless crystals
m.p.	145-147° C
$[\alpha]_D^{20}$	-25.0 (*c* 0.1 MeOH)
UV (MeOH) λ_{max} (logε)	298 nm (2.01)
IR (KBr)	3491, 3347, 2960, 1730, 1700, 1660, 1473, 1430, 1386, 1265, 1191 and 1030 cm^{-1}
HRESIMS *m/z* $[M+Na]^+$	511.2310 calcd 511.2308
^1H and ^{13}C NMR ($CDCl_3$)	See Table 3.10

Compound **9** was obtained as colorless crystals and the molecular formula was determined to be $C_{27}H_{36}O_8$ by HR-ESI-MS at *m/z* 511.2310 $[M + Na]^+$ (calcd for $C_{27}H_{36}O_8Na$ 511.2308), corresponding to 10 degrees of unsaturation. IR absorptions implied the presence of ester (1730 cm^{-1}), *α*,*β*-unsaturated ketone (1700 cm^{-1}) and hydroxyl (3491 cm^{-1}) functionalities. On the basis of ^{13}C NMR (Table 3.10) and HSQC data, compound **9** contained six methyls (one methoxy), four methylenes, eight methines (five olefinic), six quaternary carbons (one olefinic) and three carbonyls (two esters and one ketone). These data indicated that six out of 10 degrees of unsaturation came from three carbon-carbon double bonds and three carbonyl groups, and the remaining degrees thus required **9** to possess a tetracyclic core.

Analysis of 1D and 2D (^{1}H-^{1}H COSY, HSQC and HMBC) NMR spectra revealed the existence of a *β*-furanyl ring [δ_H 6.35 (br, s), 7.37 (br, s), 7.38 (br s); δ_C 109.9 CH, 120.9 qC, 140.7 CH, 142.8CH), a methoxycarbonyl group [δ_H 3.63 (s); δ_C 52.1 CH_3, 174.4 qC), and an *α*,*β*-unsaturated ketone group [δ_H 5.90 (d, J = 10.8 Hz), 6.86 (d, J = 10.8 Hz); δ_C 125.4 CH, 153.8 CH, 203.8 qC). A proton singlet at δ_H 5.67 was assigned to be H-17 by HMBC correlations with the carbon signals of the furan ring (C-20, C-21 and C-22). A *δ*-lactone ring was corroborated by HMBC cross peaks from H-17 to both bridgehead carbons (C-13 and C-14) and the ester carbonyl at δ_C 172.5 (C-16), from Me-18 to C-13, C-14 and C-17, and from H_2-15 to C-14 and C-16. The above NMR data suggested that compound **9** might be an adirobin-type limonoid closely related to methyl angolensate [91]. HMBC correlations between C-7 (δ_C 174.4) and H_2-6 (δ_H 2.48) and the methoxy protons at δ_H 3.63 confirmed the characteristic C-6–C-7 appendage of andirobin limonoids. A tertiary methyl singlet at δ_H 1.57 was assigned to be Me-30 through the strong HMBC correlations with C-9, C-10 and C-14, indicating that an exomethylene of methyl angolensate was replaced by a tertiary methyl group for **9**. Additionally, HMBC cross peaks from another tertiary methyl singlet at δ_H 1.41 (Me-19) to C-1, C-5, C-8 and C-10, clarified the connection between A-ring and B-ring through C-8–C-10 bond. The single-crystal X-ray diffraction analysis of **9** (Figure 3.21) confirmed its planar structure and allowed the determination of its relative configuration. This compound was found to be new and thus named as xylomoluccensin A.

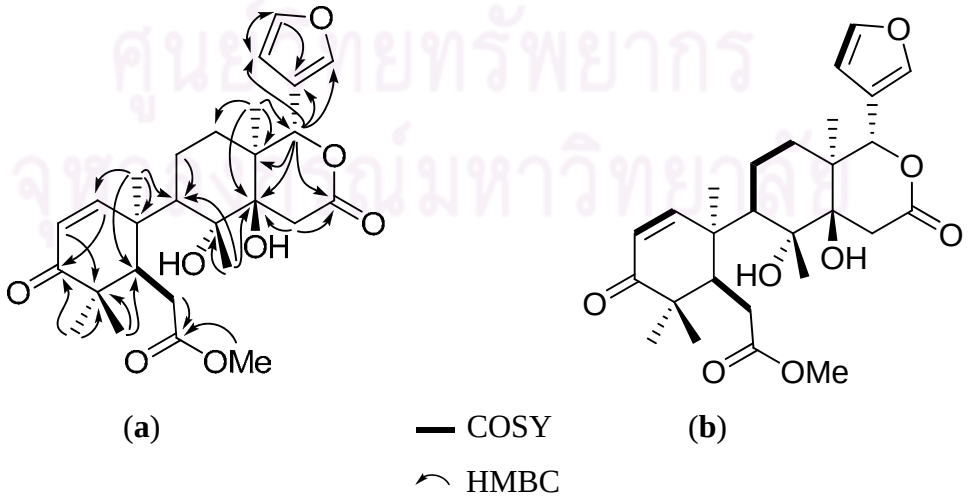

Figure 3.20 Key HMBC (**a**) and COSY (**b**) correlations of compound **9**

Table 3.10 The NMR data of compound **9**

Positions	δ_H (mult, *J* in Hz)	δ_C	COSY	HMBC
1	6.86 (d, *J*= 10.8 Hz, 1H)	153.8	H-2	C-3, C-8
2	5.90 (d, *J*= 10.8 Hz, 1H)	125.4	H-1	C-4
3		203.8		
4		46.2		
5	2.65 (s, 1H)	44.1	H-6	
6	2.48 (m, 2H)	32.2	H-5	C-7
7		174.4		
8		43.7		
9		78.5		
10	1.88 (m, 1H)	49.7	H-11	
11	1.59 (m, 2H)	20.6	H-10, H-12a, H-12b	C-9
12	1.73 (dd, *J*= 4.4, 13.6 Hz,1H) 1.36 (d, *J*= 5.2 Hz, 1H)	32.8	H-11	
13		38.0		
14		80.0		
15	3.30 (d, *J*= 18.4 Hz, 1H) 2.56 (d, *J*= 18.0 Hz, 1H)	36.8		C-14, C-16
16		172.5		
17	5.67 (s, 1H)	81.9		C-13, C-14, C-16, C-20, C-21, C-22
18	1.13 (s, 3H)	20.3		C-12, C-13, C-14, C-17
19	1.41 (s, 3H)	19.4		C-1, C-5, C-8, C-10
20		120.9		
21	7.37 (s, 1H)	140.7		C-20, C-23
22	6.35 (s, 1H)	109.9		C-21, C-23
23	7.38 (s, 1H)	142.8		C-20, C-22
28	1.10 (s, 3H)	23.0		C-3, C-4, C-5, C-29
29	0.99 (s, 3H)	22.8		C-3, C-4, C-5, C-28
30	1.57 (s, 3H)	21.1		C-9, C-10, C-14
7-OMe	3.63 (s, 3H)	52.1		C-7

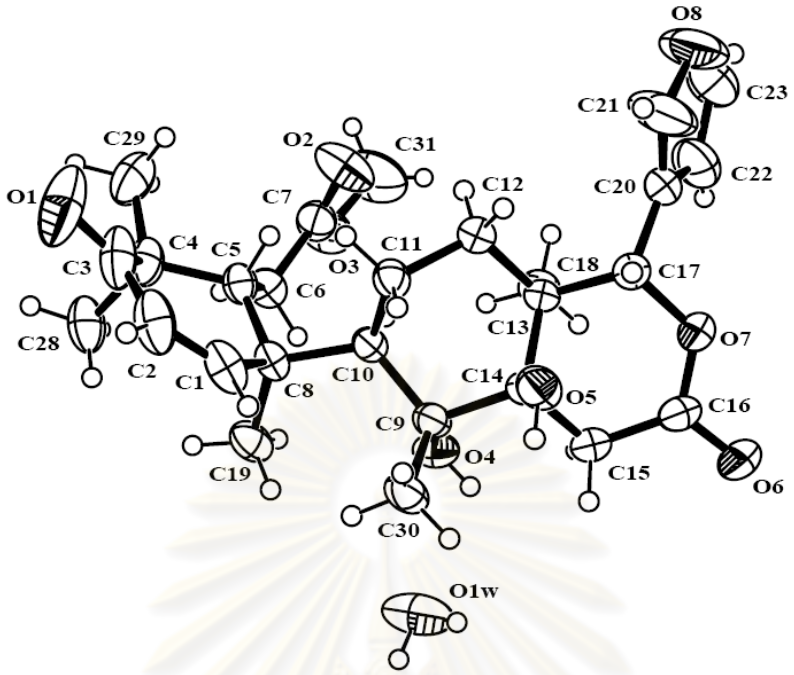

Figure 3.21 ORTEP diagram of compound **9**

Table 3.11 Crystal data and structure refinement for compound **9**

Formula	$C_{27}H_{36}O_8 \cdot H_2O$
Molecular weight	503.55
Crystal size (mm)	0.48× 0.40× 0.20
Crystal system	Orthorhombic
Space group	$P2_12_12_1$
***a* (Å)**	6.5514 (3)
***b* (Å)**	17.1962 (10)
***c* (Å)**	23.7727 (13)
***V* (Å^3)**	2678.2 (2)
Z	4
D_{calc} (g/cm^{-3})	1.269
μ (mm^{-1})	0.089
***F*(000)**	2832
Independent reflections/ Observed reflections [$I > 4\sigma(I)$], R_{int}	6624/ 2930, 0.0374
R_1	0.0530
wR_2 [$I > 2\sigma(I)$]	0.1423

3.2.10 Structure elucidation of compound 10

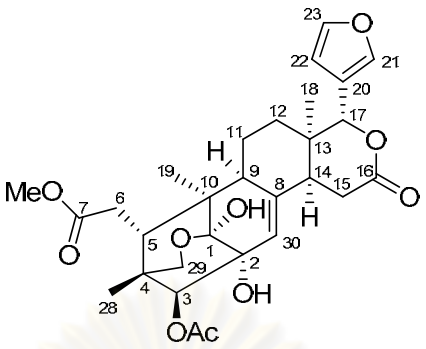

Figure 3.22 Compound **10**

Molecular formula	$C_{29}H_{36}O_{10}$
Appearance	White amorphous solid
m.p.	188-190° C
$[\alpha]_D^{20}$	-49.0 (*c* 0.1, MeOH)
UV (MeOH) λ_{max} (logε)	202 nm (2.18)
IR (KBr)	3491, 2926, 2856,1730, 1466, 1430, 1378, 1230,1152, 1091 and 1097 cm^{-1}
HRESIMS *m/z* $[M+Na]^+$	567.2209 calcd. 567.2206
^1H and ^{13}C NMR ($CDCl_3$)	See Table 3.12

Compound **10**, a white, amorphous solid, had the molecular formula $C_{29}H_{36}O_{10}$ as established by HR-ESI-MS at *m/z* 567.2209 $[M + Na]^+$ (calcd for $C_{29}H_{36}O_{10}Na$ 567.2206), implying 12 degrees of unsaturation. Its ^{13}C NMR data (Table 3.12) showed that six units of unsaturation came from three ester carbonyls and three carbon-carbon bonds. Therefore, the remaining degrees of unsaturation required **2** to be hexacylcic. A combined analysis of 1D and 2D (^1H-^1H COSY, HSQC and HMBC) NMR spectra revealed the presence of a *β*-furanyl ring [δ_H 6.44 (br s), 7.41 (br s), 7.74 (br s); δ_C 109.9 CH, 120.6 qC, 141.8 CH, 143.0 CH], a methoxycarbonyl group [δ_H 3.71 s; δ_C 52.2 CH_3, 173.9 qC], an acetoxy group [δ_H 2.13 s; δ_C 20.3 CH_3, 173.6 qC], a 1,29-oxygen bridge [δ_H 3.57 (dd, *J* = 1.6, 9.6 Hz), 3.97

(d, J = 9.6 Hz); δ_C 68.1], and three tertiary methyls [δ_H 0.68 s, 1.09 s, 1.15 s; δ_C 14.7, 21.9, 14.1]. The aforementioned NMR data strongly suggested that **2** was a phragmalin-type limonoid and closely related to that of godavarin D [95]. The presence of a $\Delta^{8,30}$ double bond was confirmed by HMBC correlations of H-9/C-8, H-15/C-8, H-30/C-1, H-30/C-9 and H-30/C-14. Moreover, observed HMBC cross peak from H-3 [δ_H 4.56 (s)] to carbonyl carbon (δ_C 173.6) of acetyl group clarified the location of acetoxyl group at C-3, and the correlation from H-3 to C-2 (δ_C 74.9) also revealed the existence of C-2 hydroxyl in **2**. The relative configuration of **2** was established on the basis of NOE interactions. Significant NOE interaction (Figure 3.23c) from H-3 to $H_{pro\text{-}R}$-29 [δ_H 3.57 (dd, J = 1.6, 9.6 Hz)] established 3α-H and the corresponding 3β-acetoxy group. Furthermore, interactions of H_3-18/H-14, H_3-18/H_3-19, H-9/H_3-19 and HO-2/H-3 indicated the α-orientation of Me-18, Me-19, H-14, H-9 and HO-2, whereas interactions of H-5/H_3-28 and H-5/H-17 suggested the β-orientation of H-5 and H-17. Thus, compound 10 was determined to be new and was named as xylomoluccensin B.

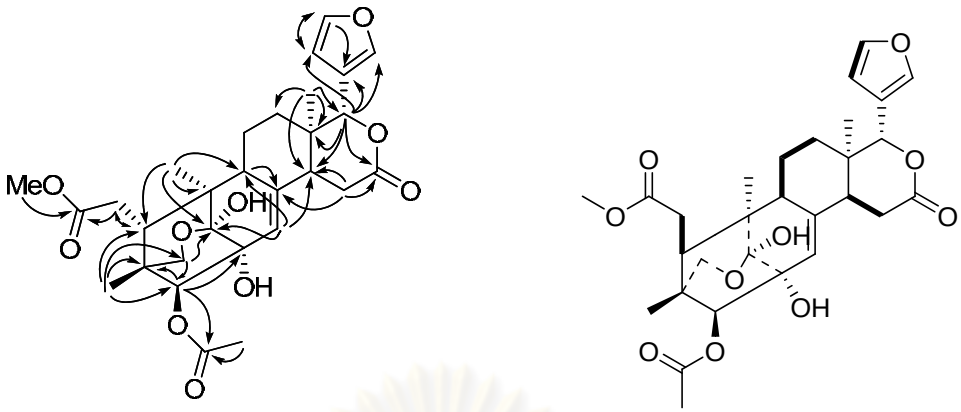

(**a**) (**b**)

COSY

HMBC

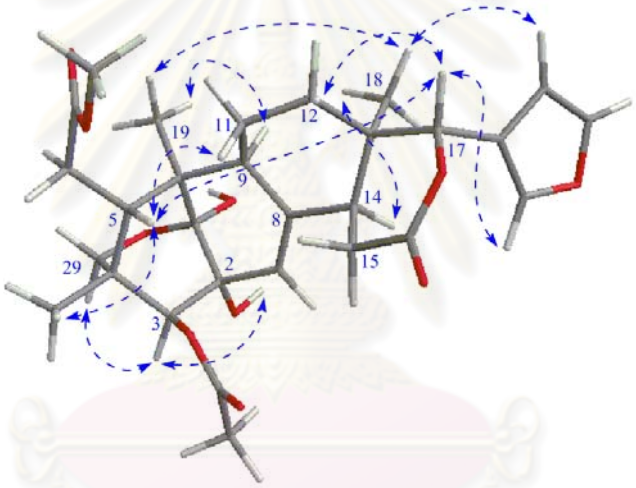

NOESY (**c**)

Figure 3.23 Key HMBC (**a**), COSY (**b**) and NOESY (**c**) correlations of compound **10**

Table 3.12 The NMR data of compound **10**

Positions	δ_H (mult, *J* in Hz)	δ_C	COSY	HMBC
1		96.7		
2		74.9		
3	4.56 (s, 1H)	85.1		C-2, C-4, C-1′
4		36.8		
5	2.72 (d, *J*= 10.4 Hz, 1H)	35.3	H-6	C-7, C-10, C-29,
6	2.31 (m, 2H)	31.6	H-5	C-5, C-7
7		173.9		
8		138.5		
9	2.23 (dd, *J*= 5.6, 12.4 Hz, 1H)	47.1	H-11	C-8
10		41.9		
11	1.73 (m, 1H)	19.1	H-9, H-12a,	
	1.66 (m, 1H)		H-12b	
12	1.61 (m, 1H)	34.2	H-11a, H1b	C-17
	1.45 (m, 1H)			
13		36.7		
14	2.30 (m, 1H)	44.7	H-15	C-13
15	2.88 (m, 2H)	30.0	H-14	C-8, C-13, C-14, C-16
16		169.8		
17	5.51 (s, 1H)	77.1		C-13, C-14, C-16,
				C-20, C-21, C-22
18	1.09 (s, 1H)	21.9		C-12, C-13, C-14,
				C-17
19	1.15 (s, 1H)	14.1		C-1, C-5, C-9, C-10
20		120.6		
21	7.74 (s, 1H)	141.8		C-20, C-22
22	6.44 (s, 1H)	109.9	H-23	C-20, C-21, C-23
23	7.41 (s, 1H)	143.0	H-22	C-20, C-21, C-22
28	0.68 (s, 1H)	14.7		C-3, C-4, C-5, C-29
29	3.97 (d, *J*= 9.6 Hz, 1H)	68.1		C-1, C-3, C-5
	3.57 (dd, *J*= 1.6, 9.6 Hz, 1H)			
30	5.09 (s, 1H)	124.0		C-1, C-9, C-14
3-OAc		173.6		
	2.13 (br, s, 1H)	20.3		C-1′
1-OH				
2-OH	5.30 (s, 1H)			
7-OMe	3.71 (s, 3H)	52.2		C-7

3.2.11 Structure elucidation of compound 11

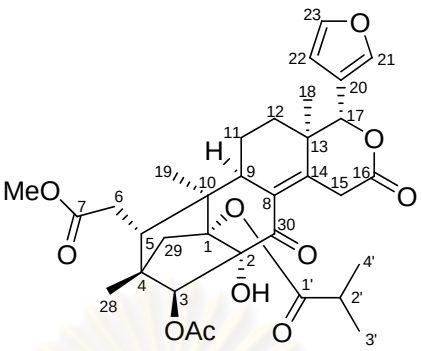

Figure 3.24 Compound **11**

Molecular formula	$C_{33}H_{40}O_{11}$
Appearance	White amorphous solid
m.p.	107-109 ° C
$[\alpha]_D^{20}$	-9.0 (*c* 0.1, MeOH)
UV (MeOH) λ_{max} (logε)	217 nm (1.35)
IR (KBr)	3452, 3139, 2973, 1730, 1691, 1621, 1460, 1378, 1213, 1156, and 1073 cm^{-1}
HRESIMS *m/z* $[M+H]^+$	613.2646 calcd. 613.2649
^1H and ^{13}C NMR ($CDCl_3$)	See Table 3.13

Compound **11** was obtained as a white, amorphous solid. The molecular formula $C_{33}H_{40}O_{11}$ was determined by HR-ESI-MS at *m/z* 613.2646 $[M + H]^+$ (calcd for $C_{33}H_{41}O_{11}$ 613.2649), accounting for 14 degrees of unsaturation. The NMR data also displayed characteristic signals associated with a phragmalin limonoid, including a *β*-furanyl ring [δ_H 6.43 (br s), 7.41 (br s), 7.43 (br s); δ_C 109.6 CH, 120.1 qC, 141.7 CH, 143.7 CH], a methoxycarbonyl group [δ_H 3.67 s; δ_C 52.0 CH_3, 176.5 qC], a 1,29-bridge [δ_H 1.97 (d, *J* = 11.2 Hz), 2.22 (d, *J* = 11.2 Hz); δ_C 41.6], and three tertiary methyls [δ_H 0.85 s, 1.09 s, 1.19 s; δ_C 14.5, 17.8, 18.8]. Moreover, analysis of 1D and 2D NMR revealed the presence of an acetoxy [δ_H 1.97

s; δ_C 20.7 CH_3, 169.7 qC], and isobutyryl [δ_H 1.12 (d, J = 6.8 Hz), 1.10 (d, J = 6.8 Hz), 2.56 (sep); δ_C 17.8 CH_3, 18.9 CH_3, 33.9 CH, 176.5 qC] group. HMBC correlation from H-3 [δ_H 5.08 (s)] to carbonyl carbon of acetyl group (δ_C 169.7) confirmed its location at C-3, whereas the downfield chemical shift of C-1 (δ_C 90.3), similar to those in moluccensins A-E [87], suggested the location of isobutyryl group at this position. A $\Delta^{8,14}$ double bond was corroborated by HMBC cross peaks of H_2-15/C-8, H_2-15/C-14, H-9/C-8 and H-9/C-14, and a C-30 ketone group was indicated by those of H_2-15/C-30, H-3/C-30 and HO-2/C-30 (Figure 3.25a). The relative configuration of **11** was virtually identical to that of **10** on the basis of similar NOE interaction. Thus, compound **11** was determined to be new and was named as xylomoluccensin C.

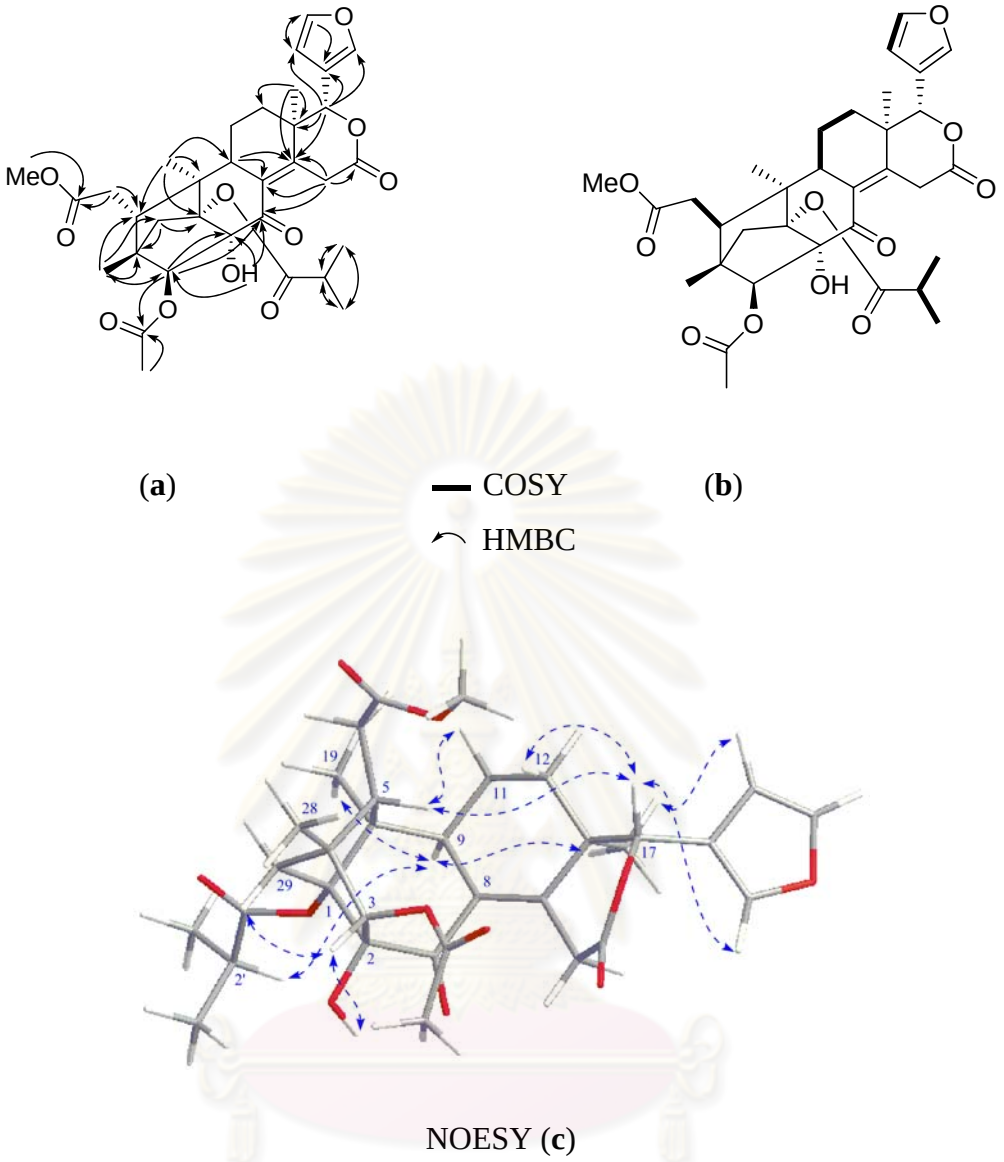

Figure 3.25 Key HMBC (**a**), COSY (**b**) and NOESY (**c**) correlations of compound **11**

Table 3.13 The NMR data of compound **11**

Positions	δ_H (mult, *J* in Hz)	δ_C	COSY	HMBC
1		90.3		
2		80.2		
3	5.08 (s, 1H)	89.5		C-2, C-28, C-30, C-1″
4		43.4		
5	2.95 (m, 1H)	39.0	H-6	C-4, C-6, C-29
6	2.36 (m, 2H)	33.8	H-5	C-4, C-5, C-7
7		173.3		
8		130.7		
9	2.79 (s, 1H)	44.5	H-11a, H-11b	C-8, C-12, C-13, C-14
10		47.7		
11	1.75 (m, 1H)	19.7	H-9, H-12a,	
	1.62 (m, 1H)		H-12b	
	1.62 (m, 1H)			
12	1.69 (m, 1H)	30.3	H-11a, H-11b	C-9, C-14, C-17, C-18
	1.31 (m, 1H)			
13		38.9		
14		145.8		
15	3.90 (s, 2H)	36.2		C-8, C-13, C-14, C-16, C-30
16		168.9		
17	5.49 (s, 1H)	80.0		C-13, C-14, C-20, C-21, C-22
18	1.19 (s, 3H)	18.8		C-12, C-13, C-14, C-17
19	1.09 (s, 3H)	17.8		
20		120.1		
21	7.41 (s, 1H)	141.7		C-20, C-22, C-23
22	6.43 (s, 1H)	109.6	H-23	C-20, C-23
23	7.43 (s, 1H)	143.7	H-22	C-20, C-22
28	0.85 (s, 3H)	14.5		C-3, C-4, C-5, C-29
29	2.22 (d, *J*= 11.2 Hz, 1H)	41.6		C-1, C-4
	1.97 (m, 1H)			
30		198.1		
2-OH	4.47 (br, s, 1H)			C-2, C-3, C-30
3-OAc		169.7		
2″	1.97 (s, 1H)	20.7		C-1″
1-*O*-isobutylryl				
1′		176.5		
2′	2.56 (sep)	33.9		C-1′, C-3′, C-4′
3′	1.11 (d, *J*= 6.8 Hz, 3H)	18.9		C-2′, C-4′
4′	1.10 (d, *J*= 6.8 Hz, 3H)	17.8		C-2′, C-3′
7-OMe	3.67 (s, 3H)	52.0		C-7

3.3 Anti-inflammatory activity of isolated compounds

NO production inhibitory effects of compounds **1**-**9** and **11** were evaluated at two doses of 5 and 10 μg/mL (Figure 3.26). Only gedunin-type limonoids, **4** and **5**, exhibited potent anti-inflammatory activity, particularly 7-deacetylgedunin (**4**). Compounds **9** and **11** showed moderate inhibitory effect at 10 μg/mL, while compounds **2** and **3** gave weak activity though at 10 μg/mL, and compounds **1** and **6**-**8** did not display any detectable activity at both screening doses.

Compounds **4** and **5** were subsequently tested for their acute toxicity on unstimulated cell lines. As a result, despite compound **4** gave more potent activity than **5**, it also showed higher toxicity (IC_{50} = 7.3 μg/mL for **4**; 16.5 μg/mL for **5**) as shown in Figure 3.27 and 3.28. This result implied that reduced form of ketone function at C-7 in **4** might play an important role for both activities.

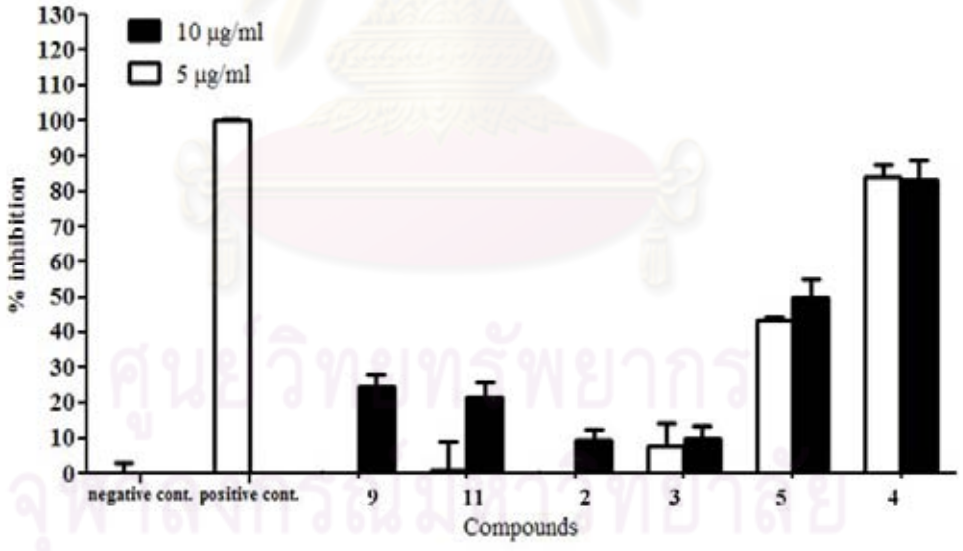

Figure 3.26 NO production inhibitory effects of compounds at 5 and 10 µg/mL

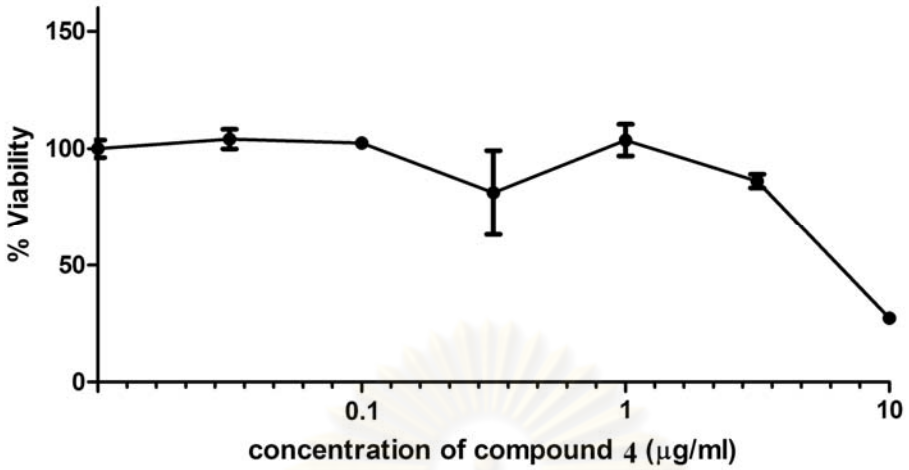

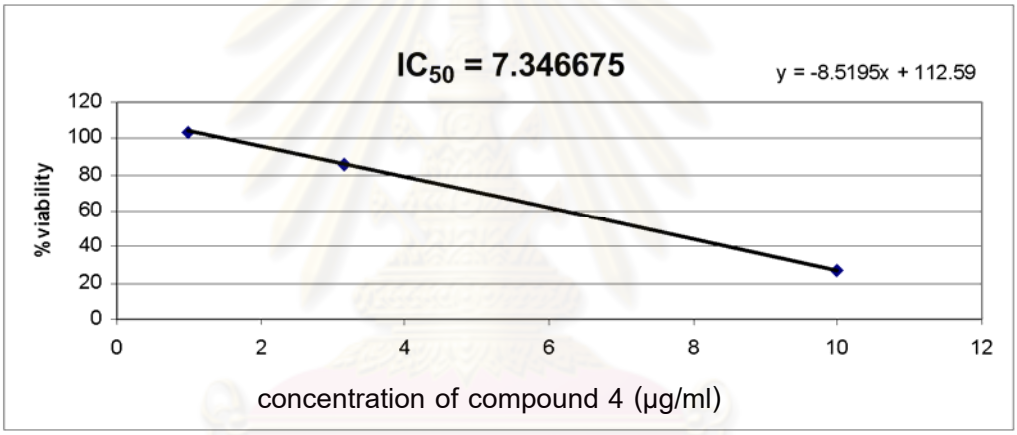

Figure 3.27 Toxicity assay of compound **4**

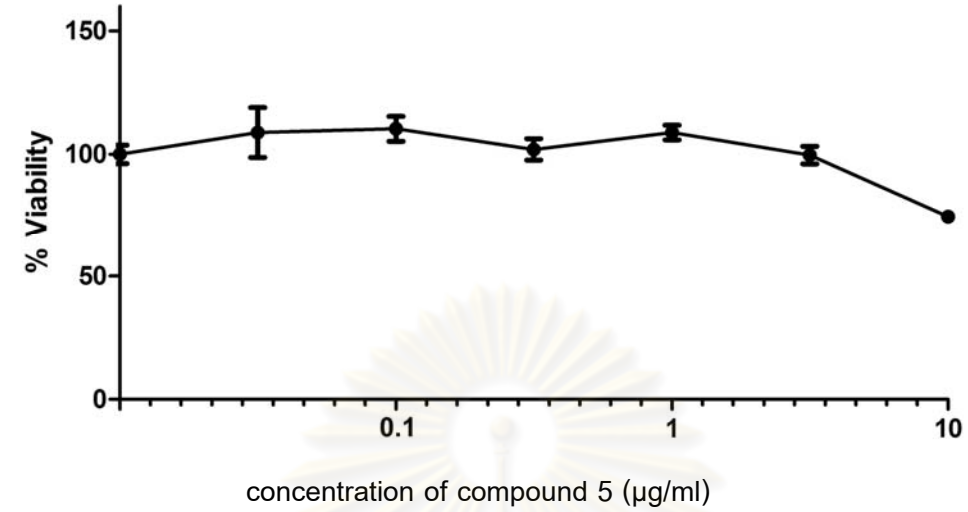

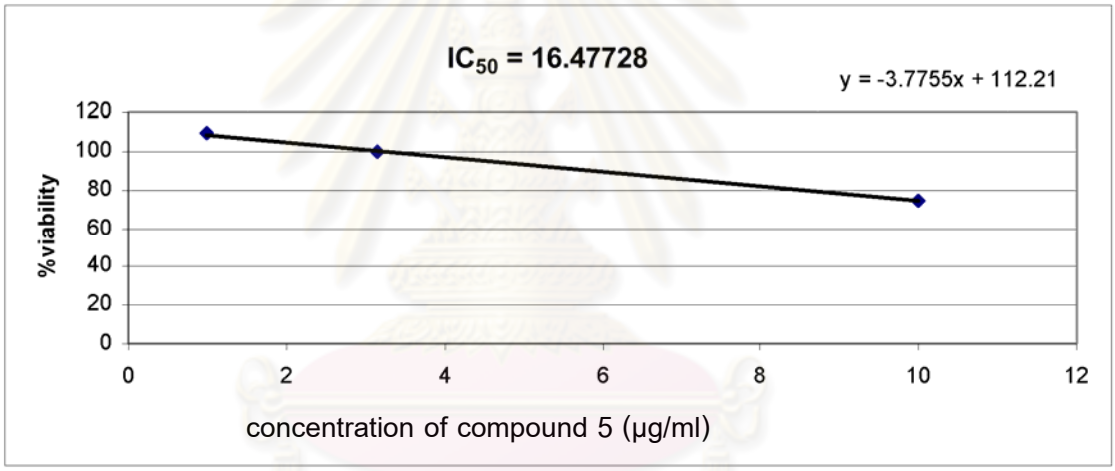

Figure 3.28 Toxicity assay of compound **5**

CHAPTER IV

CONCLUSION

Chemical examination of the seed kernels of *Xylocarpus moluccensis* Roem. collected from Phuket province led to the isolation of a new andirobin, xylomoluccensin A (**9**), and two new phragmalin-type limonoids, xylomoluccensins B (**10**) and C (**11**), together with eight known limonoids namely mexicarnolide (**1**), 3*β*-deacetylfissinolide (**2**), 2-hydroxyfissinolide (**3**), 7-deacetylgedunin (**4**), 7-oxo-7-deacetoxygedunin (**5**), moluccensin H (**6**), moluccensin I (**7**) and xyloccensin E (**8**) as shown below. The structures of novel compounds were elucidated by analysis of spectroscopic data, as well as single-crystal X-ray diffraction analysis, while those of known compounds were determined on the basis of 1D and 2D NMR spectroscopic data and by comparing with those previously reported in literature.

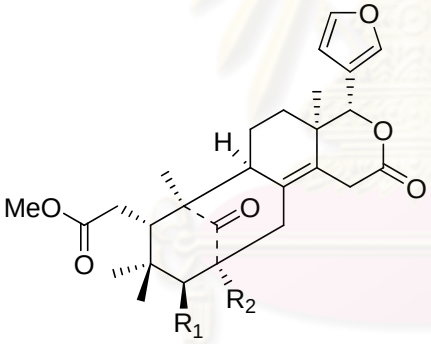

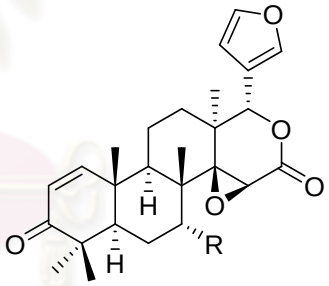

1: R^1= =O, R^2= H

2: R^1= OH, R^2= H

3: R^1= OAc, R^2= OH

4: R= OH

5: R= =O

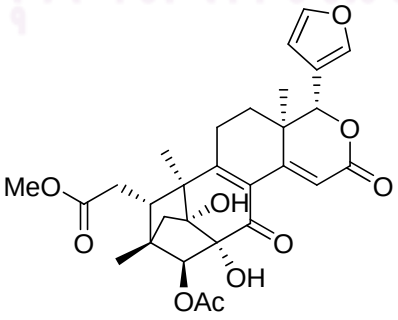

6

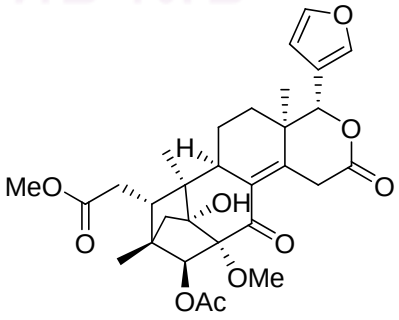

7

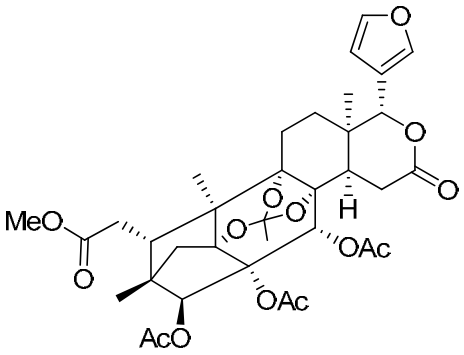

8

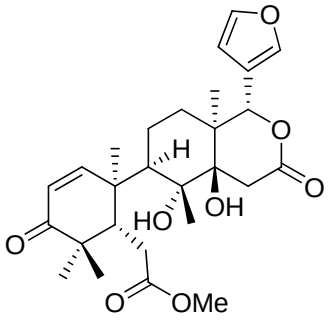

9

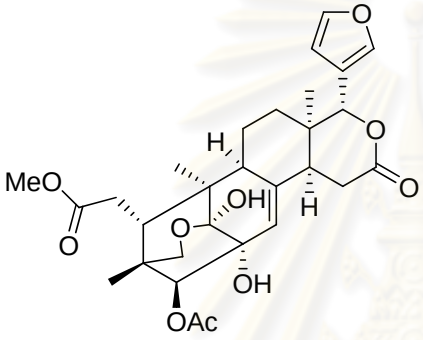

10

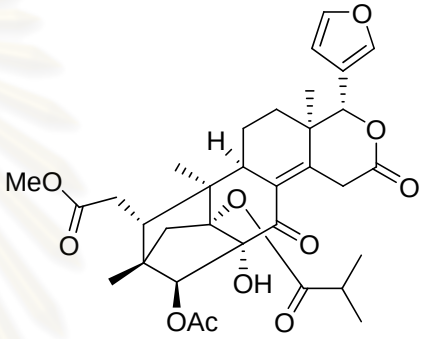

11

Furthermore, all isolated compounds, except for compound **10**, were evaluated for their anti-inflammatory activity using the model of inhibitory activity against nitric oxide production from activated macrophages. Only gedunin-type limonoids, 7-deacetylgedunin (**4**) and 7-oxo-7-deacetoxygedunin (**5**) exhibited significant NO production inhibitory activity at a concentration of 10 µg/mL, particularly 7-deacetylgedunin (**7**), suggesting that these compounds have potent anti-inflammatory activity. However, when compounds **4** and **5** were subsequently tested for their acute toxicity on unstimulated cell lines, compound **4** showed higher toxicity (IC_{50} = 7.3 µg/mL for **4**; 16.5 µg/mL for **5**), despite it gave more potent activity than **5**, This result implied that reduced form of ketone function at C-7 in **4** might play an important role for both activities.

REFERENCES

[1] Newman, D. J., Cragg, G. M., and Snader, K. M. 2000. The influence of natural products upon drug discovery. Nat Prod Rep. 17: 215-234.

[2] Newman, D. J., Cragg, G. M., and Snader, K. M. 2003. Natural products as sources of new drugs over the period 1981-2002. J Nat Prod. 66: 1022-1037 .

[3] Koehn, F. E., and Carter, G. T. 2005. The evolving role of natural products in drug discovery. Nat Rev Drug Discov . 4 : 206-220 .

[4] Balunas, M. J., and Kinghorn, A. D. 2005. Drug discovery from medicinal plants. Life Sci . 78: 431-441 .

[5] Drahl, C., Cravatt, B. F., and Sorensen, E. J. 2005. Protein-reactive natural products. Angew Chem Int Ed Engl . 44: 5788-5809 .

[6] Grifo, F., Newman, D., Fairfield, A., Bhattacharya, B., and Grupenhoff, J. The origins of prescription drugs. In: Grifo F., and Rosenthal J. (eds.), Biodiversity and Human Health, pp.131-163. Washington DC : Island Press, 1997.

[7] Butler, M.S. The role of natural product chemistry in drug discovery. 2004. J Nat Prod. 67: 2141-2153.

[8] Thayer, A. Bristol-Myers to settle suits. 2003. Chem Eng News . 81: 6 .

[9] Oberlies, N.H., and Kroll, D. J. Camptothecin and taxol: historic achievements in natural products research. 2004. J Nat Prod. 67: 129-135.

[10] Dewick, P. M. 2002. Medicinal Natural Products: A Biosynthetic Approach. 2nd ed. Chichester, UK : John Wiley & Sons.

[11] Fabricant, D. S., and Farnsworth, N. R. 2001. The value of plants used in traditional medicine for drug discovery. Environ Health Perspect. 109: 69-75.

[12] Kinghorn, A. D. The discovery of drugs from higher plants. In: Gullo, V. P. (ed.), The Discovery of Natural Products with Therapeutic Potential, pp.81-108. Boston MA : Butterworth-Heinemann Press, 1994.

[13] Butler, M. S. 2005. Natural products to drugs: natural products derived compounds in clinical trials. Nat Prod Rep. 22: 162-195.

[14] Cirla, A., and Mann, J. 2003. Combrestatins: from natural products to drug discovery. Nat Prod Rep. 20: 558-564.

[15] Pinney, K. G., Jelinek, C., Edvardsen, K., Chaplin, D. J., and Pettit, G. R. The discovery and development of the combrestatins. In: Cragg, G. M., Kingston, D. G. I. and Newman, D. J. (eds.), Anticancer Agents from Natural Products, pp.23-46. Boca Raton FL : CRC Press, 2005.

[16] West, C. M. L., and Price, P. 2004. Combrestatin A4 phosphate. Anticancer Drugs. 15: 179-187.

[17] Young, S. L., and Chaplin, D. J. 2004. Combrestatin A4 phosphate: background and current clinical status. Expert Opin Investig Drugs. 13: 1171-1182.

[18] Powell, R. G., Weisleder, D., Smith C. R., and Rohwedder, W. K . 1970. Structures of harringtonine, isoharringtonine, and homoharringtonine. Tetrahedron Lett. 11: 81-818.

[19] Kantarjian, H. M.,*et.al*. 2001. Homoharringtonine: history, current research, and future direction. Cancer. 92: 1591-1603.

[20] Kedei, N., *et.al*. 2004. Characterization of the interaction of ingenol 3-angelate with protein kinase C. Cancer Res. 64: 3243-3255.

[21] Ogbourne, S. M., Suhrbier, A., and Jones, B. 2004. Antitumor activity of ingenol 3-angelate: plasma membrane and mitochondrial disruption and necrotic cell death. Cancer Res. 64: 2833-2839.

[22] Kamsteeg, M., Rutherford, T., and Sapi, E. 2003. Phenoxodiol – an isoflavone analog - induces apoptosis in chemoresitant ovarian cancer cells. Oncogene. 22: 2611 -2620.

[23] Constantinou, A. I., Mehta, R., and Husband, A. 2003. Phenoxodiol, a novel isoflavone derivative, inhibits dimethylbenz [*a*] anthracene (DMBA)-induced mammary carcinogenesis in female Sprague-Dawley rats. Eur J Cancer. 39: 1012- 1018.

[24] Shibata, S., Tanaka, O., Sado, M., and Tsushima, S. 1963. The genuine sapogenin of ginseng. Tetrahedron Lett. 4: 795-800.

[25] Jia, W., Yan, H., Bu, X., Liu, G., and Zhao, Y. 2004. Aglycone protopanaxadiol, a ginseng saponin, inhibits P-glycoprotein and sensitizes chemotherapy drugs on multidrug resistant cancer cells. J Clin Oncol. 22: 9663.

[26] Kiviharju, T. M., Lecane, P. S., Sellers, R. G., and Peehl, D. M. 2002. Antiproliferative and proapoptotic of triptolide (PG490), a natural product entering clinical trials, on primary cultures of human prostatic epithelial cells. Clin Cancer Res. 8: 2666-2674.

[27] Fidler, J. M., Li, K., and Chung, C. 2003. PG490-88, a derivative of triptolide, causes tumor regression and sensitizes tumors to chemotherapy. Mol Cancer Ther. 2: 855-862.

[28] Bandaranayake, W. M. 2002. Bioactivities, bioactive compounds and chemical constituents of mangrove plants. Wetl Ecol Manag. 10: 421-452.

[29] Spalding, M.D., Blasco, F., and Field, C. 1997. World mangrove atlas. The International Society for Mangrove Ecosystems. Okinawa. 178.

[30] Wu, J., Xiao, Q., Xu, J., Li, M. Y., and Yang, M. H. 2008. Natural products from true mangrove flora: source, chemistry and bioactivities. Nat Prod Rep. 25: 955-981.

[31] Bandaranayake, W. M. 1998. Traditional and medicinal use of Mangrove. Mangrove Salt Marshes. 2: 133-148.

[32] Patra, J. K., Panigrahi, T. K., Rath, S. K., Dhal, N. K., and Thatoi, H. N. 2009 Phytochemical screening and antimicrobial assessment of leaf extracts of Excoecaria agallocha L.: a mangal species of Bhitarkanika, Orissa, India. Adv Nat Appl Sci. 3(2): 241-246.

[33] Patra, J. K., Das, M. A., Rath, S. K., Dhal, N. K., and Thatoi, H. N. 2009. Screening of antioxidant and antifilarial activity of leaf extracts of Excoecaria agallocha L. Int J Integr Biol. 7(1): 9-15.

[34] Kathiresan, K., and Bingham, B. L. Biology of mangrove and mangrove ecosystem. In: Southward, A. J., Tyler, A. A., Young, C. M., and Fuiman, L. A. (eds.) Advances in marine biology, pp 84–25. New York: Academy Press, 2001.

[35] Pattanaik, C., Reddy, C. S., Dhal, N. K., and Das, R. 2008. Utilization of Mangrove forests in Bhitarkanika wildlife Sanctuary Orissa. Indian J Tradit Knowl 7(4): 598-603.

[36] Bamroongrugsa, N. 1999. Bioactive substances from mangrove resources. Songklanakarin J Sci Technol. 21(3): 377-386.

[37] Kathiresan, K., Boopathy, N. S., and Kavitha, S. 2006. Coastal vegetation: an underexplored source of anticancer drugs. Nat Prod Radiance. 5(2): 114-119.

[38] Bose, S., and Bose, A. 2008. Antimicrobial activity of *Acanthus ilicifolius* (L.). Indian J Pharm Sci. 70(6): 821-823.

[39] Singh, A., Duggal, S., and Suttee, A. 2009. *Acanthus ilicifolius* Linn.-lesser known medicinal plants with significant pharmacological activities. Int J Phytomed. 1: 001-003.

[40] Manilal, A., Sujith, S., Kiran, S., and Selvin, S. C. 2009. Biopotentials of mangroves collected from southwest coast of India. Glob J Biotechnol Biochem. 4(1): 59–65.

[41] Chandrasekaran, M., Kannathasan, K., Venkatesalu, V., and Prabhakar, K. 2009. Antibacterial activity of some salt marsh halophytes and mangrove plants against methicillin resistant *Staphylococcus aureus*. World J Microbiol Biotechnol. 25: 155-160.

[42] Chumkaew, P., Kato, S., and Chantrapromma, K. 2006. Potent cytotoxic rocaglamide derivatives from the fruits of Amoora cucullata. Chem Pharm Bull. 54(9) 1344-1346.

[43] Abeysinghe, P. D., Wanigatunge, R. P., and Pathirana, R. P. 2006. Evaluation of antibacterial activity of different mangrove plant extracts. Ruhuna J Sci. 1: 108-116.

[44] Vadlapudi, V., and Naidu, K. C. 2009. Bioefficiency of mangrove plants *Lumintzera racemosa* and *Bruguiera gymnorhiza*. J Pharm Res. 2(10): 1591-1592.

[45] Ashihara, H., *et, al*. 2003. Comparison of adenosine metabolism in leaves of several mangrove plants and a poplar species. Plant Physiol Biochem. 41:133-139.

[46] Feng, Y., Li, X. M., Duan, X. J., and Wang, B. G. 2006. A new Acylated Iridoid Glucoside from *Avicennia marina*. Chin Chem Lett. 17(9): 1201-1204.

[47] Bobbarala, V., Vadlapud, V. R., and Naidu, K. C. 2009. Antimicrobial potentialities of Mangrove plant *Avicennia marina*. J Pharm Res. 2(6): 1019-1021.

[48] Abeysinghe, P. D. 2010. Antibacterial activity of some medicinal mangroves against antibiotic resistant pathogenic bacteria. Indian J Pharm Sci. 72(2): 167-172.

[49] Kumar, T., Ray, S., Brahmachary, R. L., and Ghose, M. 2009. Preliminary GC–MS analysis of compounds present in the root exudates of three mangrove species. Acta Chromatogr. 21(1): 117-125.

[50] Raju, A. J. S., Jonathan, K. H., and Rao, S. P. 2008. Traditional extraction of bark tannin from the mangrove tree, *Ceriops decandra* (Griff.) Ding Hou and its use in treating cotton fishing nets. Nat Prod Radiance. 7(2): 173-175.

[51] Masuda, T., *et, al*. 1999. Evaluation of the antioxidants activity of environmental plants. J Agric Food Chem. 47: 1749-1754.

[52] Anjaneyulu, A. S. R., and Rao, V. L. 2000. Five diterpenoids(agallochins A-E) from the mangrove plant *Excoecaria agallocha* Linn. Phytochemistry. 55: 891-901.

[53] Kathiresan, K. 2000 A review of studies on Pichavaram mangrove south east India. Hydrobiologia. 430: 185-205.

[54] Konishi, T., Konoshima, T., Fujiwara, Y., and Kiyosawa, S. 2000. Exococcarins D, E and K from *Excoecaria agallocha*. J Nat Prod. 63: 344-346.

[55] Li, L., *et, al*. 2008 A-seco-oleane-type triterpenes from *Phomopsis sp*. (strain HKI0458) isolated from the mangrove plant *Hibiscus tiliaceus*. Phytochemistry. 69: 511-517.

[56] Biber, P. C. 2006. Measuring the effects of salinity stress in the red mangrove, *Rhizophora mangla* L. Afr J Agric Res. 1(1): 001-004.

[57] Hewag, C. M., *et, al*. 1998. Antibacterial activity of some medicinal plants of Srilanka. J Nat Sci Counc Srilanka. 26: 27-34.

[58] Taylor, J. L. S., Rabe, T., McGaw, L. J., Jäger A. K., and van Staden, J. 2001. Towards the scientific validation of traditional medicinal plants. Plant Growth Regul. 34(1): 23-37.

[59] Ncube, N. S., Afolayan, A. J., and Okoh, A. I. 2008. Assessment techniques of antimicrobial properties of natural compounds of plant origin: current methods and future trends. Afr J Biotechnol. 7(12): 1797-1800.

[60] Konishi, T., Takasaki, M., Tokuda, H., Kiyosawa, S., and Konoshima, T. 1998. Anti-tumor-promoting activity of diterpenes from *Excoecaria agallocha*. Biol Pharm Bull. 21: 993-996.

[61] Konishi, T., Konoshima, T., Fujiwara, Y., and Kiyosawa, S. 2000. Exococcarins D, E and K from *Excoecaria agallocha*. J Nat Prod. 63: 344-346.

[62] Rao, E. V. 2007. Drug discovery from plants. Curr Sci. 93(8): 1060.

[63] Roy, A., and Saraf, S. 2006. Limonoids: Overview of Significant Bioactive Triterpenes Distributed in Plants Kingdom. Biol. Pharm. Bull. 29(2): 191-201.

[64] Somrutai J., Chantachum S., Ratanaphan A., and Chantrapromma K., 2005. Stability of limonin from lime seeds. Electron. J. Environ. Agric. Food chem. 4: 938-944.

[65] Lakshmi, V., and Gupta, P. 2008. An Overview of the genus *Xylocarpus*. Nat Prod Res. 22: 1197: 1224.

[66] Champagne, D. E., Koul, O., Isman, M. B., Scudder, G. G. E., and Neil Towers, G. H. 1992. Biological activity of limonoids from the rutals. Phytochemistry. 31: 337-349.

[67] Wu, J., Zhang, S., Xiao, Q., Li, Q., Huang, J., Xiao, Z., and Huang, L. 2004. Xyloccensin L, a novel limonoid from *Xylocarpus granatum*. Tetrahedron Lett. 45: 591-593.

[68] Jacob, R., Hasegawa, S., and Manners, G. 2000. The potential of Citrus Limonoids as anticancer agents. Perishables Handling. 102: 6-8.

[69] Okamura, H., Yamauchi, K., Miyawaki, K., Iwagawa, T., and Nakatani, M. 1997. Synthesis and biological activities of degraded limonoids. (±)-fraxinellonone and its related compounds. Tetrahedron Lett. 38: 263-266.

[70] Akuduge, L., Gade, G., and Bohm, L. 2001. Cytotoxicity of azadirachtin A in human gliblastoma cell lines. Life Sci. 68: 1153-1160.

[71] Jung, H., *et, al*. 2000. Potentiating effect of obacunone from *Dictamnus dasycarpus* on cytotoxicity of microtubule inhibitors, vincristine, vinblastine and taxol. Planta Med. 66: 74-76.

[72] Manners, G. D., Jacob, R. A., Breksa, I. A. P., Hasegawa, S., and Schoch, T. K. 2003. Simultaneous separation and identification of limonoids from citrus using liquid chromatography-collision-induced dissociation mass spectra J. Agric. Food Chem. 51: 4156-4161.

[73] Saxena, S., Pant, N., Jain, D. C., and Bhakuni, R. S. 2003. Antimalarial agents from plant sources. Curr. Sci. 85: 1314-1329.

[74] Bickii, J., Njifutie, N., Ayafo,r F. J., Basco, L. K., and Ringwald, P. 2000. *In vitro* antimalarial activity of limonoids from *Khaya grandifoliola* C.D.C. (Maliaceae).J.Ethnopharmacology. 69: 27-33.

[75] Krief, S., Martin, M. T., Grellier, P., Kasenene, J. and Sevenet, T. 2004. Novel antimalarial compounds isolated in a survey of self-medicative behavior of wild chimpanzee in Uganda. Antimicrob.Agents Chemother. 48: 3196-3199.

[76] Abdelgaleil, S. A., Hashinaga, F., and Nakatani M. 2005. Antifungal activity of limonoids from *Khaya ivorensis*. Pest Manag. Sci. 61: 186-190.

[77] Govindachari, T. R., *et, al*. 1999. Swietenolide diacetate from the seeds of *Swietenia macrophylla*. J. Chem. Ecol. 25: 923-933.

[78] Sunthitikawinsakul, A., *et, al*. 2003. Anti-HIV-1 limonoid: first isolation from *Clausena excavata*. Phytother. Res. 17: 1101-1103.

[79] Sastri, B. N. 1950. The wealth of India; Raw Materiales, Vol. 2(C), pp. 74-75, New Delhi, Publication and Infromation Directorate, CSIR.

[80] Banerji, B., and Nigam, S. K. 1984. Wood constituents of Meliaceae: A review. Fitoterapia. 55: 3-36.

[81] Chopra, R. N., Nayar, S. L., and Chopra, I. C. 1956. Glossary of Indian Medicinal Plants. Ed. V, New Delhi: CSIR.

[82] Uddin, S. J., *et, al*. 2005. Antidiarrhoeal activity of the methanol extract of the barks of *Xylocarpus moluccensis* in castor oil- and magnesium sulphate-induced diarrhoea models in mice. J.Ethnopharmacol. 101: 139-143.

[83] Choudhary, S., Sree, A., Mukherjee, S., Patnaik, P. and Bapuji, M. 2005. *In Vitro* Antibacterial Activity of Extracts of Selected Marine Algae and Mangroves against Fish Pathogens. Aisan Fisheries Sci. 18: 285.

[84] Wu, J., *et, al*. 2005. Two new mexicanolides from the fruit of the Chinese mangrove *Xylocarpus granatum*. J. Chem Sci. 60: 1291-1294.

[85] JSTOR PLANT SCIENCE. Entry for *Xylocarpus moluccensis* Lam. M. J. Roem. [family MELIACEAE]. [Online] Available from: http://plants.jstor.org/flora/fz1407 [2010, October 27]

[86] Taylor, D.A.H. 1983. Limonoid Extractive From *Xylocarpus moluccensis*. Phytochemistry. 22: 1297-1299.

[87] Li, M.Y., *et, al*. 2009. Moluccensins A-G, Phragmalins with a Conjugated C-30 Carbonyl Group from a Krishna Mangrove, *Xylocarpus moluccensis*. J. Nat. Prod, 72: 1657-1662.

[88] Pudhom, K., Sommit, D., Nuclear, P., Ngamrojanavanich, N., and Petsom, A. 2010. Moluccensins H-J, 30-Ketophragmalin Limonoids from *Xylocarpus moluccensis*. J. Nat. Prod. 73: 263–266.

[89] Wu, J., *et, al*. 2010. Limonoids and Tirucallane Derivatives from the Seeds of a Krishna Mangrove, *Xylocarpus moluccensis*. J. Nat. Prod. 73: 6446-6449.

[90] Zhang, J., *et, al*. 2010. Mexicanolides from the Seeds of a Krishna Mangrove, *Xylocarpus moluccensis*. Chem. Pharm. Bull. 58: 552-555.

[91] Adesogan, E. K., and Taylor, D. A. H. 1970. Limonoid Extractives from *Khaya ivorensis*. J. Chem. Soc. (C): 1710-1714.

[92] Kadota, S., Marpaung, L., Kikuchi, T., and Ekimoto, H. 1990. Mahagonin, a novel dimeric tetranortriterpenoid from Swietenia mahagoni Jacq. Chem. Pharm. Bull. 38: 639.

[93] Payla, P. A. *et, al*. 2006. Limonoids from Andiroba Oil and *Cedrela fissilis* and their Insecticidal Activity. J. Braz. Chem. Soc. 17: 542-547.

[94] Sarigaputi, C. 2009. Bioactive compounds from the seeds kernels of *Xylocarpus rumphii* (Kostel.) Mabb. Master's Thesis. Department of Biotechnology Faculty of Science Chulalongkorn University

[95] Li, J., *et, al.* 2010. Limonoids from the seeds of a Godavari mangrove, Xylocarpus moluccensis. Phytochemistry. 71: 1917-1924.

APPENDIX

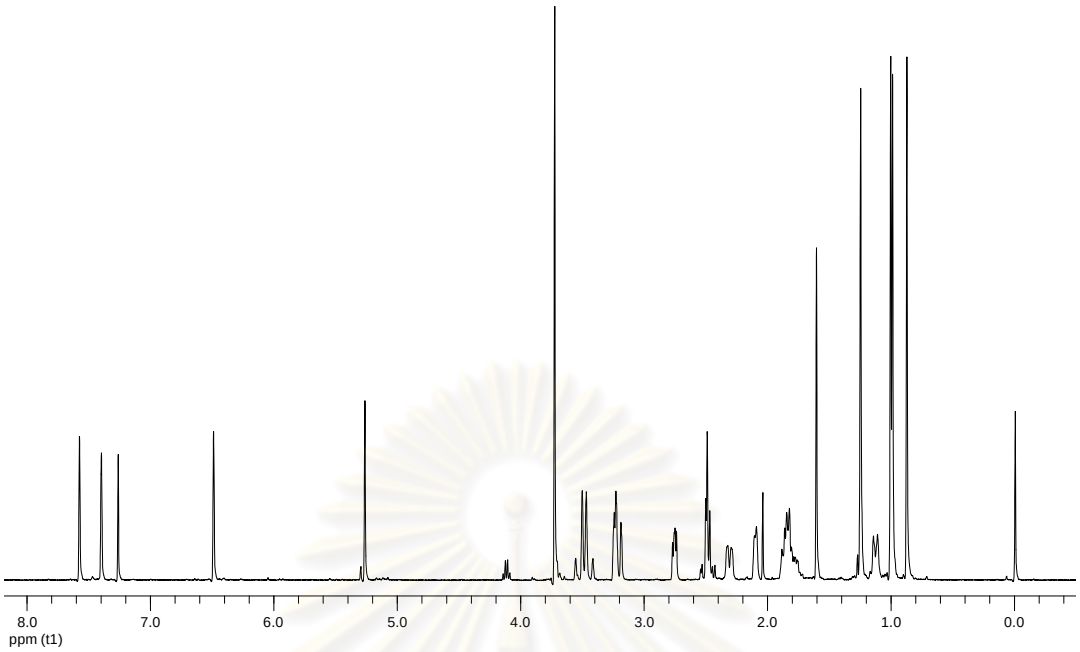

Figure S-1 ^{1}H NMR (400 MHz) spectrum of compound **1** ($CDCl_3$)

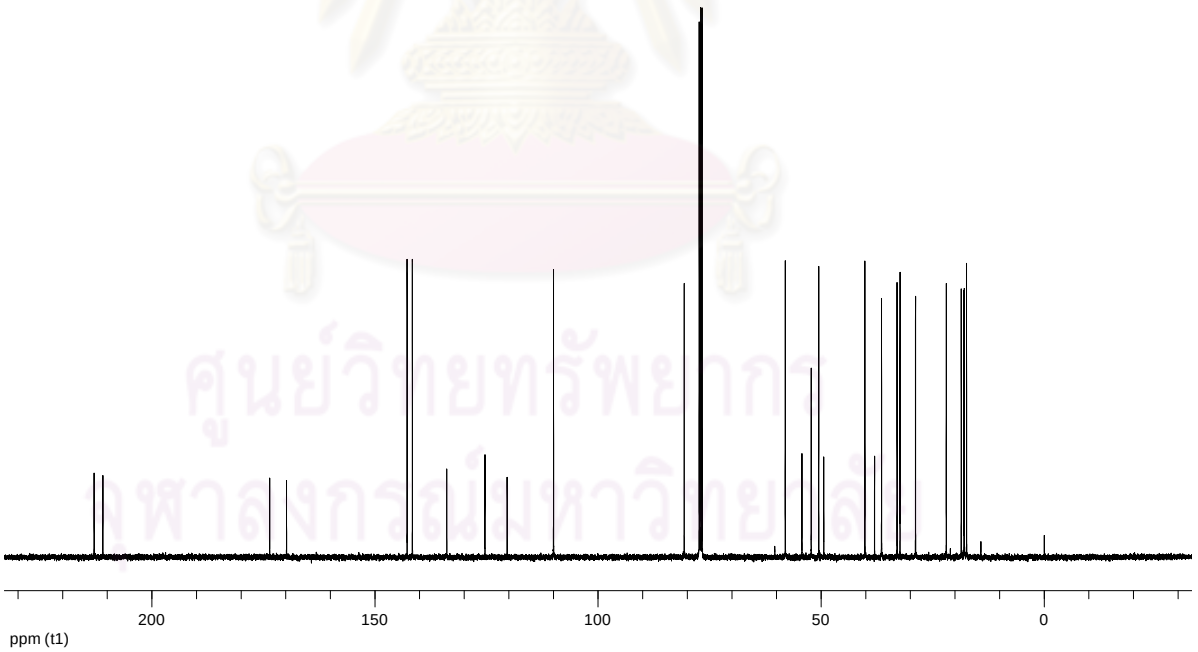

Figure S-2 ^{13}C NMR (100 MHz) spectrum of compound **1** ($CDCl_3$)

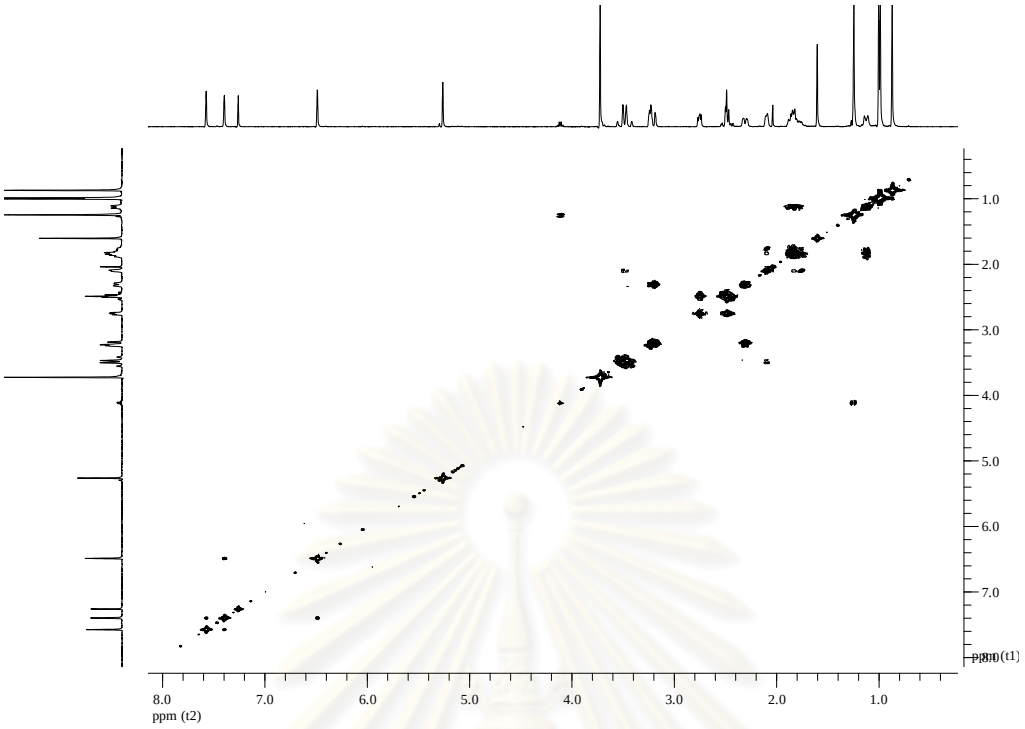

Figure S-3 ^{1}H-^{1}H COSY spectrum of compound **1** ($CDCl_3$)

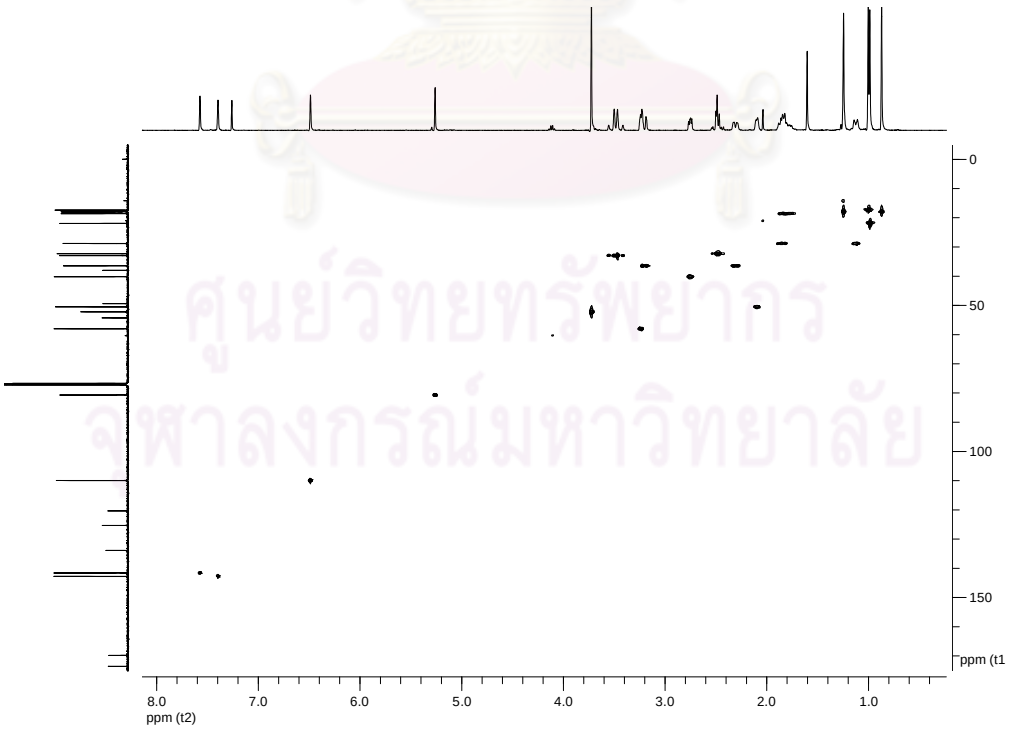

Figure S-4 HSQC spectrum of compound **1** ($CDCl_3$)

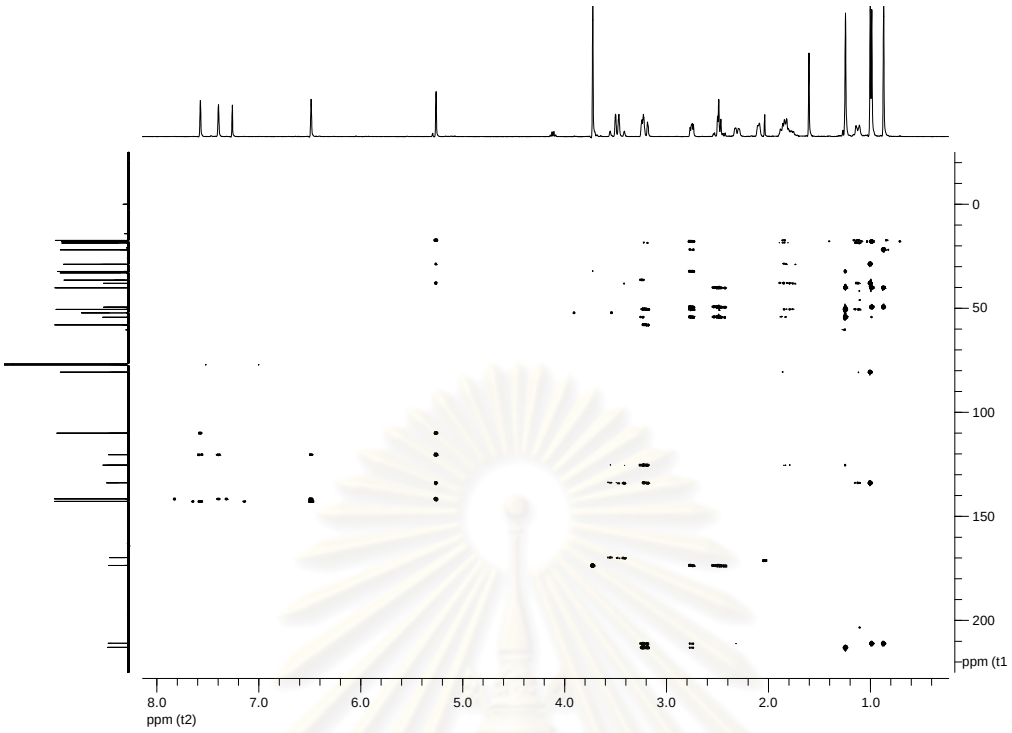

Figure S-5 HMBC spectrum of compound **1** ($CDCl_3$)

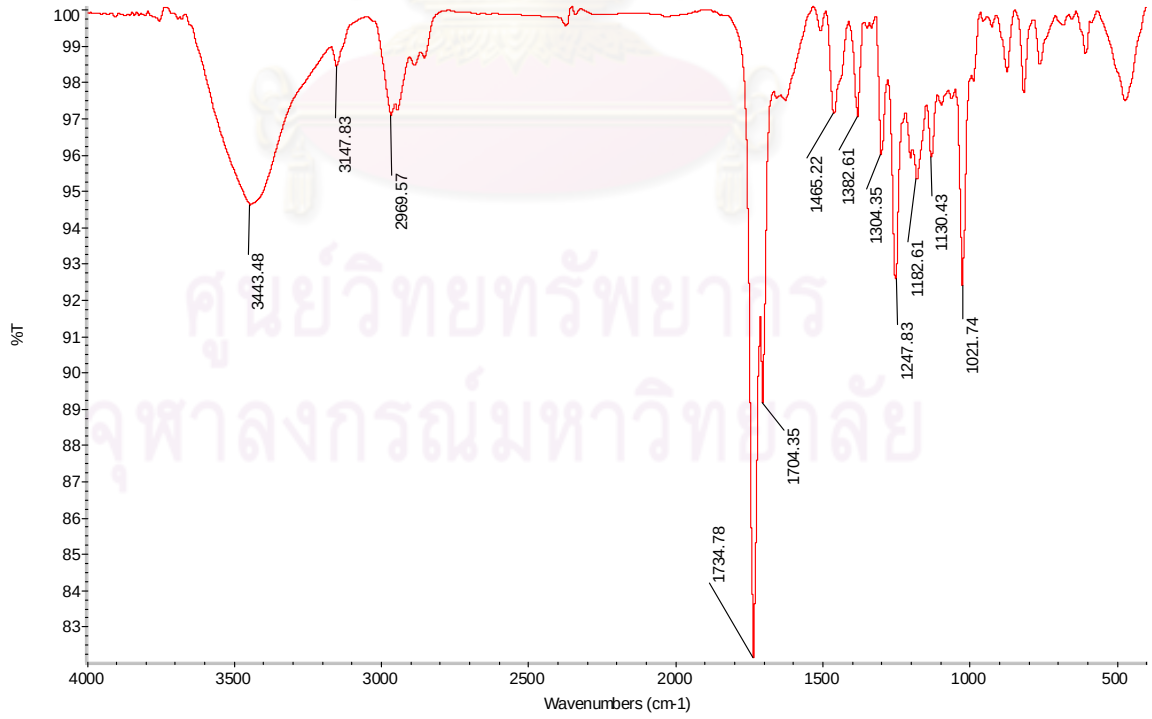

Figure S-6 IR spectrum of compound **1** (KBr)

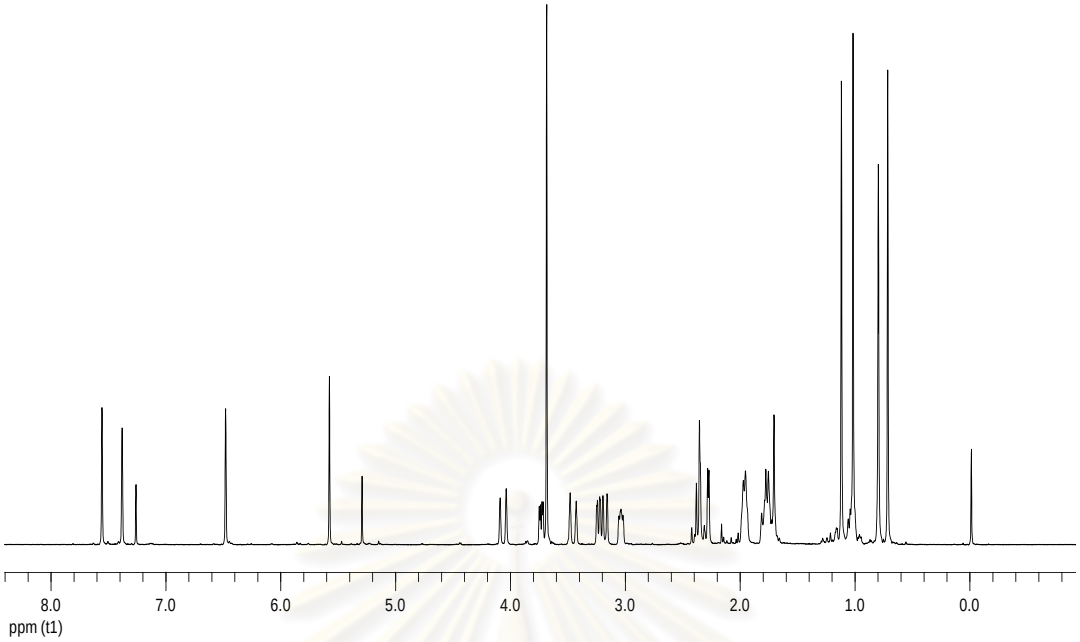

Figure S-7 ^{1}H NMR (400 MHz) spectrum of compound **2** ($CDCl_3$)

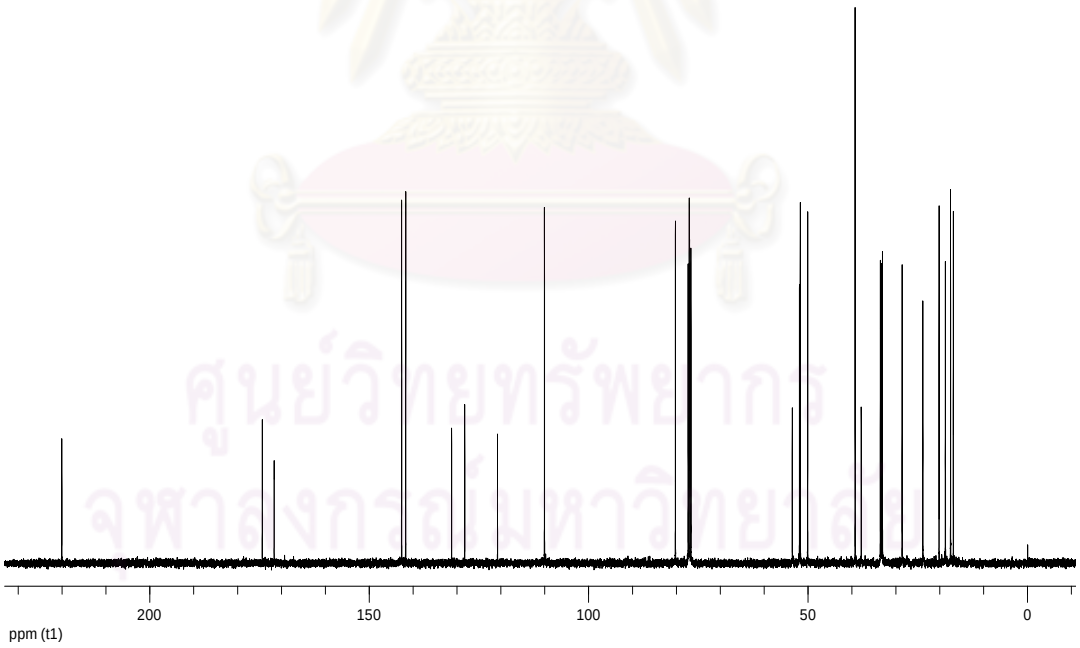

Figure S-8 ^{13}C NMR (100 MHz) spectrum of compound **2** ($CDCl_3$)

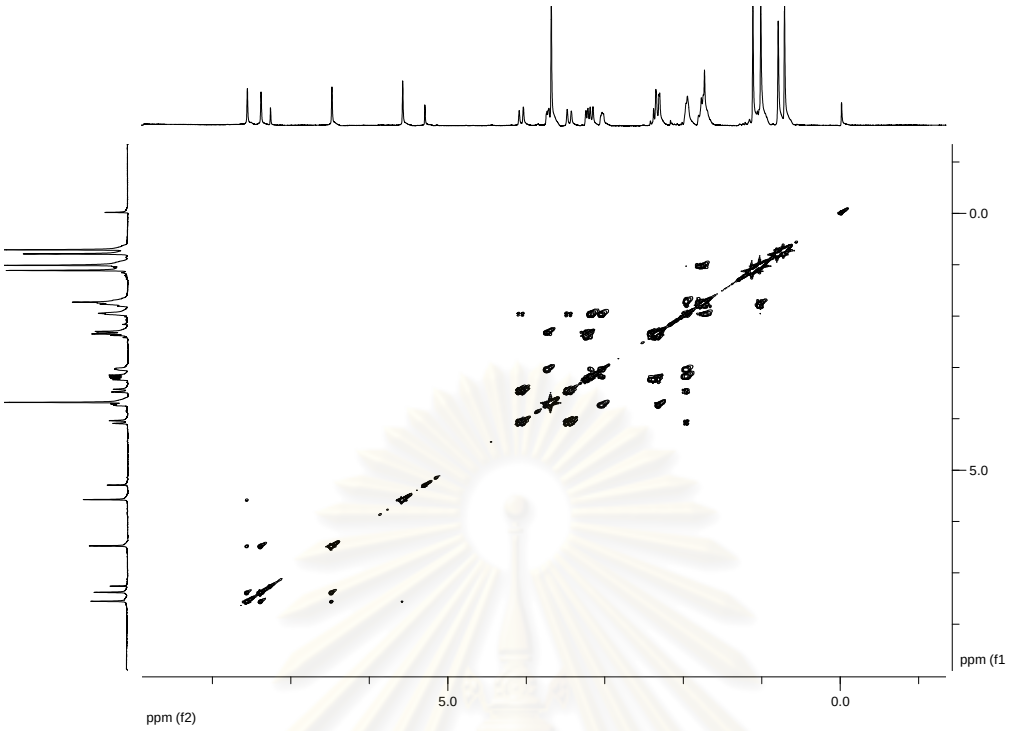

Figure S-9 ^{1}H-^{1}H COSY spectrum of compound **2** ($CDCl_3$)

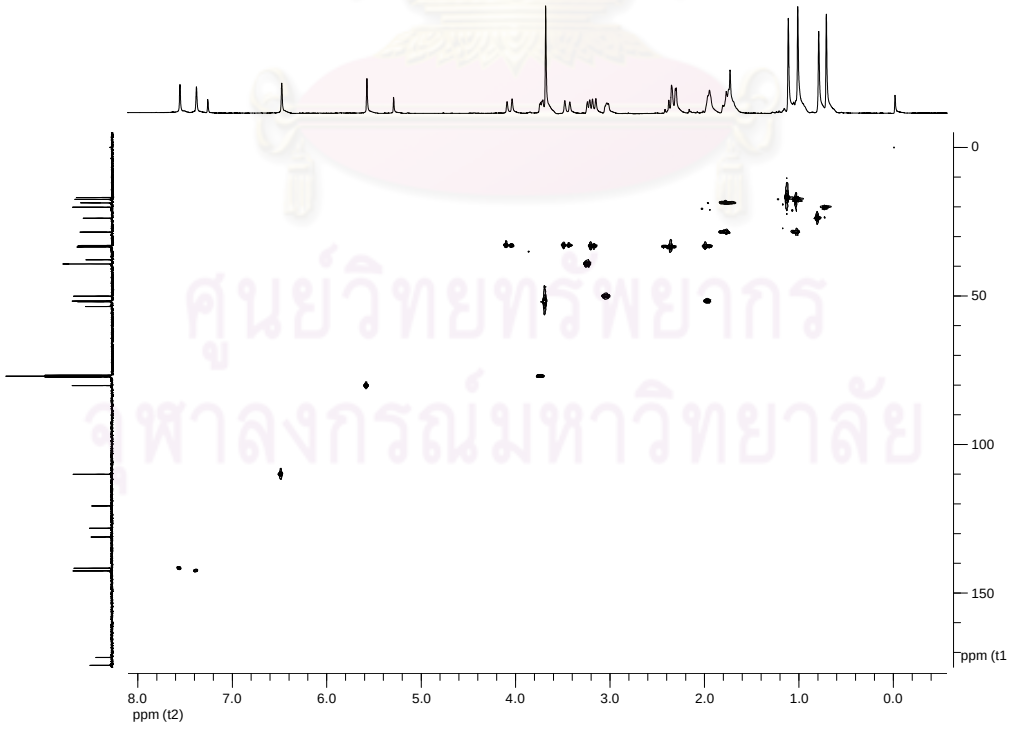

Figure S-10 HSQC spectrum of compound **2** ($CDCl_3$)

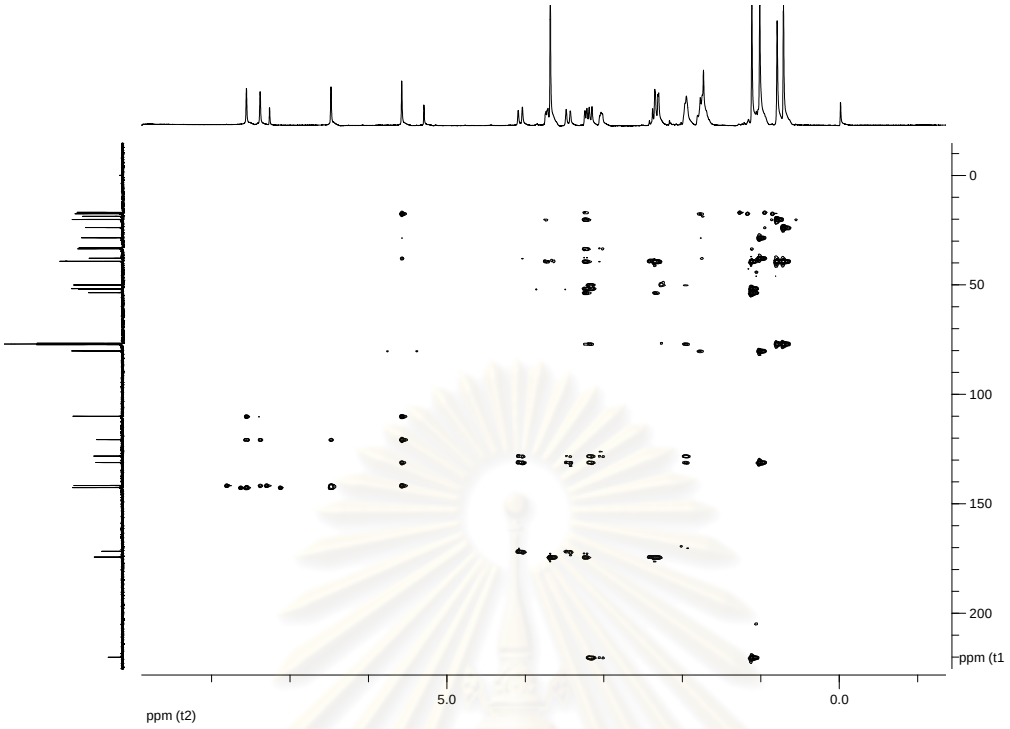

Figure S-11 HMBC spectrum of compound **2** ($CDCl_3$)

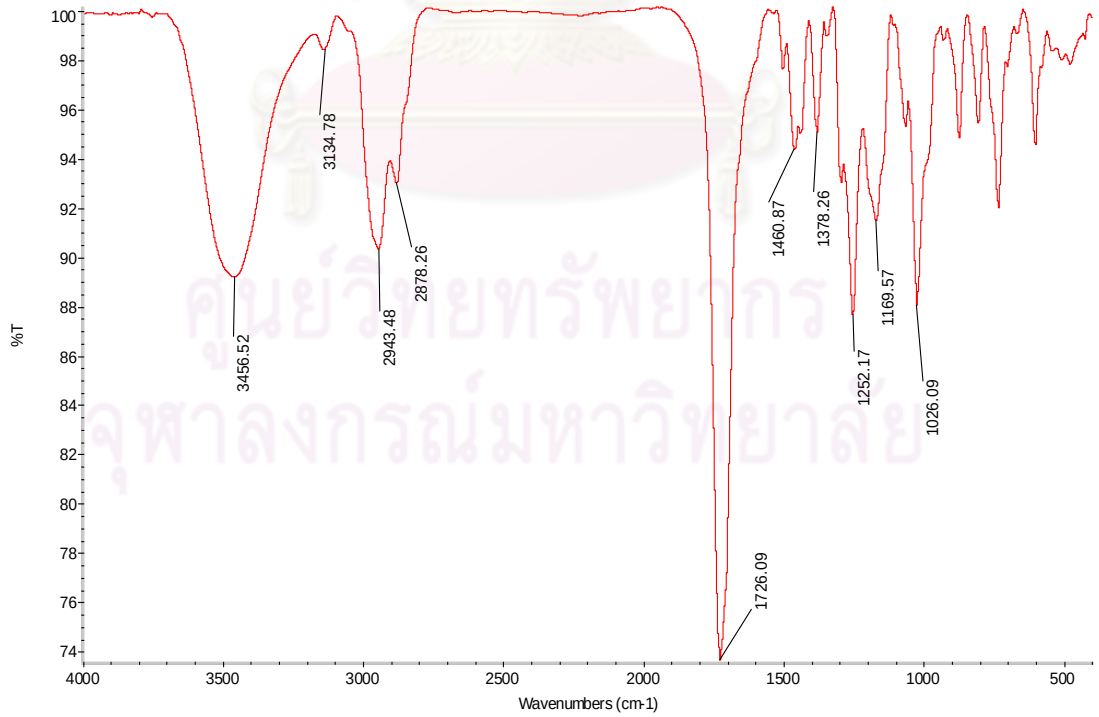

Figure S-12 IR spectrum of compound **2** (KBr)

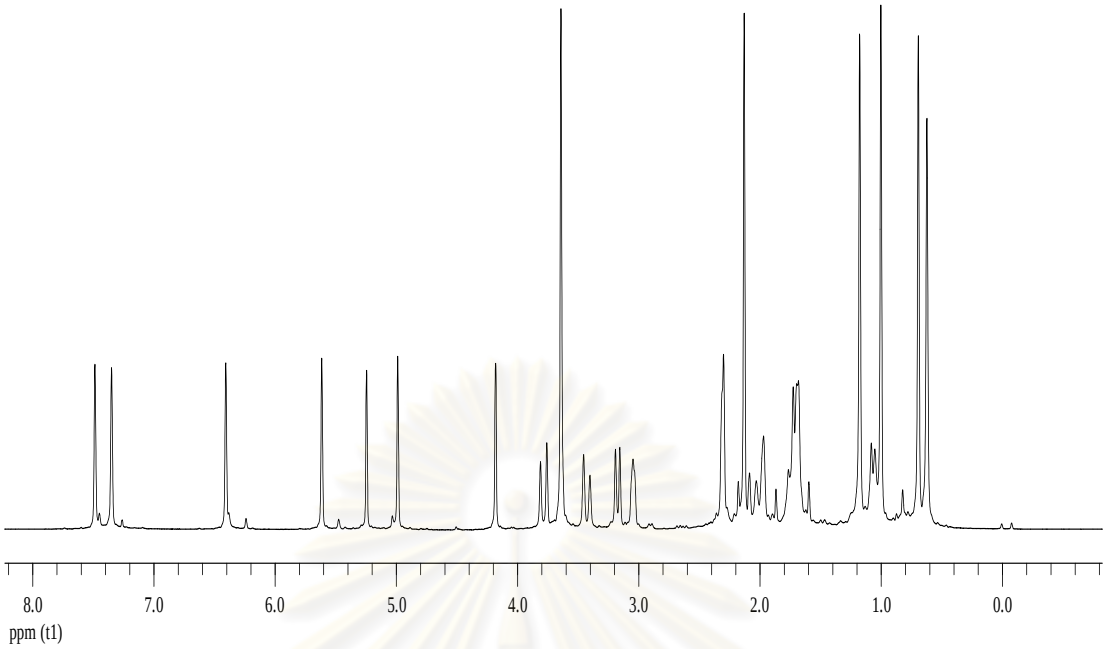

Figure S-13 ^{1}H NMR (400 MHz) spectrum of compound **3** ($CDCl_3$)

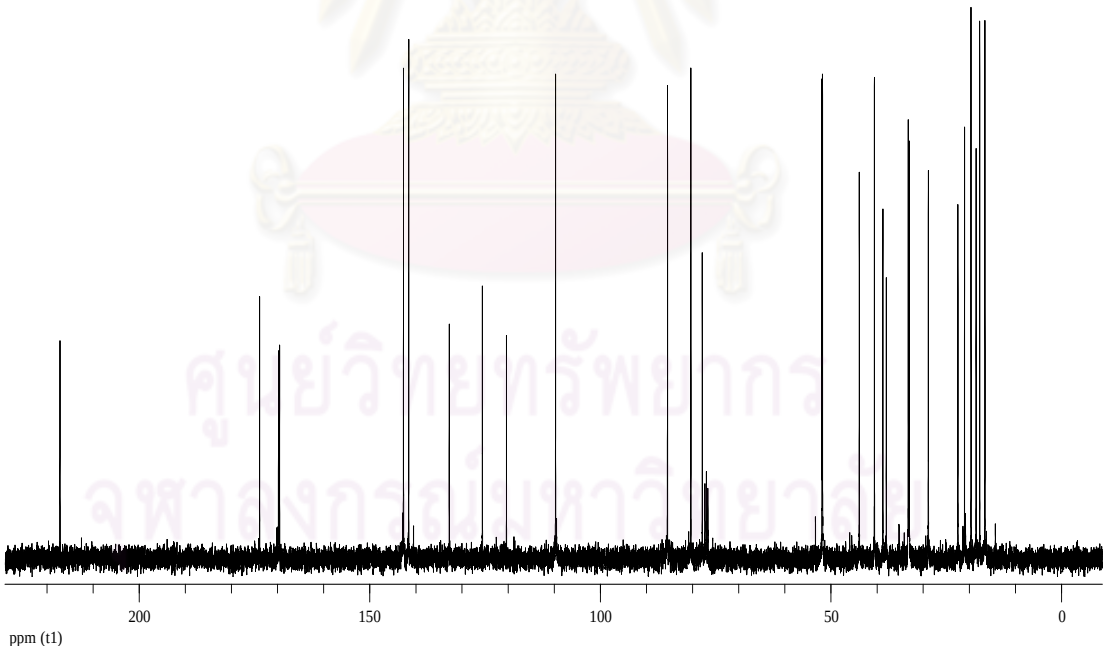

Figure S-14 ^{13}C NMR (100 MHz) spectrum of compound **3** ($CDCl_3$)

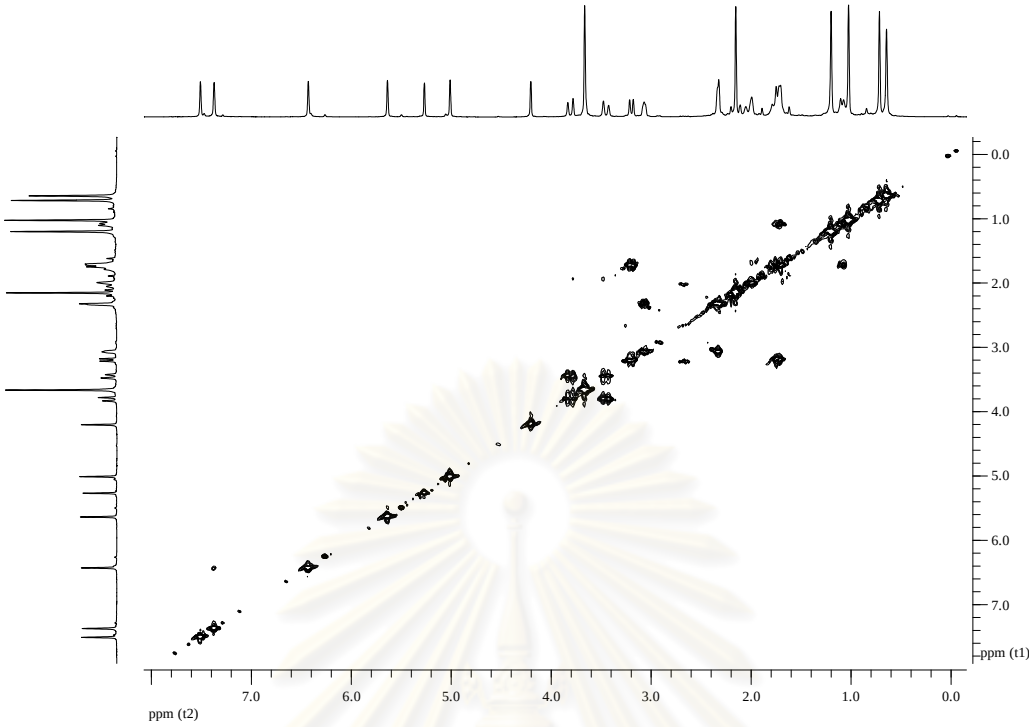

Figure S-15 ^{1}H-^{1}H COSY spectrum of compound **3** ($CDCl_3$)

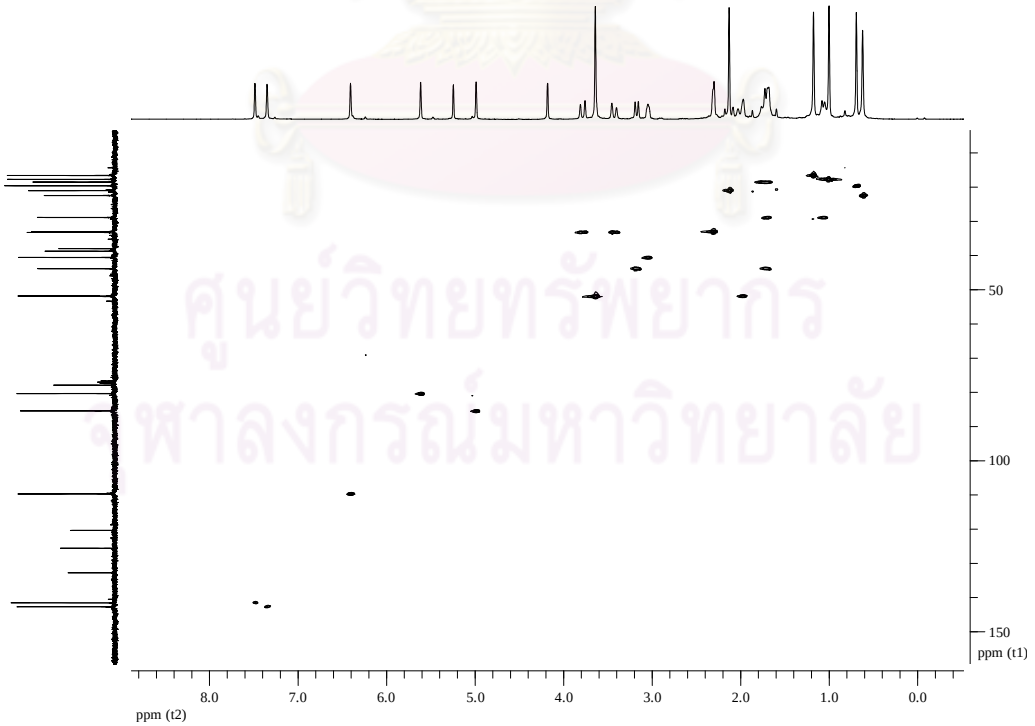

Figure S-16 HSQC spectrum of compound **3** ($CDCl_3$)

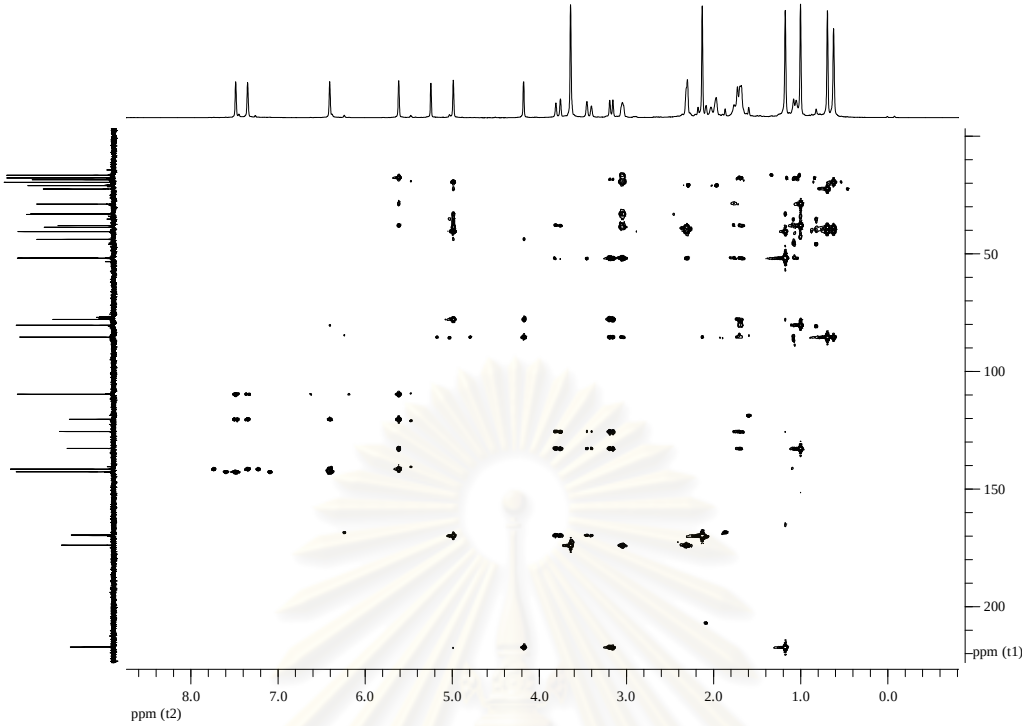

Figure S-17 HMBC spectrum of compound **3** ($CDCl_3$)

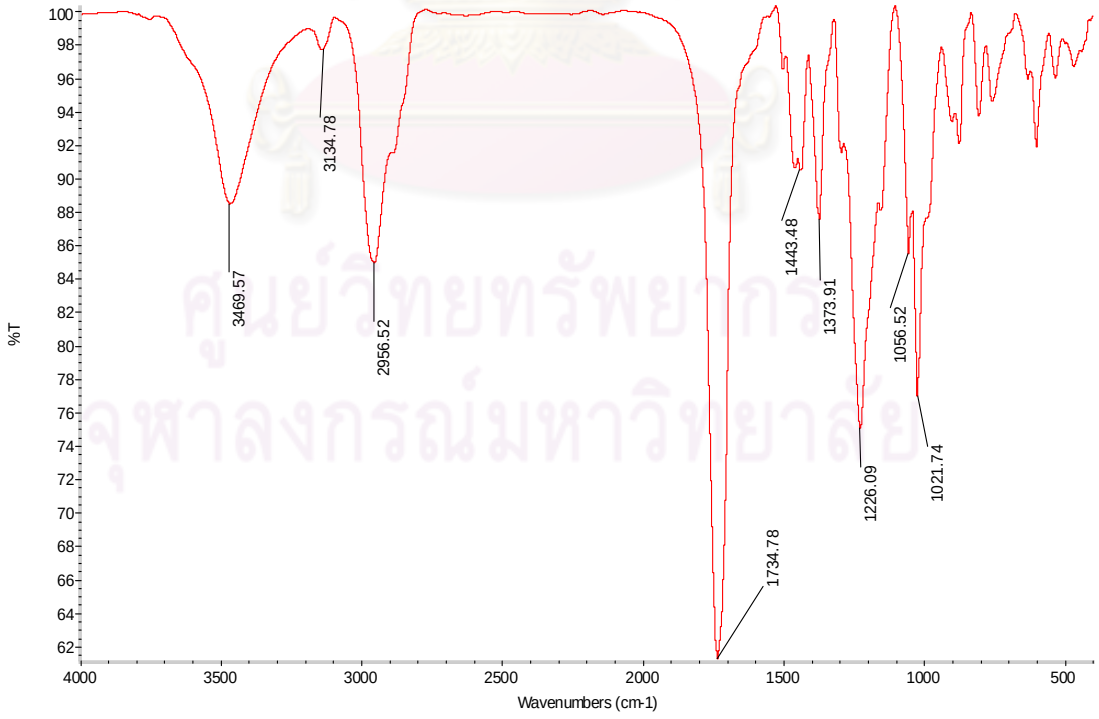

Figure S-18 IR spectrum of compound **3** (KBr)

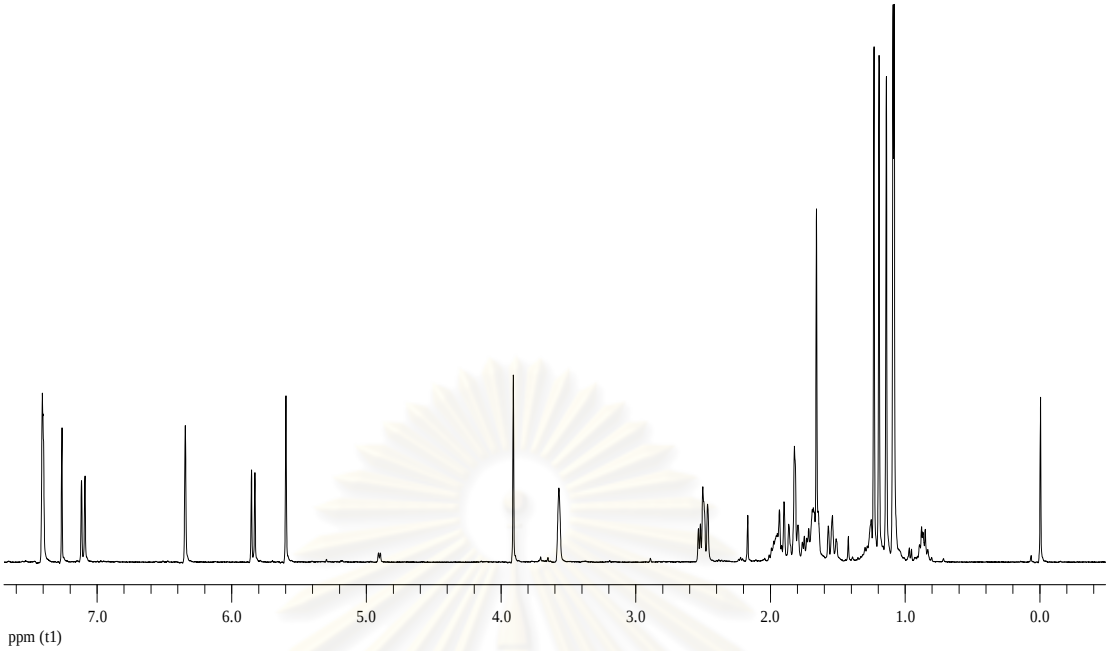

Figure S-19 ^{1}H NMR (400 MHz) spectrum of compound **4** ($CDCl_3$)

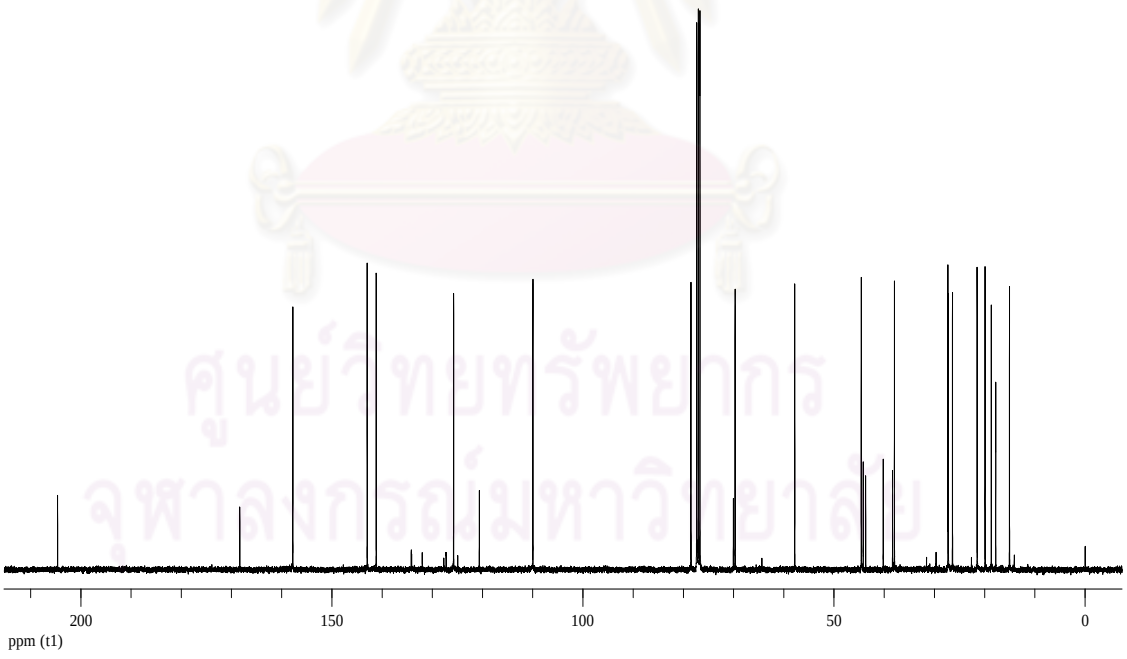

Figure S-20 ^{13}C NMR (100 MHz) spectrum of compound **4** ($CDCl_3$)

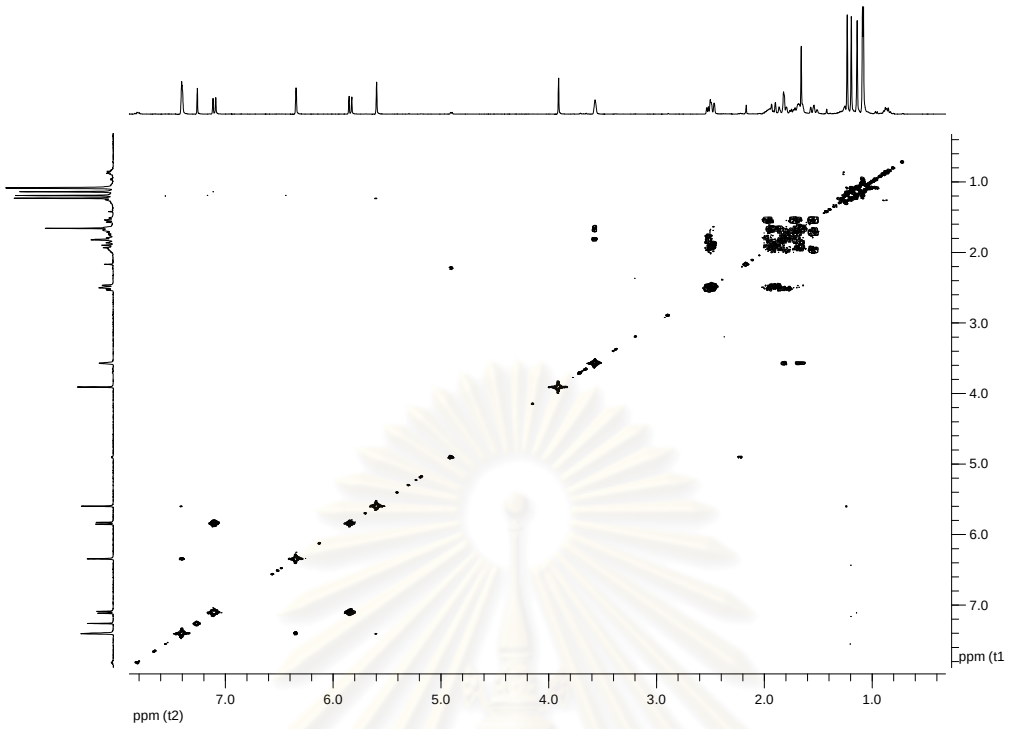

Figure S-21 ^{1}H-^{1}H COSY spectrum of compound **4** ($CDCl_3$)

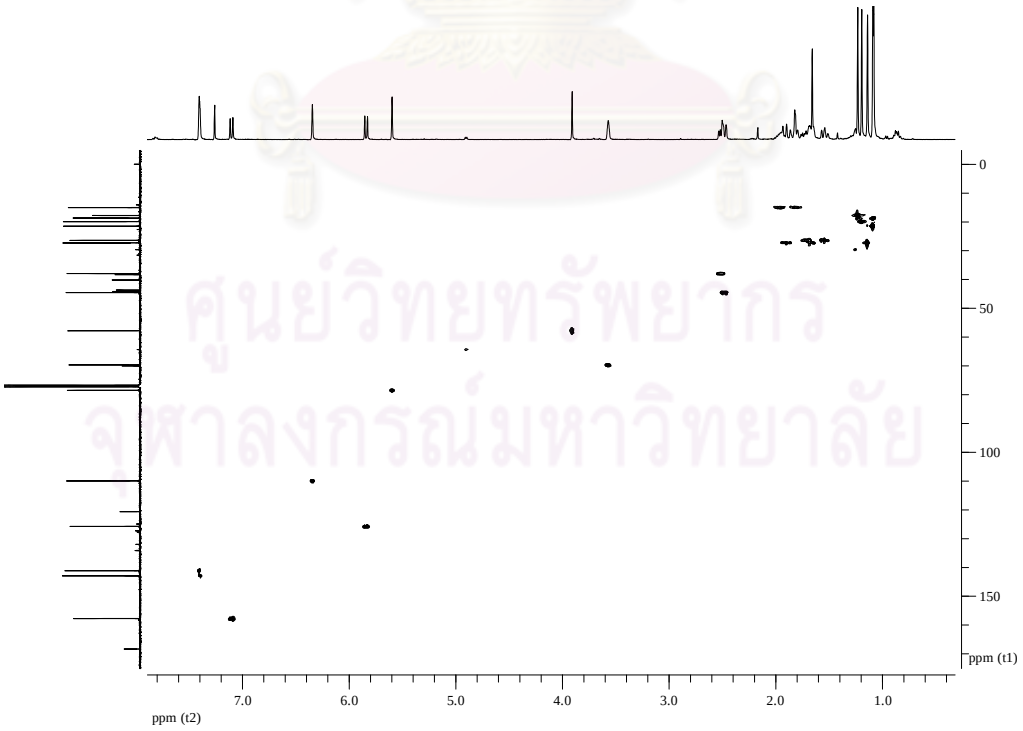

Figure S-22 HSQC spectrum of compound **4** ($CDCl_3$)

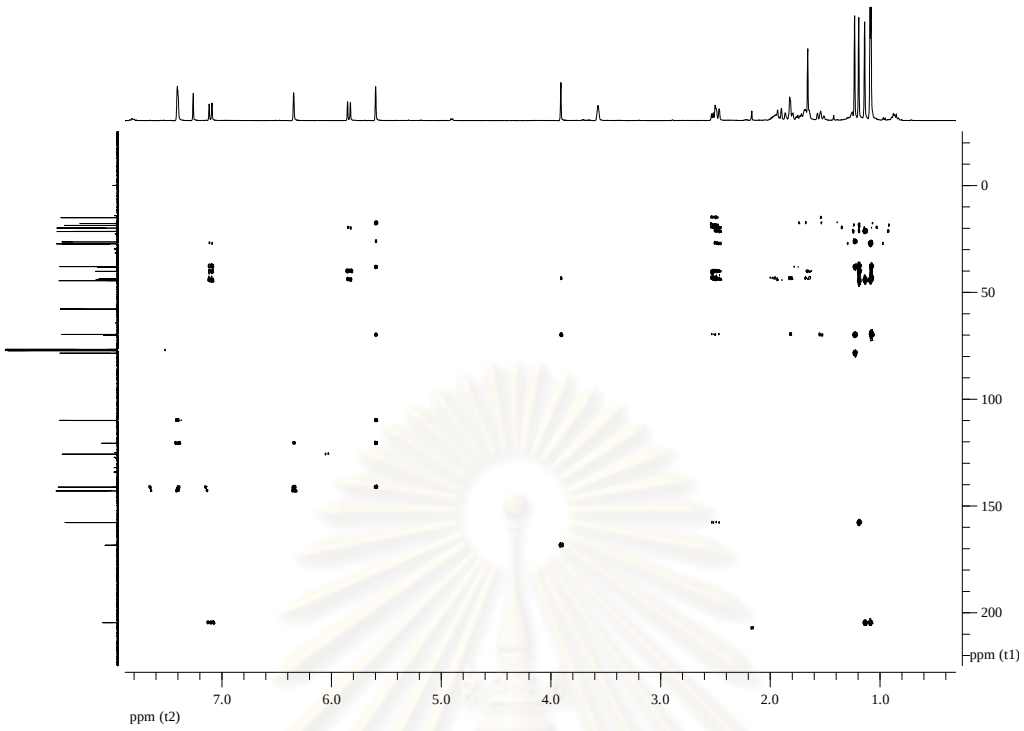

Figure S-23 HMBC spectrum of compound **4** ($CDCl_3$)

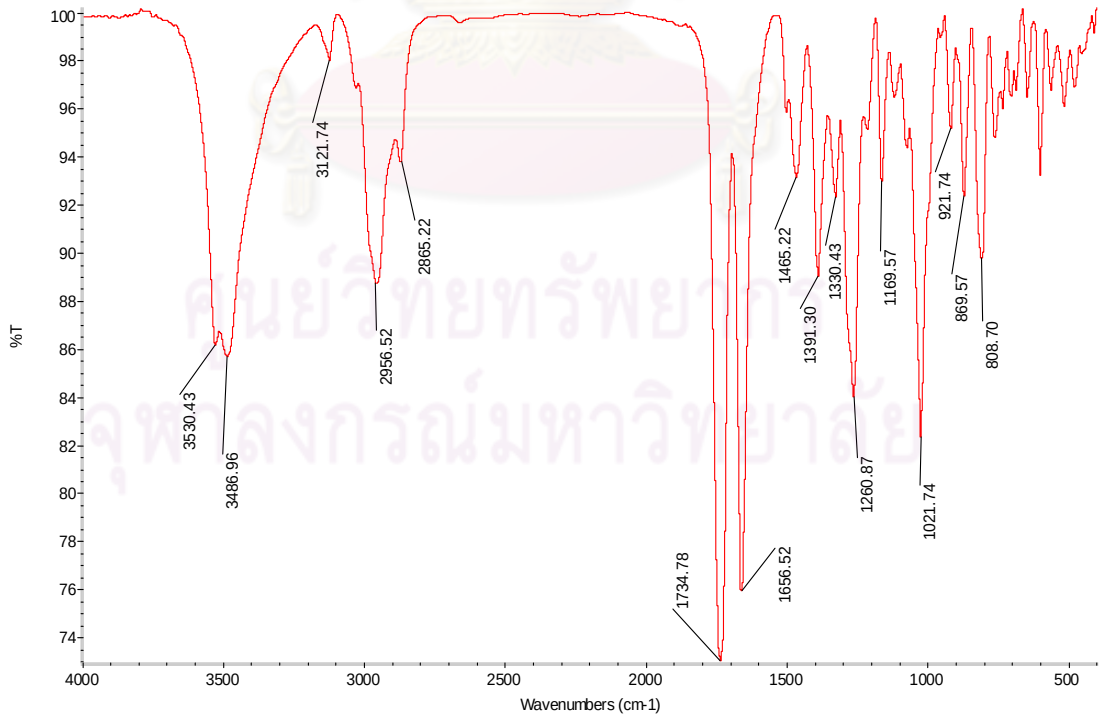

Figure S-24 IR spectrum of compound **4** (KBr)

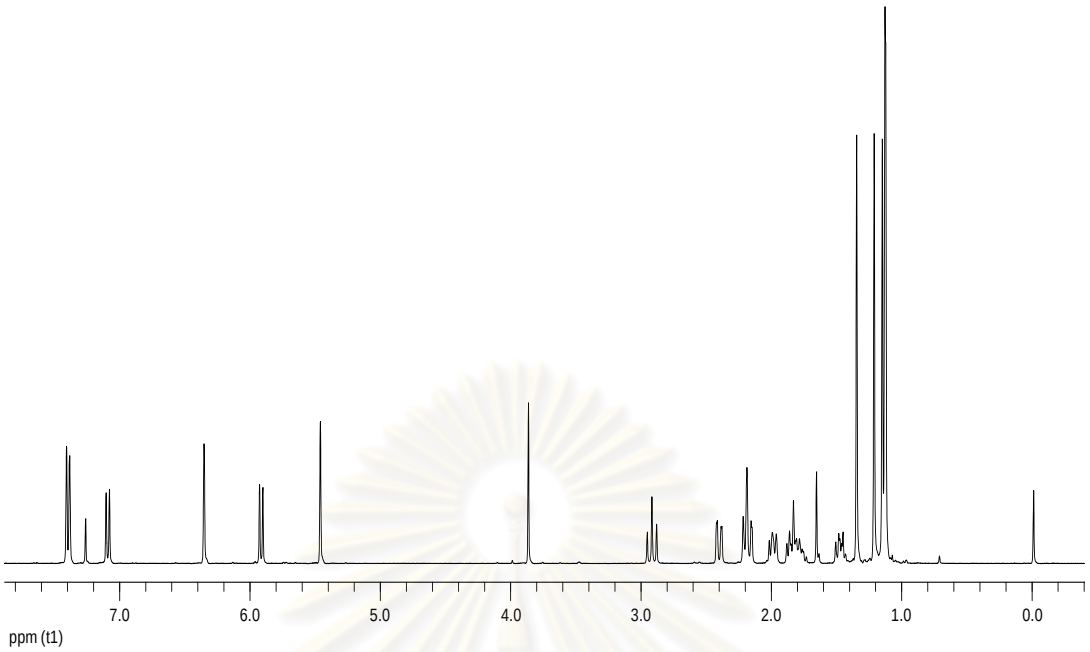

Figure S-25 ^{1}H NMR (400 MHz) spectrum of compound **5** ($CDCl_3$)

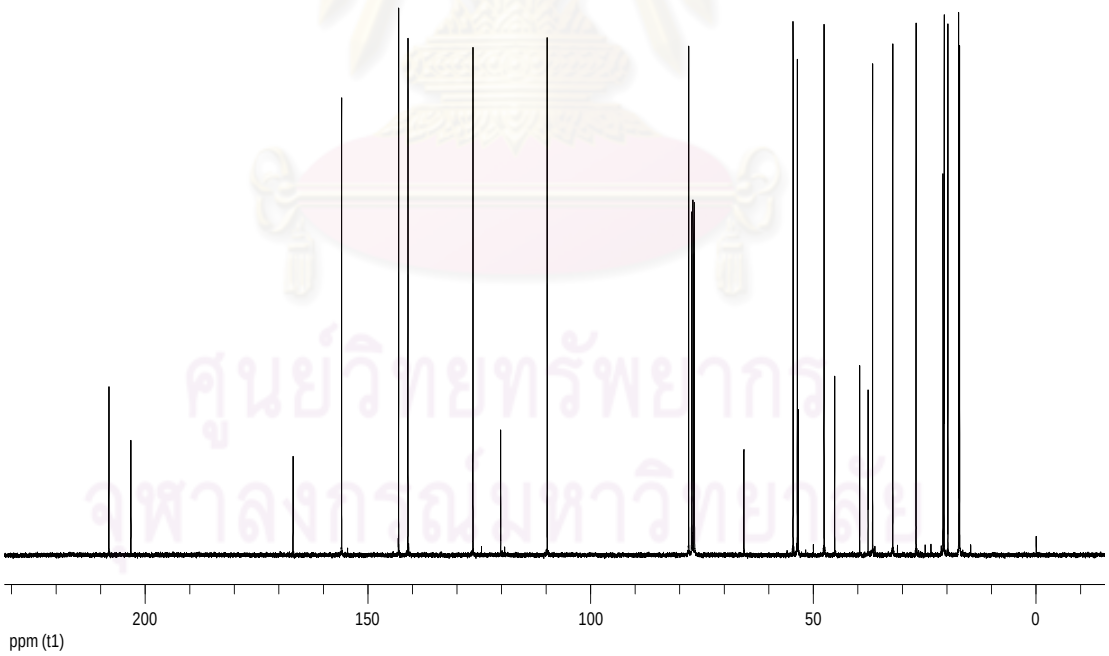

Figure S-26 ^{13}C NMR (100 MHz) spectrum of compound **5** ($CDCl_3$)

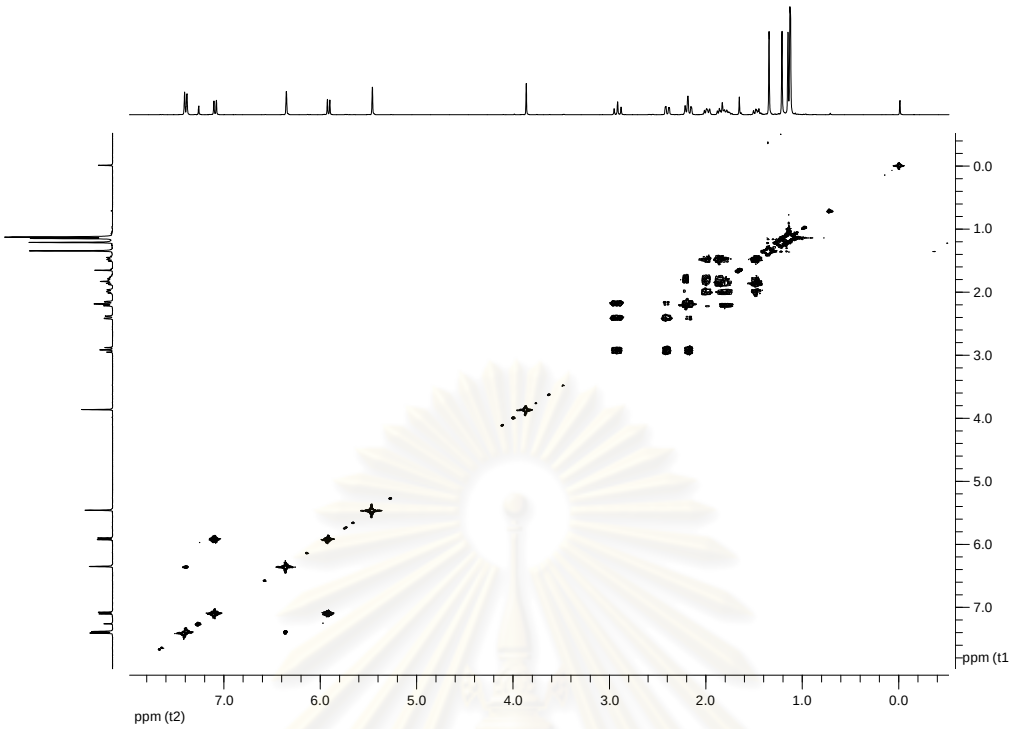

Figure S-27 ^{1}H-^{1}H COSY spectrum of compound **5** ($CDCl_3$)

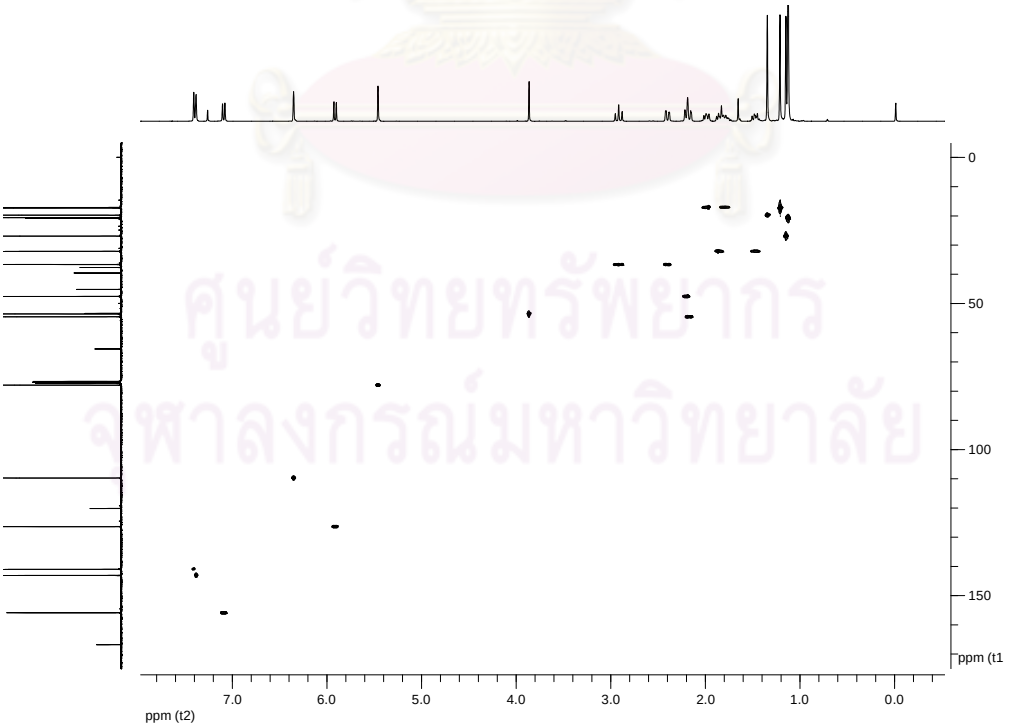

Figure S-28 HSQC spectrum of compound **5** ($CDCl_3$)

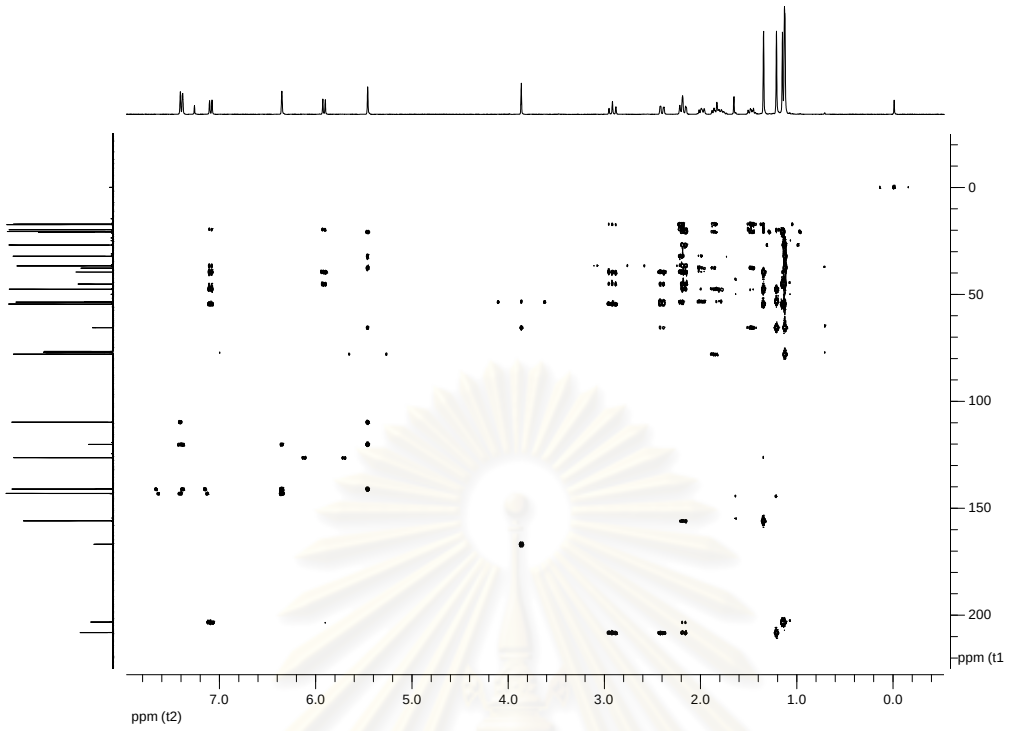

Figure S-29 HMBC spectrum of compound **5** ($CDCl_3$)

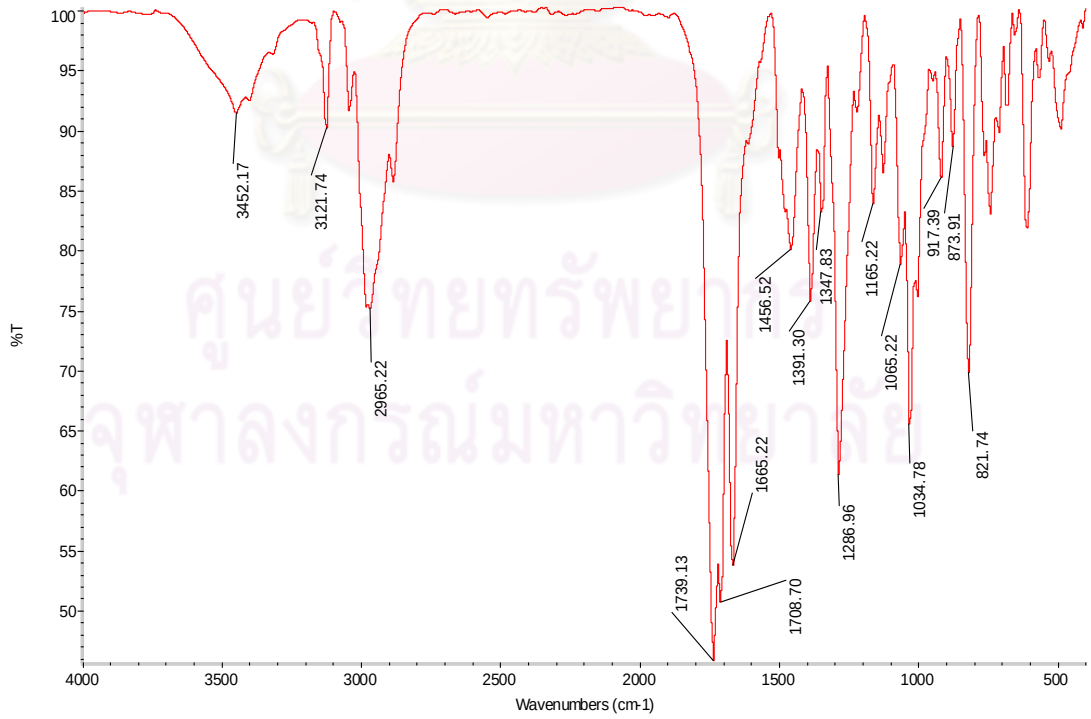

Figure S-30 IR spectrum of compound **5** (KBr)

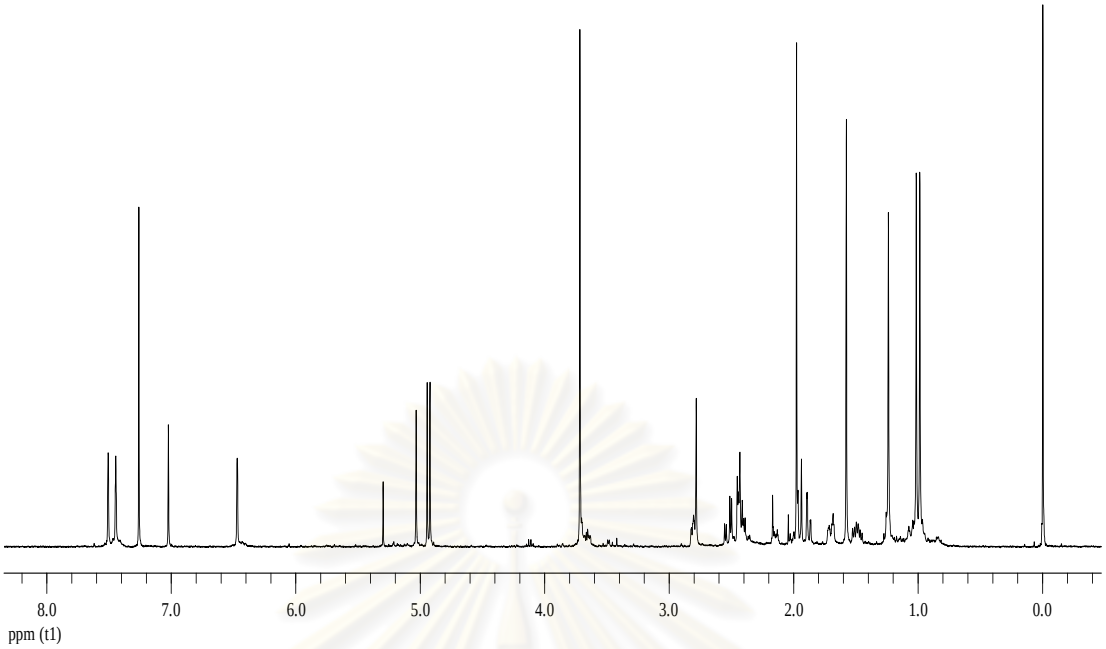

Figure S-31 ^{1}H NMR (400 MHz) spectrum of compound **6** ($CDCl_3$)

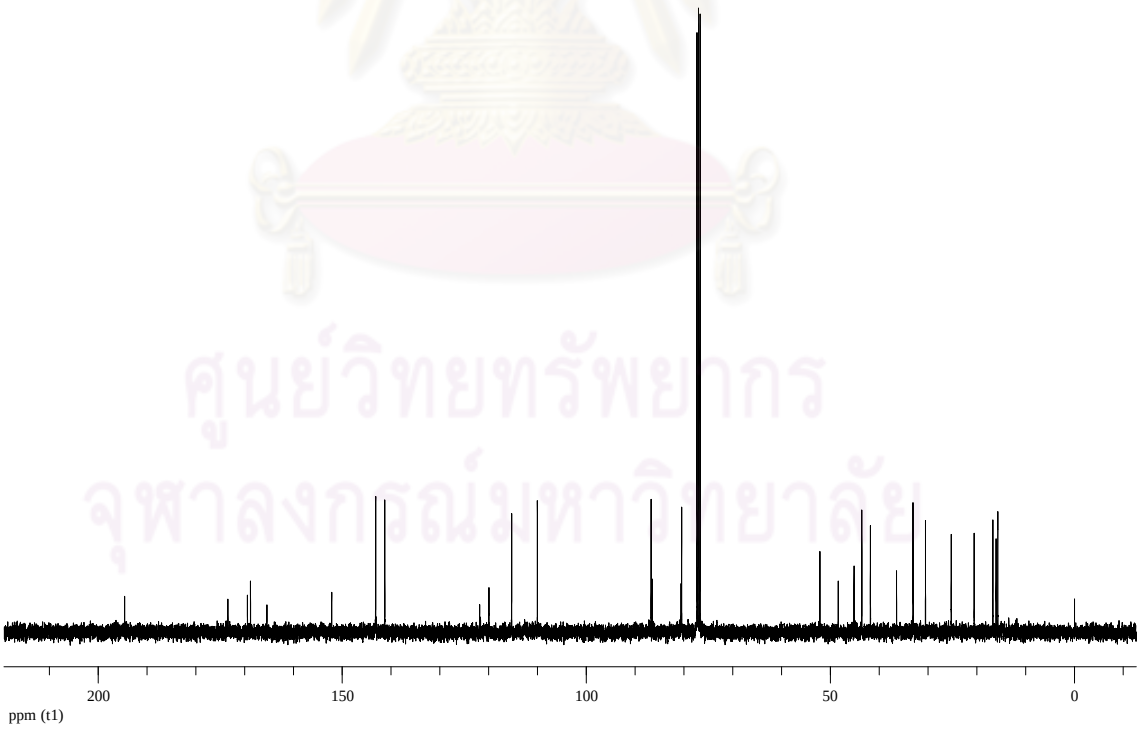

Figure S-32 ^{13}C NMR (100 MHz) spectrum of compound **6** ($CDCl_3$)

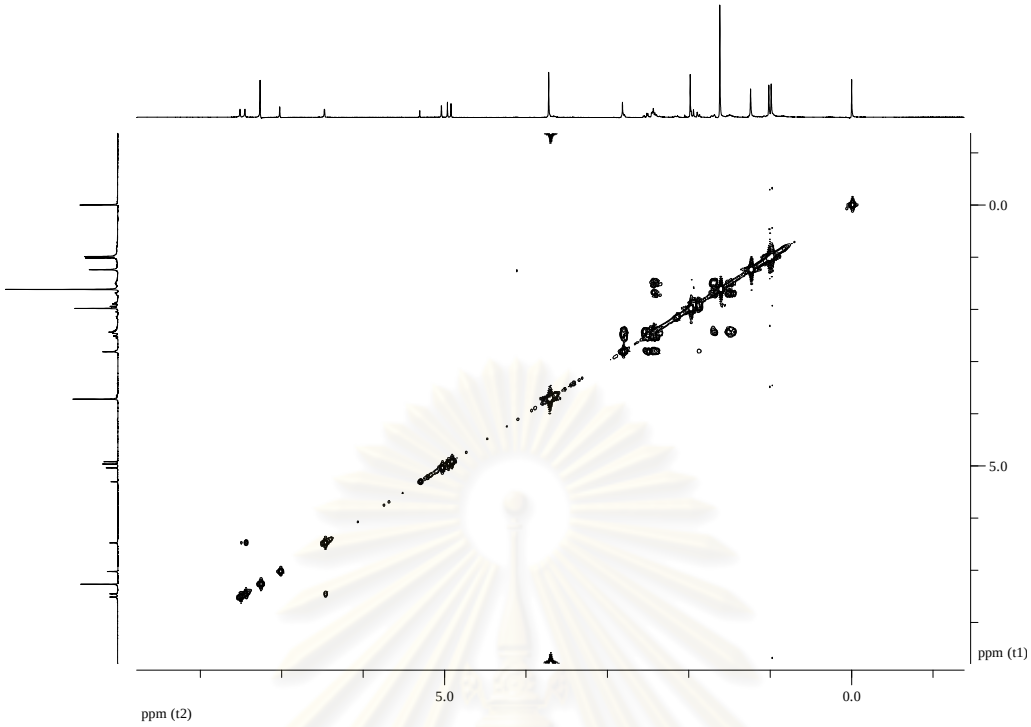

Figure S-33 ^{1}H-^{1}H COSY spectrum of compound **6** ($CDCl_3$)

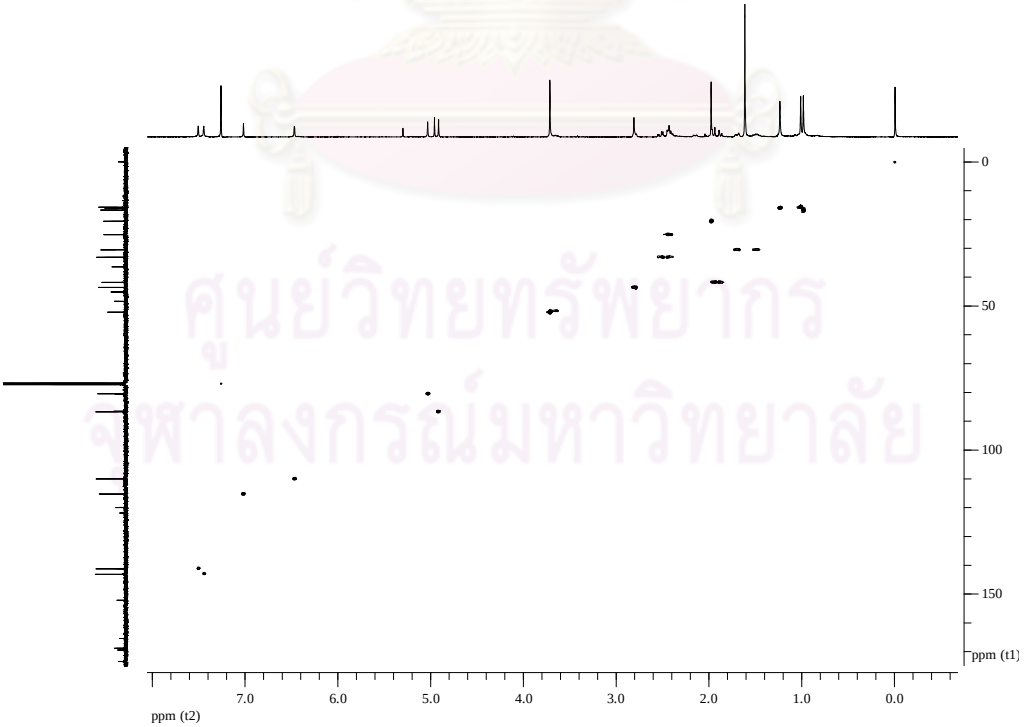

Figure S-34 HSQC spectrum of compound **6** ($CDCl_3$)

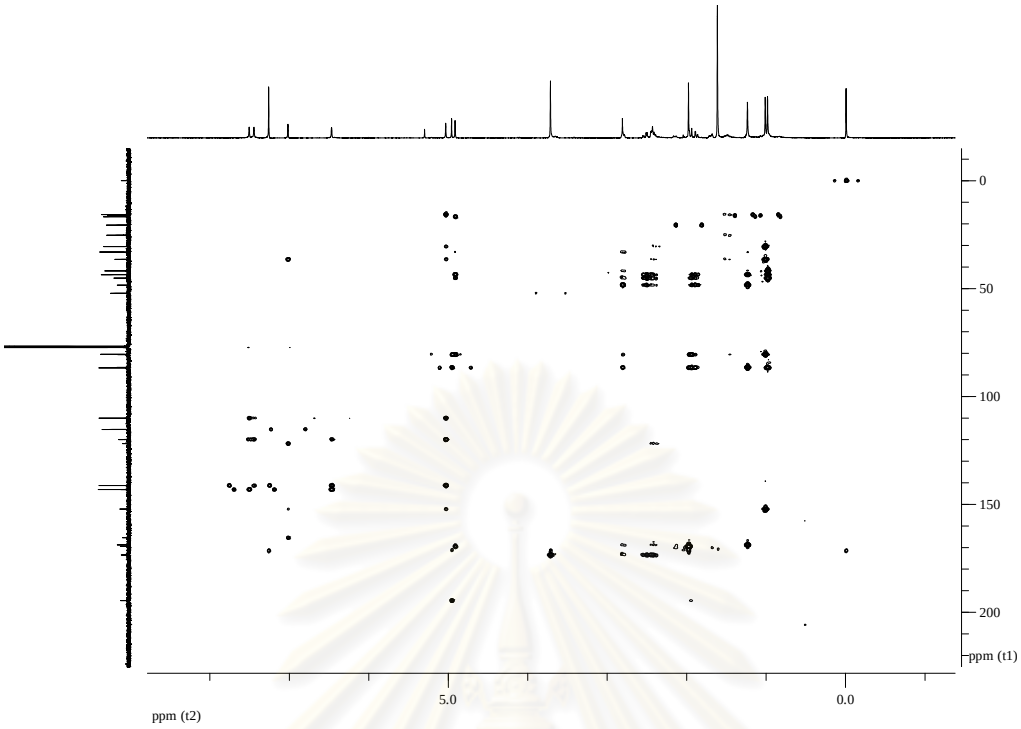

Figure S-35 HMBC spectrum of compound **6** ($CDCl_3$)

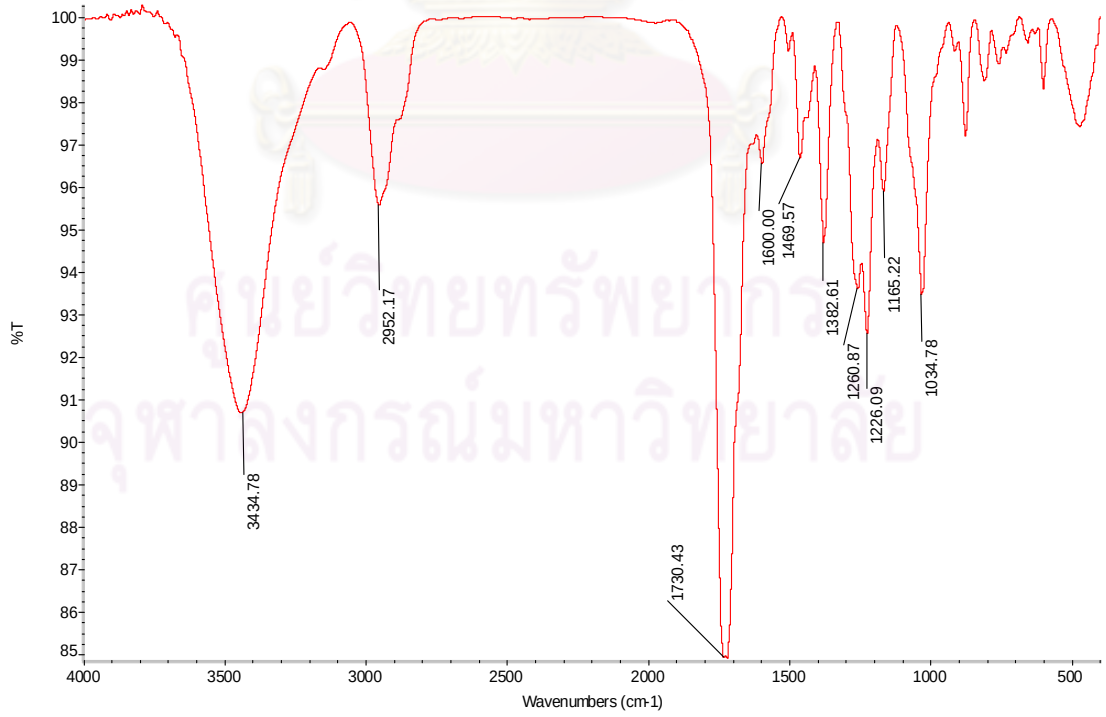

Figure S-36 IR spectrum of compound **6** (KBr)

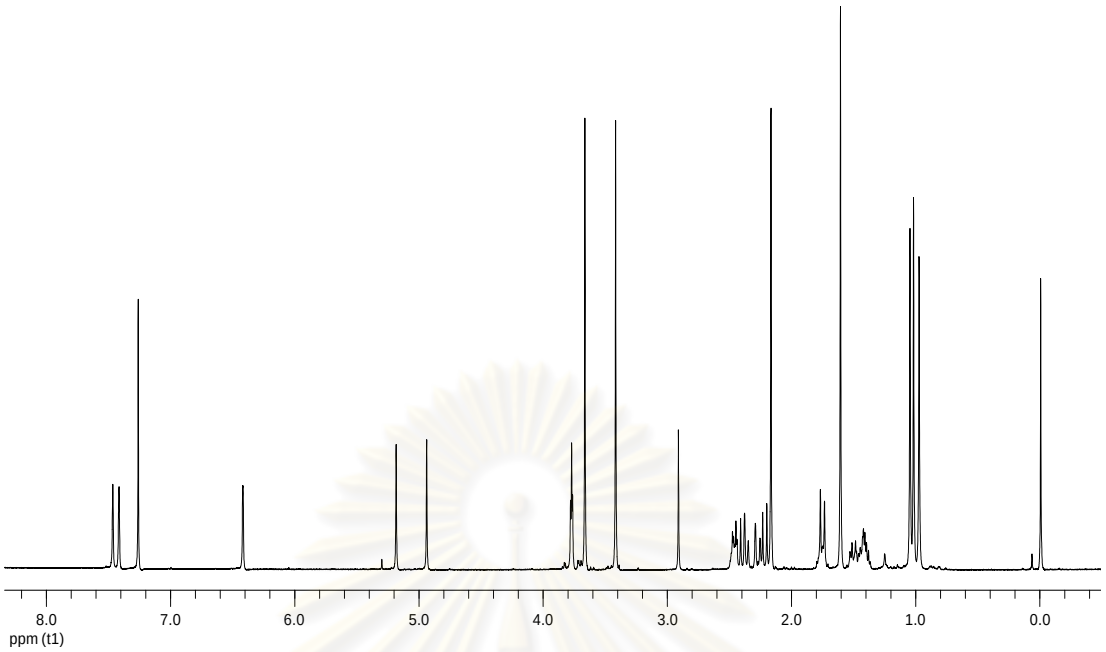

Figure S-37 ^{1}H NMR (400 MHz) spectrum of compound **7** ($CDCl_3$)

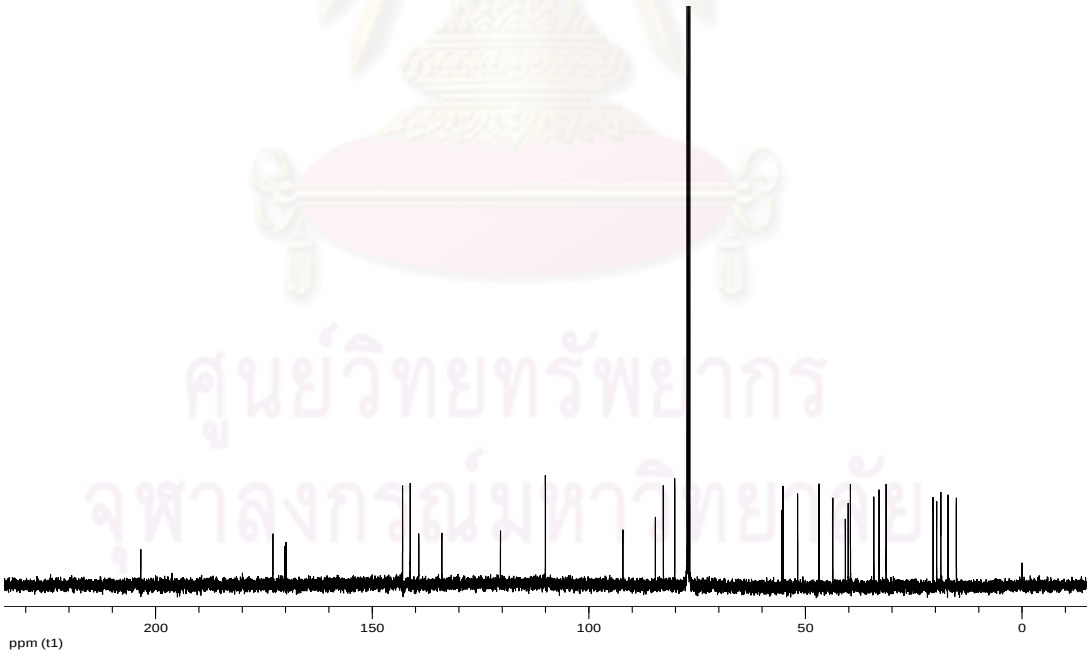

Figure S-38 ^{13}C NMR (100 MHz) spectrum of compound **7** ($CDCl_3$)

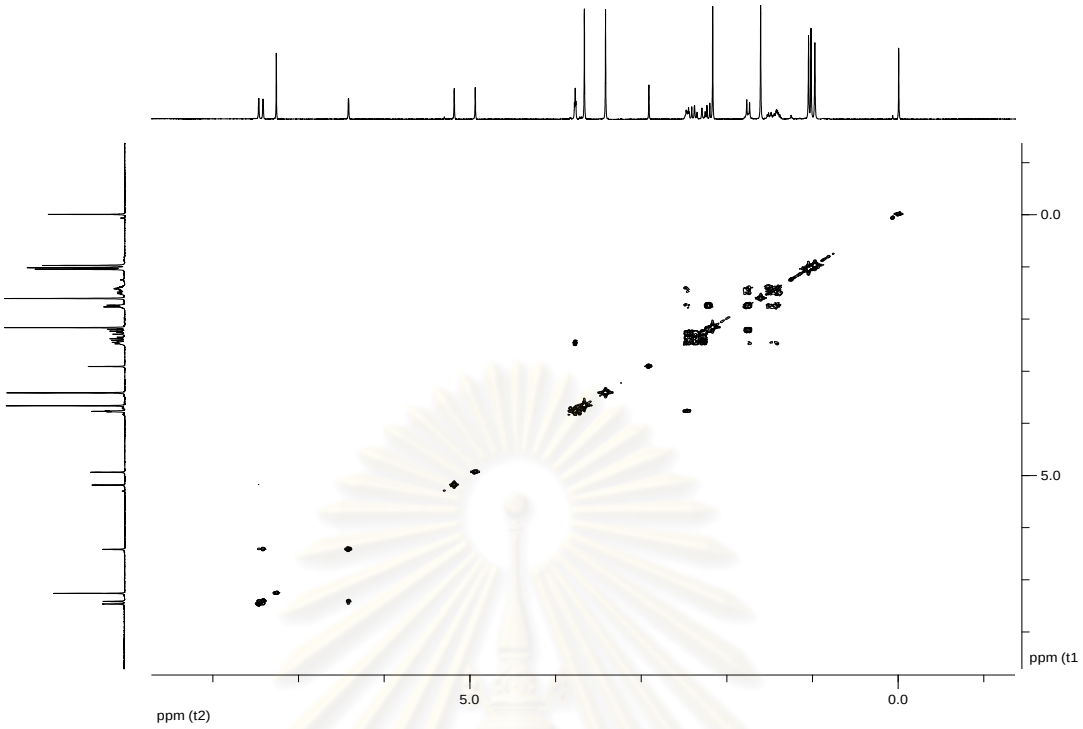

Figure S-39 ^{1}H-^{1}H COSY spectrum of compound **7** ($CDCl_3$)

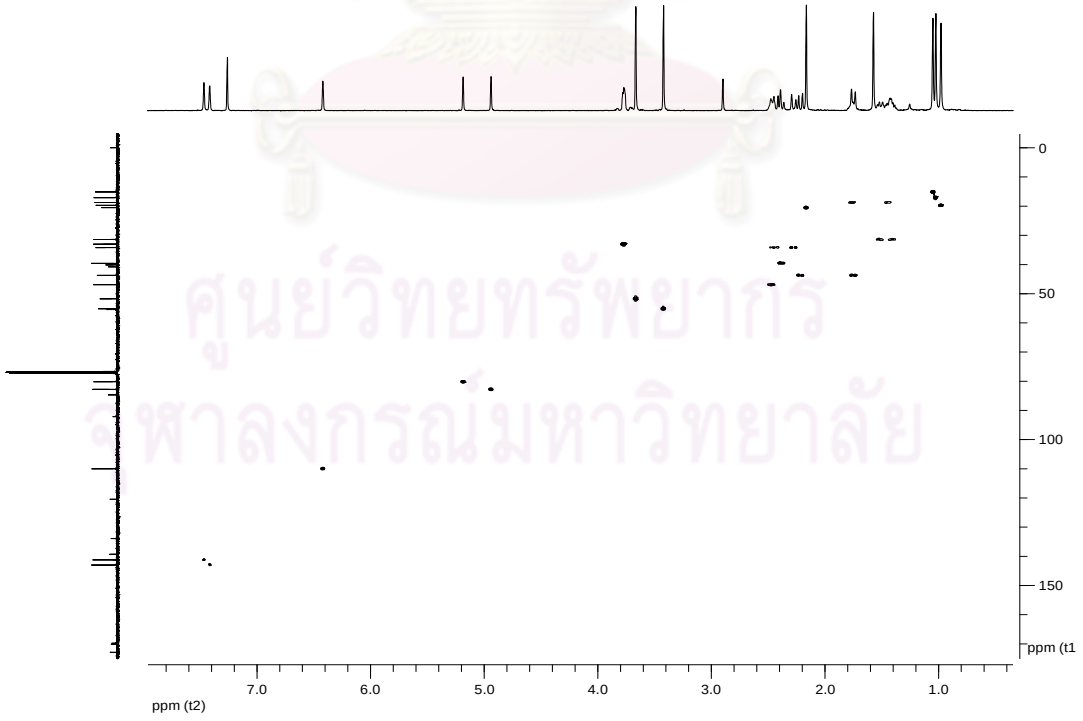

Figure S-40 HSQC spectrum of compound **7** ($CDCl_3$)

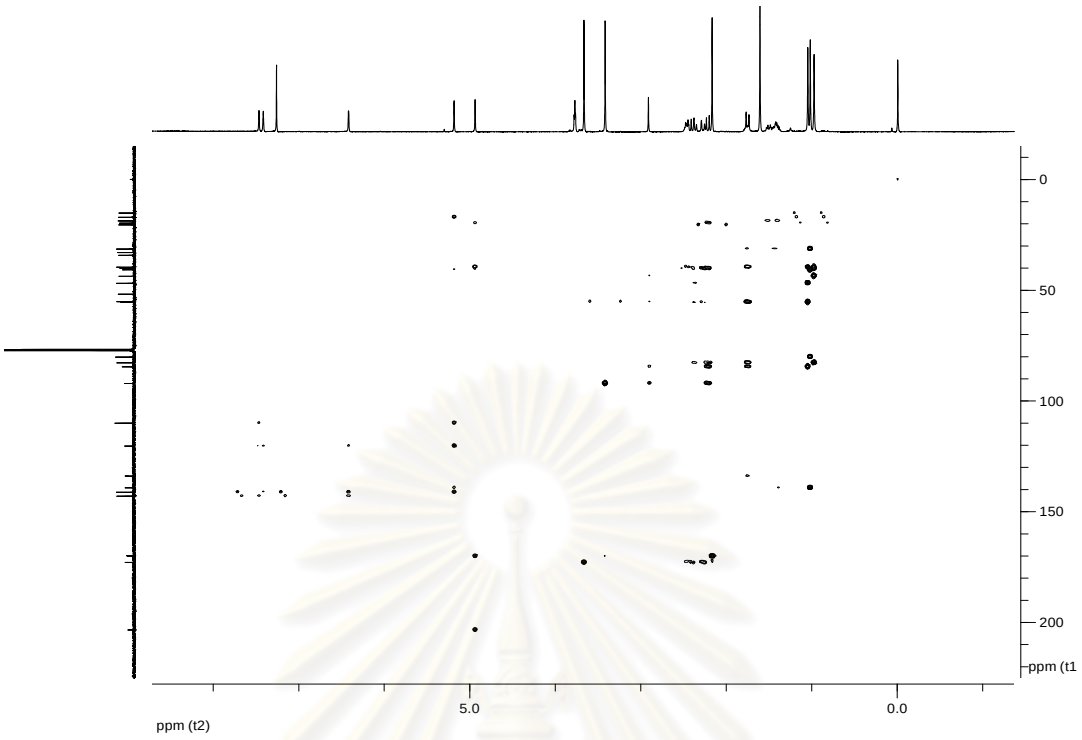

Figure S-41 HMBC spectrum of compound **7** ($CDCl_3$)

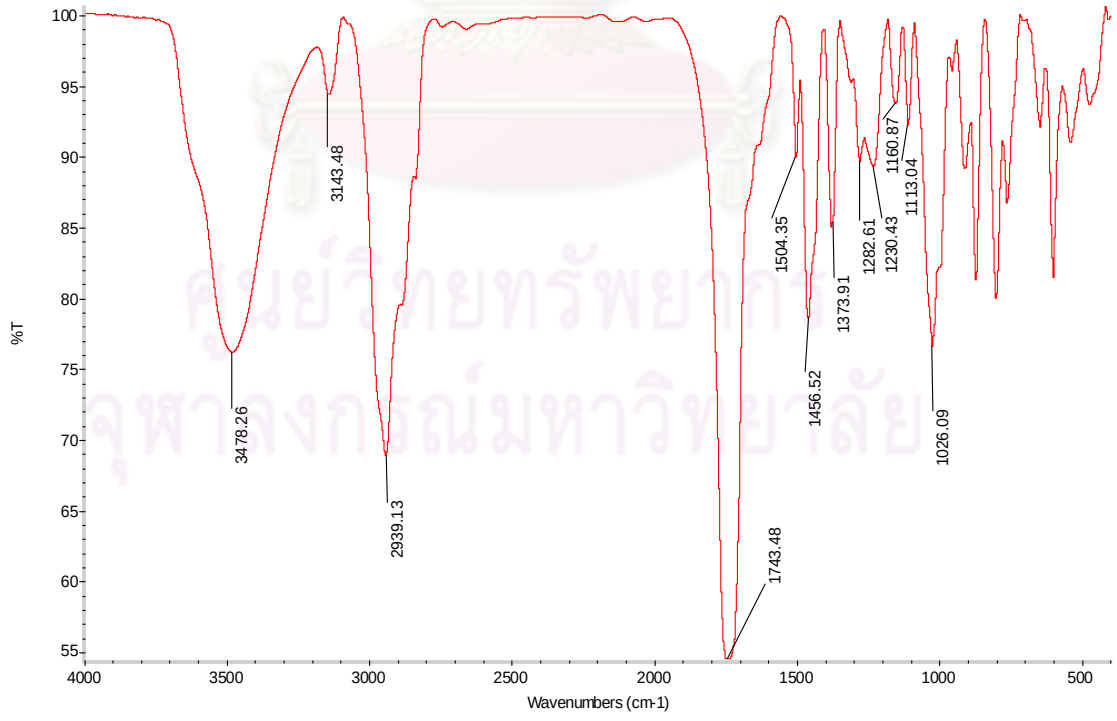

Figure S-42 IR spectrum of compound **7** (KBr)

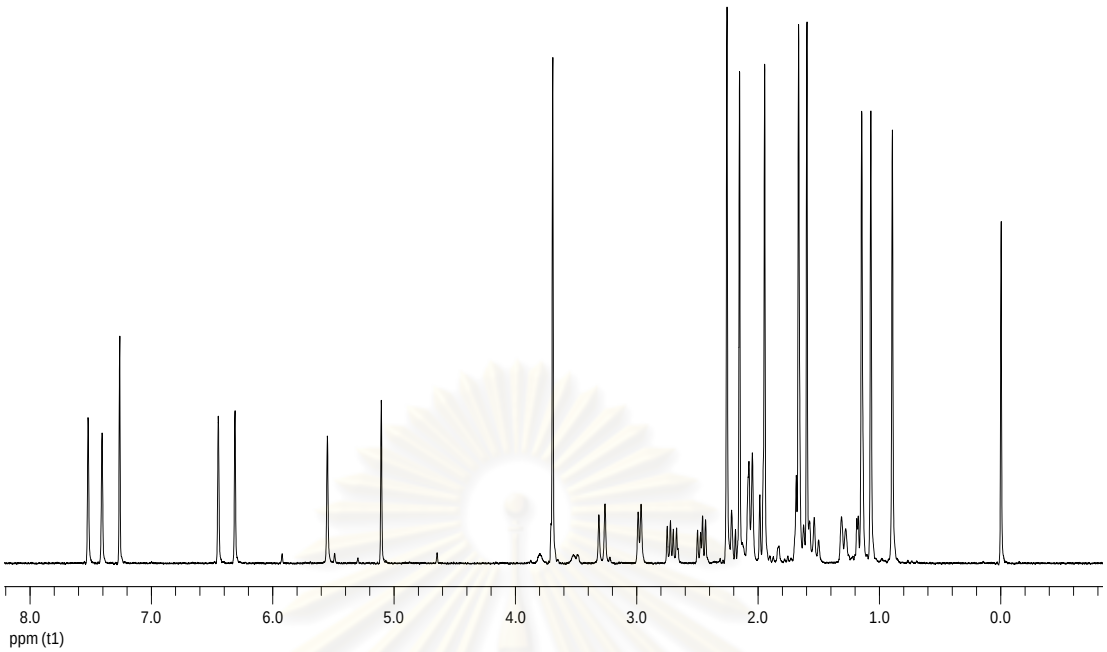

Figure S-43 ^{1}H NMR (400 MHz) spectrum of compound **8** ($CDCl_3$)

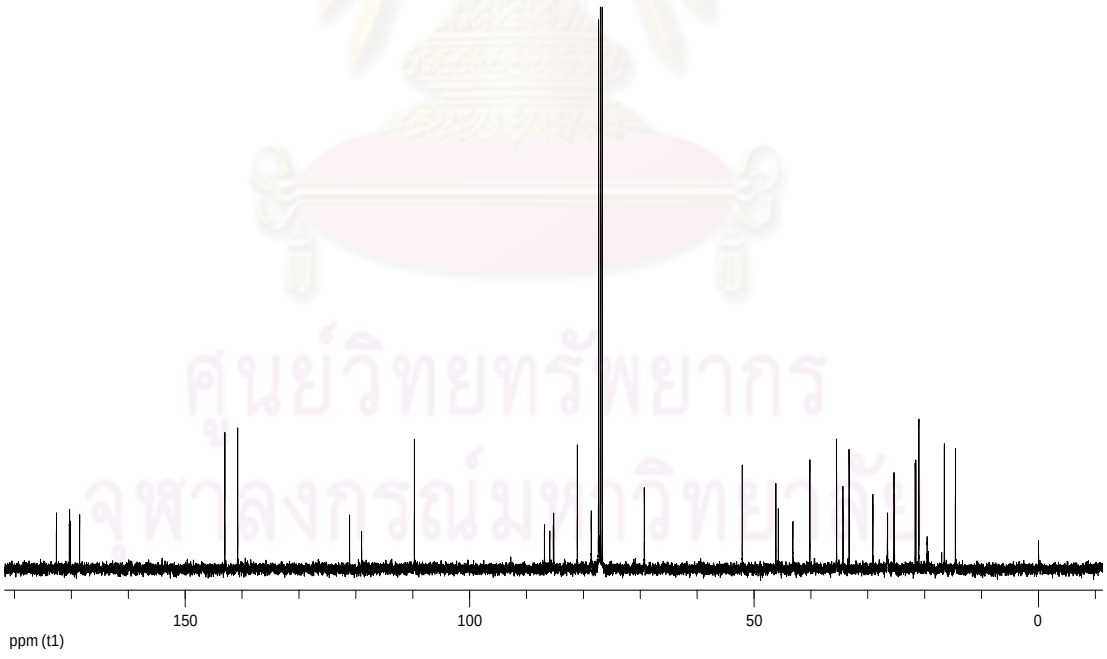

Figure S-44 ^{13}C NMR (100 MHz) spectrum of compound **8** ($CDCl_3$)

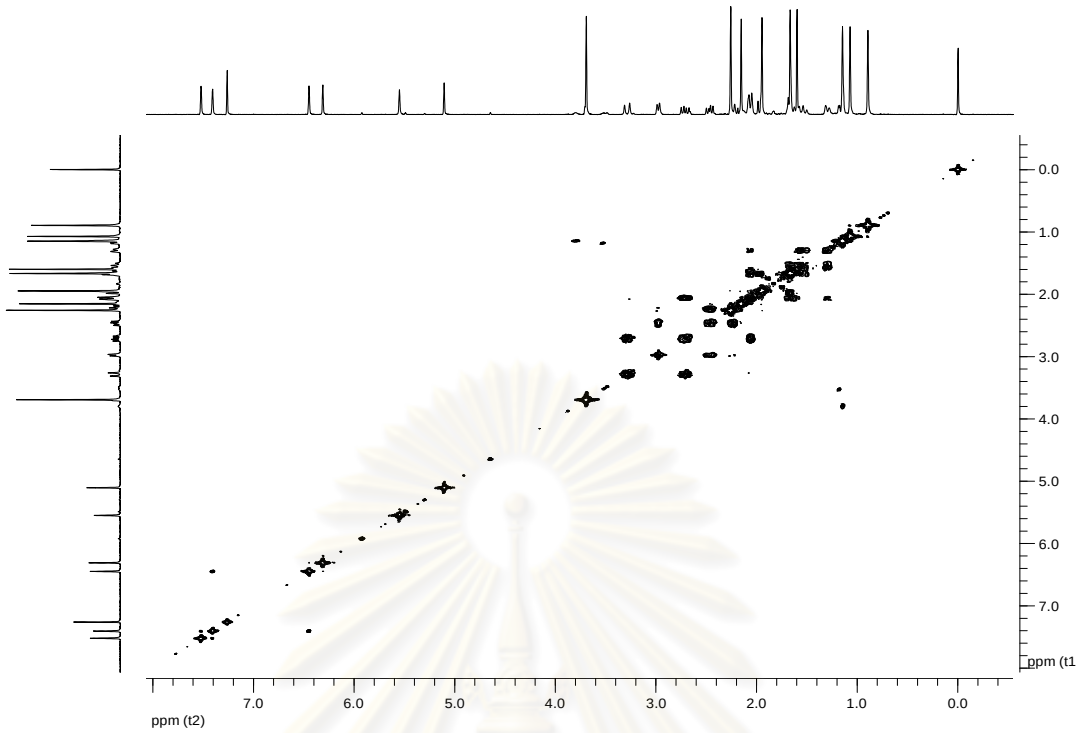

Figure S-45 ^{1}H-^{1}H COSY spectrum of compound **8** ($CDCl_3$)

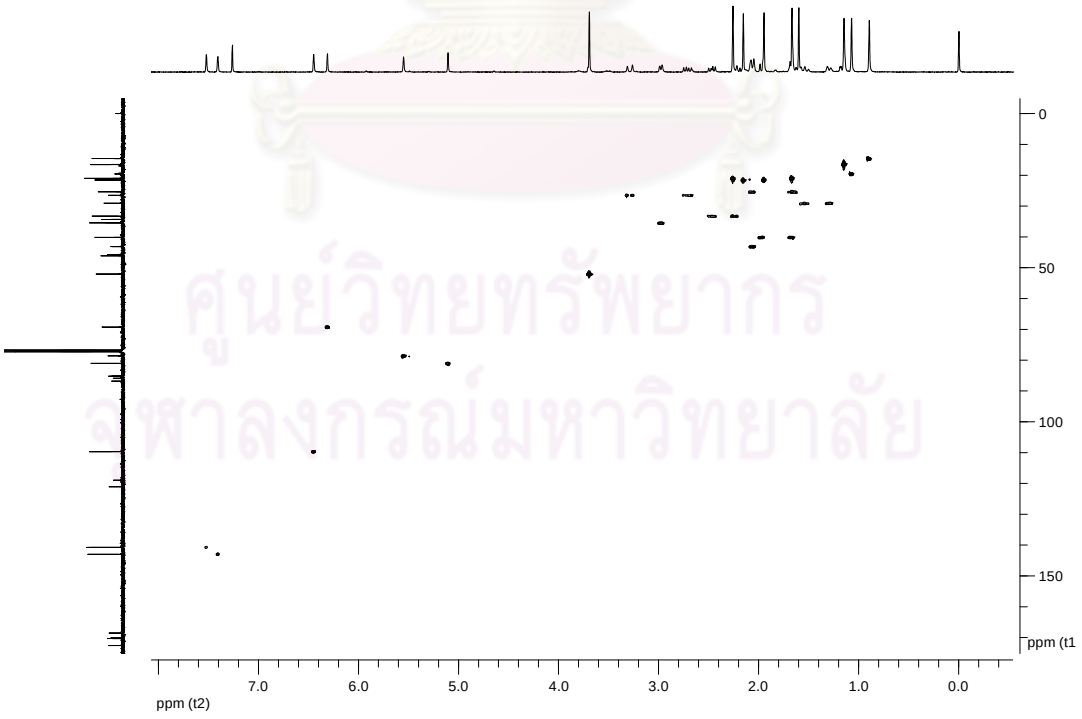

Figure S-46 HSQC spectrum of compound **8** ($CDCl_3$)

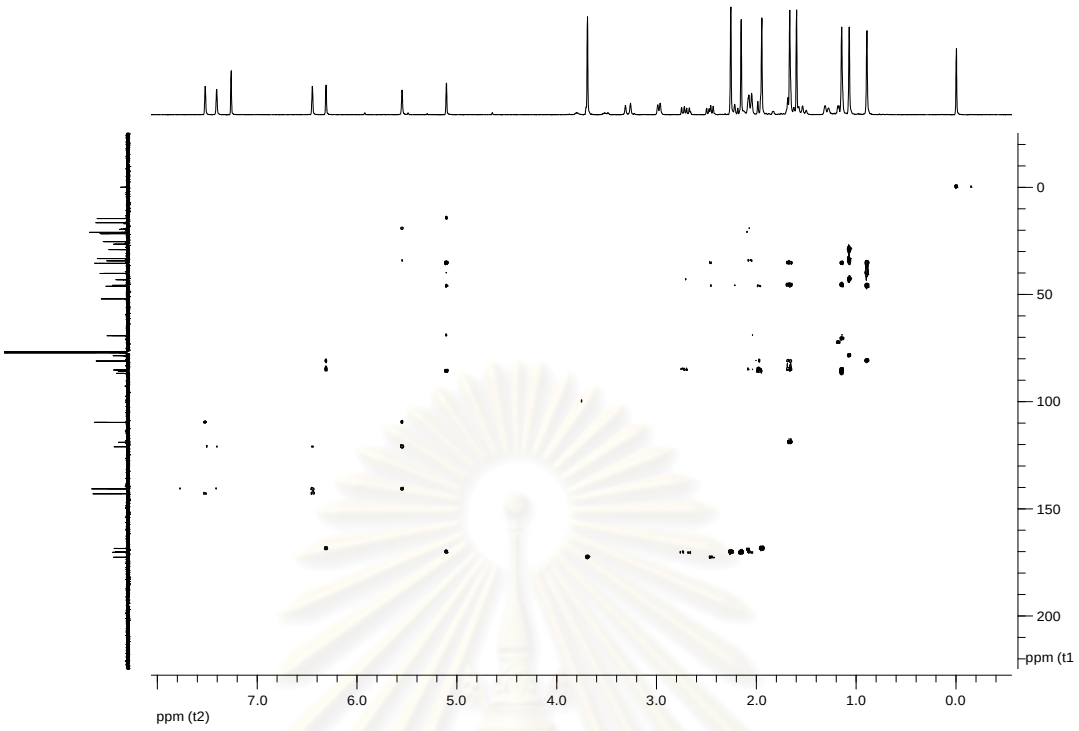

Figure S-47 HMBC spectrum of compound **8** ($CDCl_3$)

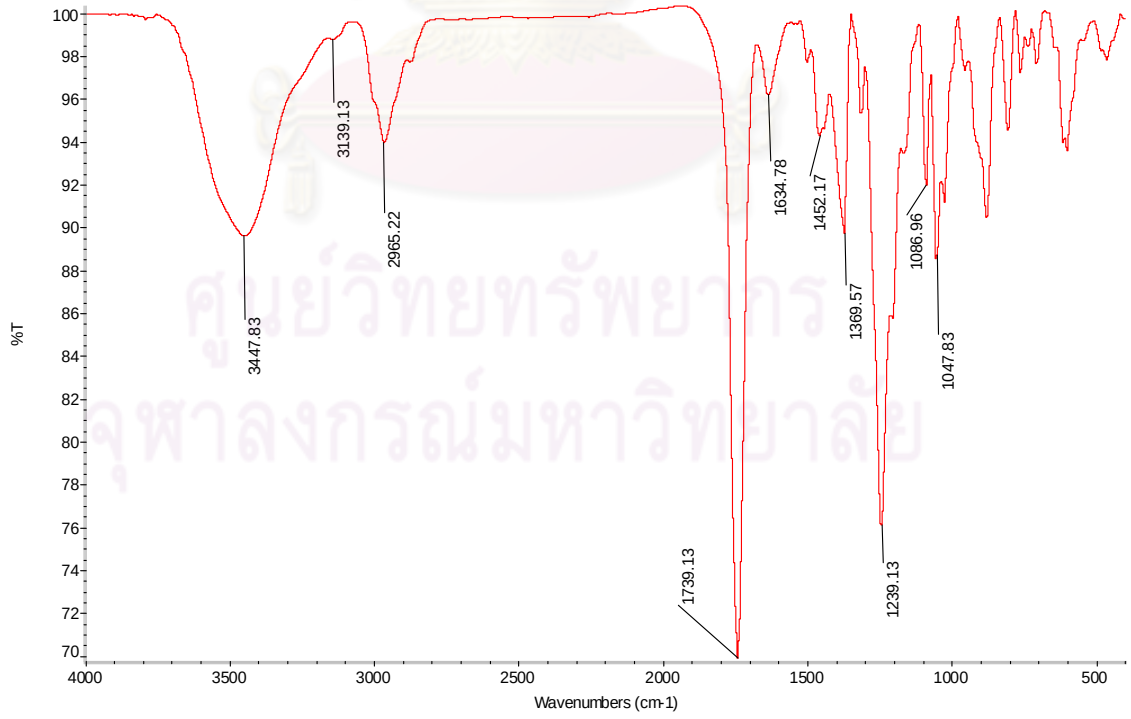

Figure S-48 IR spectrum of compound **8** (KBr)

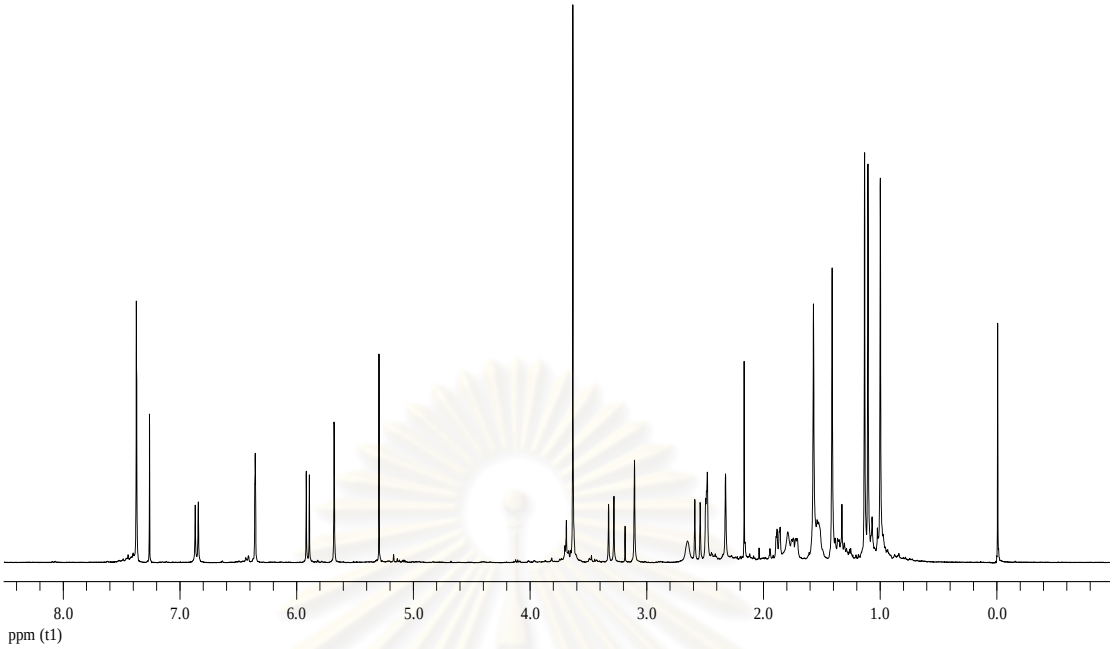

Figure S-49 ^{1}H NMR (400 MHz) spectrum of compound **9** ($CDCl_3$)

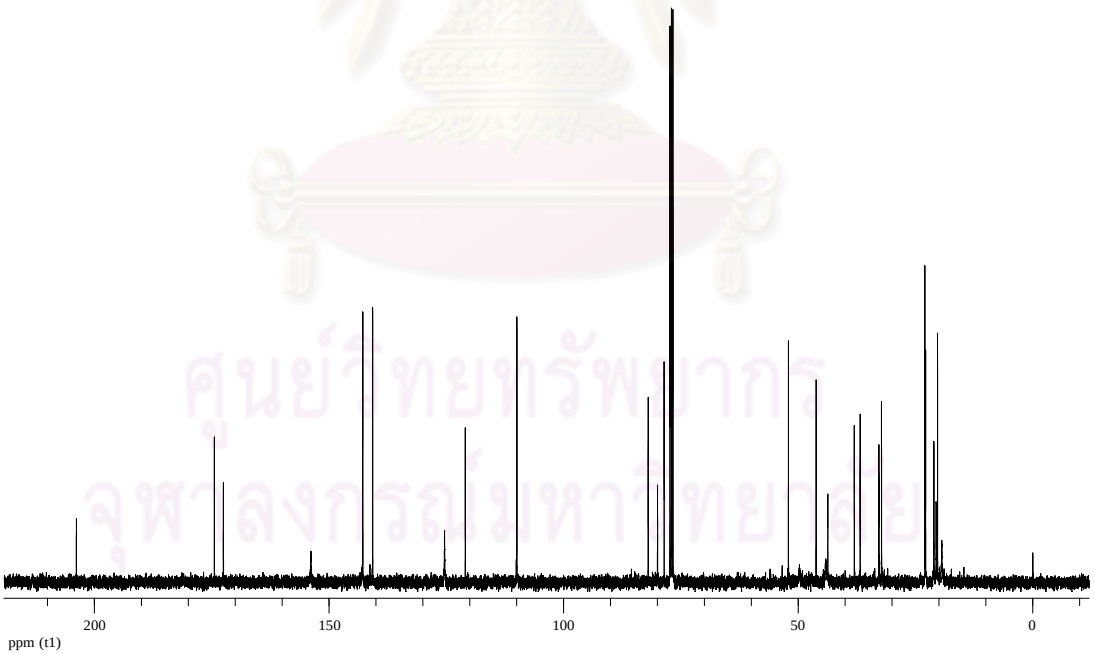

Figure S-50 ^{13}C NMR (100 MHz) spectrum of compound **9** ($CDCl_3$)

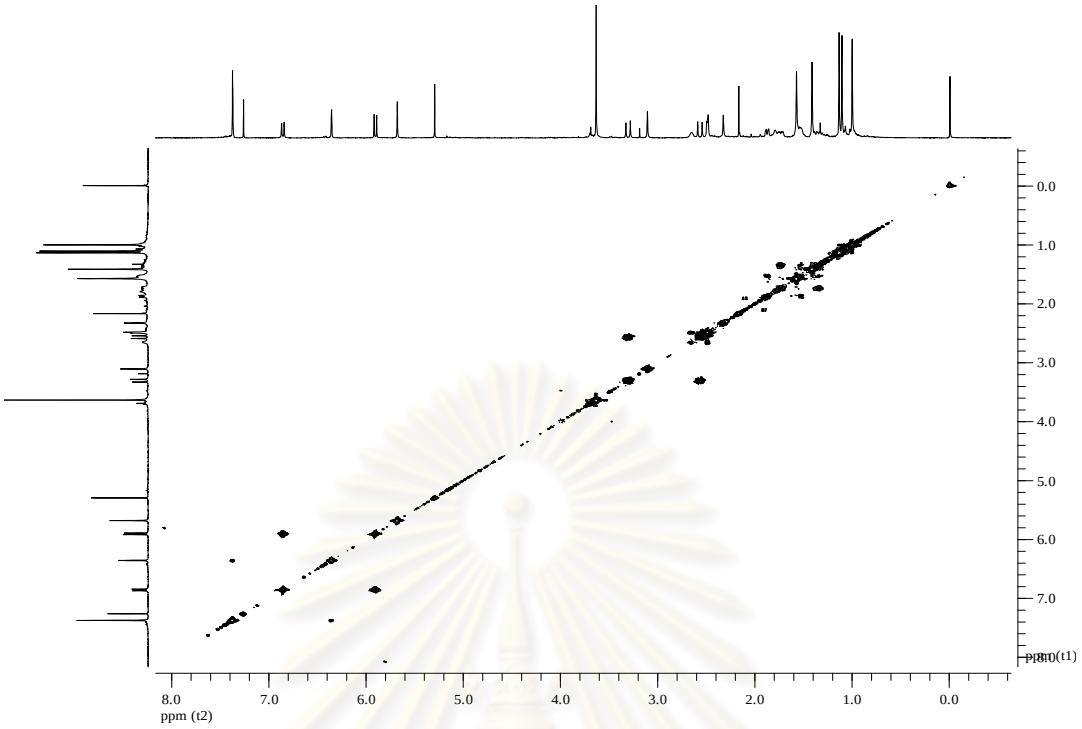

Figure S-51 ^{1}H-^{1}H COSY spectrum of compound **9** ($CDCl_3$)

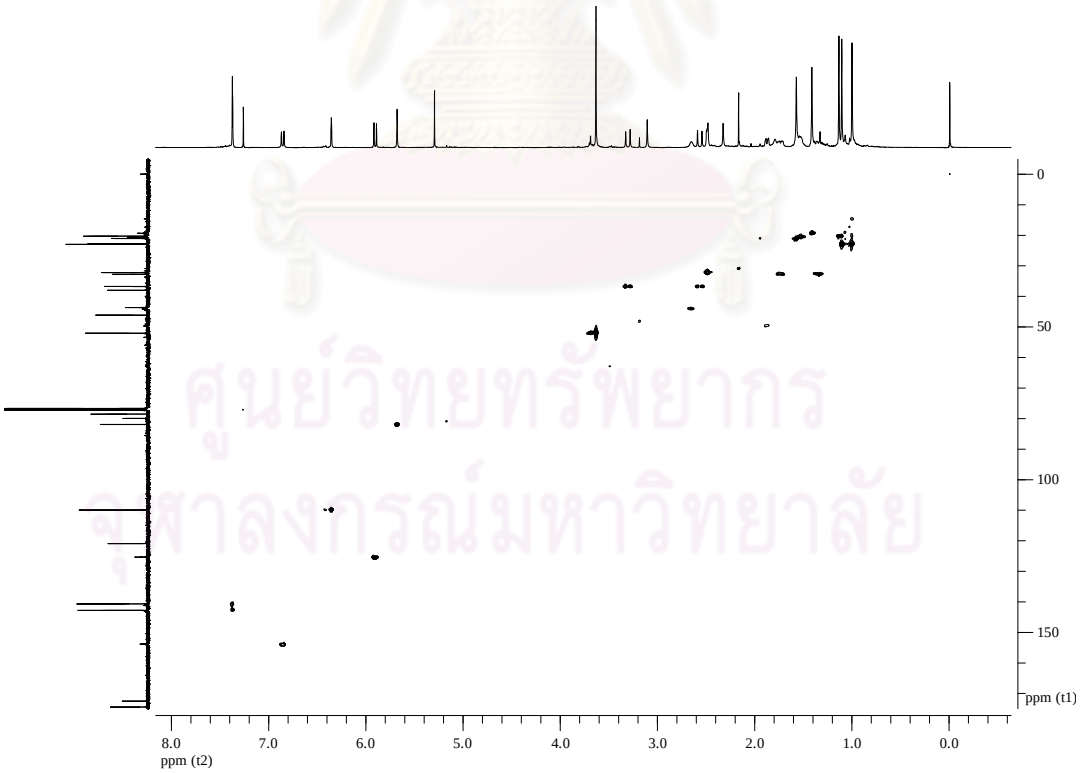

Figure S-52 HSQC spectrum of compound **9** ($CDCl_3$)

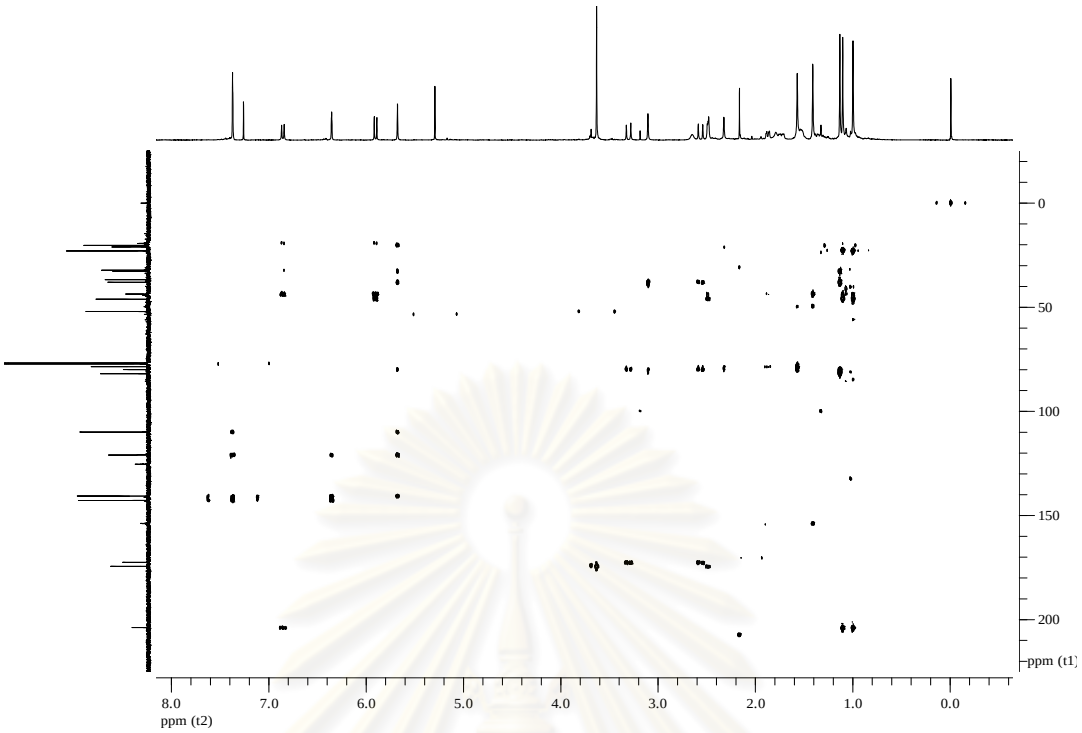

Figure S-53 HMBC spectrum of compound **9** ($CDCl_3$)

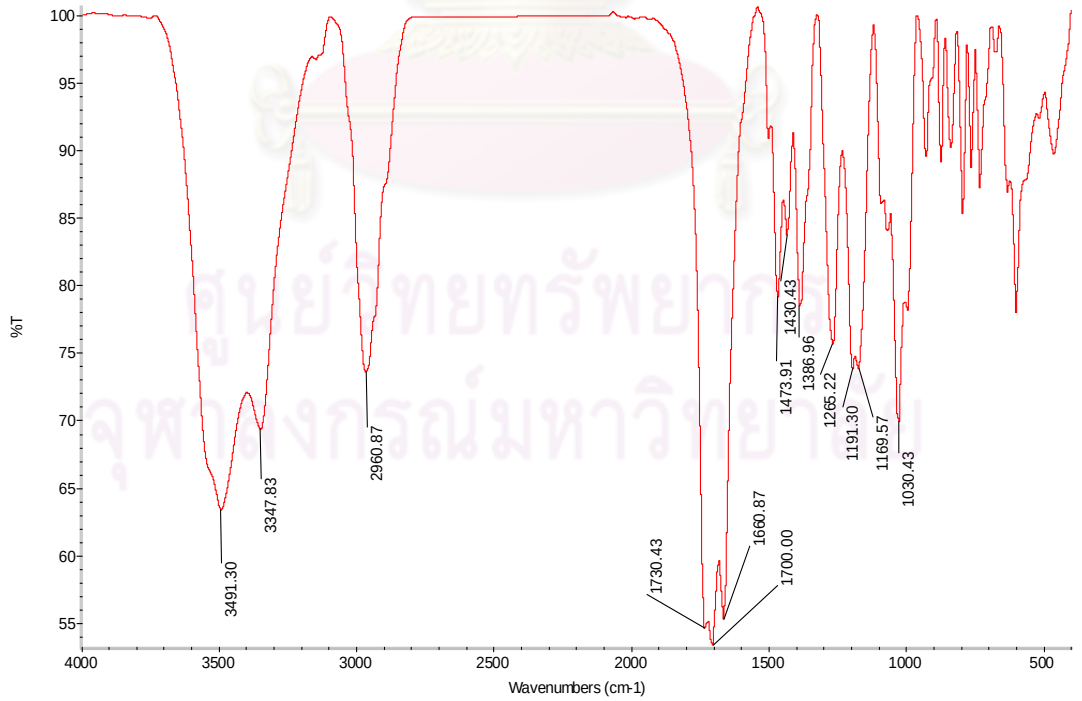

Figure S-54 IR spectrum of compound **9** (KBr)

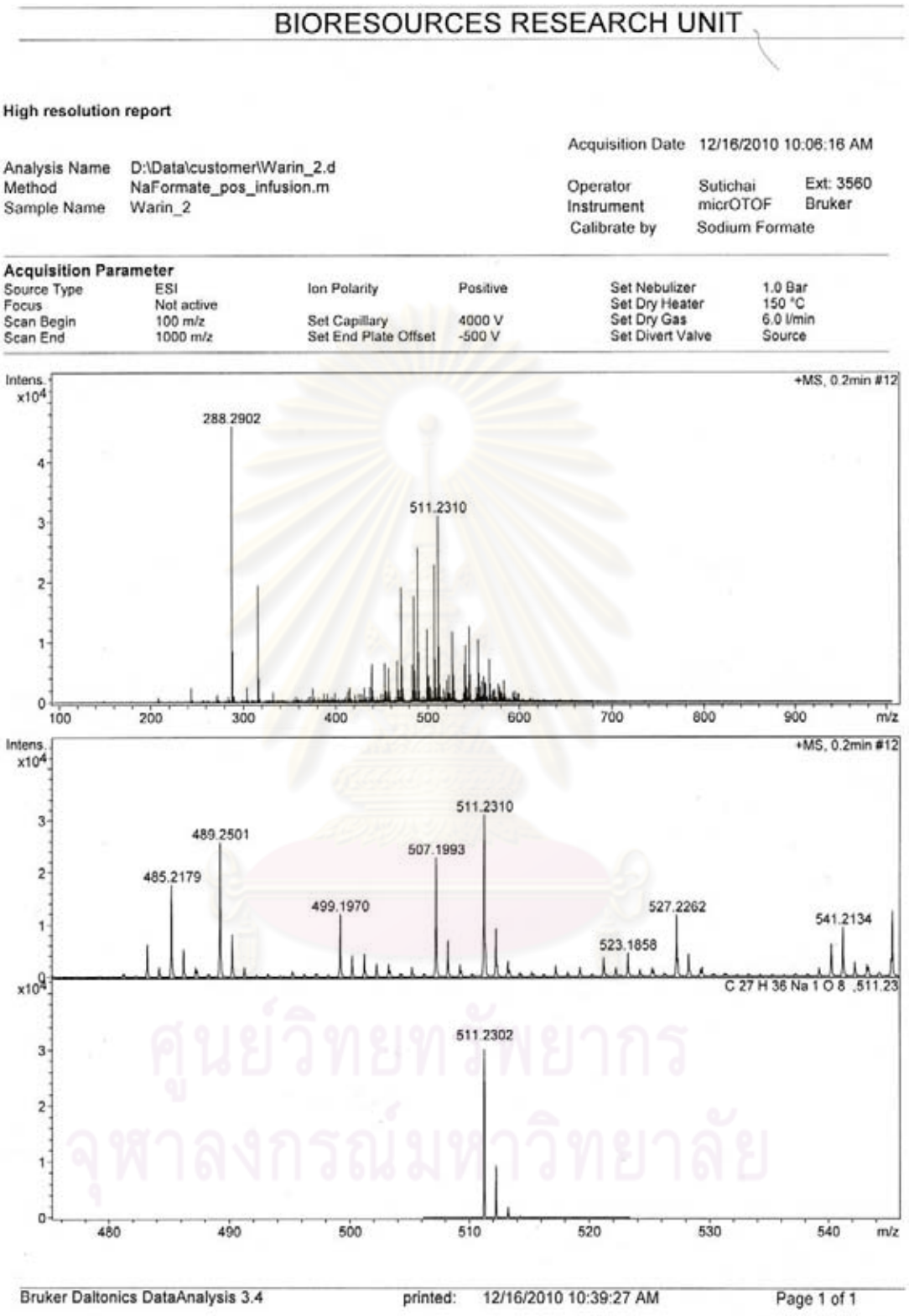

Figure S-55 HRESIMS Mass spectrum of compound **9**

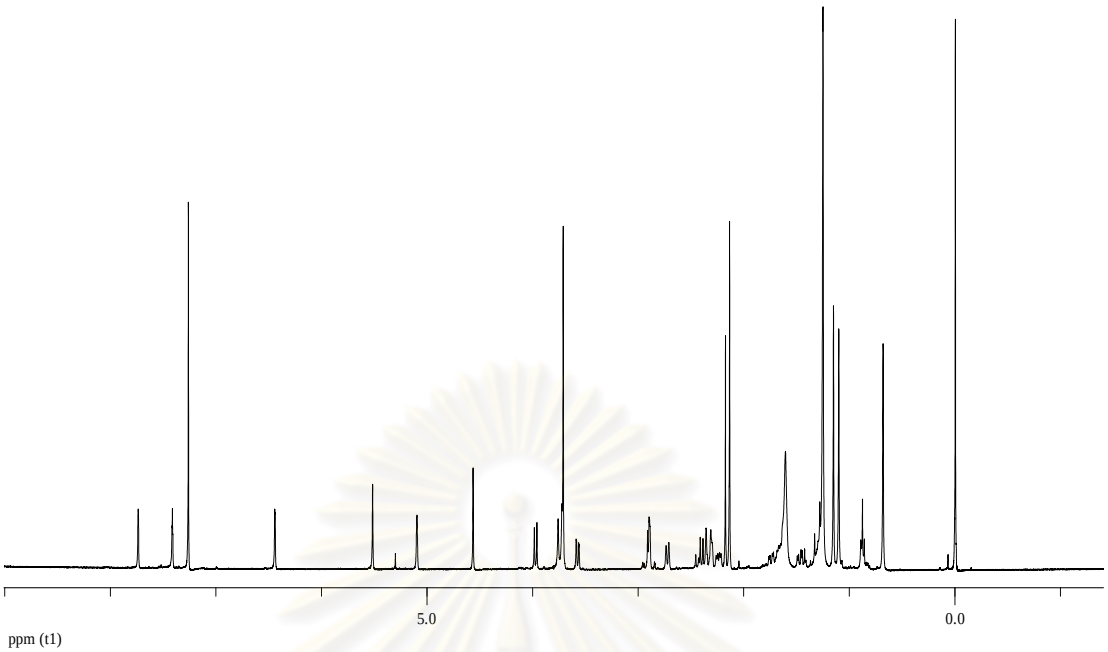

Figure S-56 ^{1}H NMR (400 MHz) spectrum of compound **10** ($CDCl_3$)

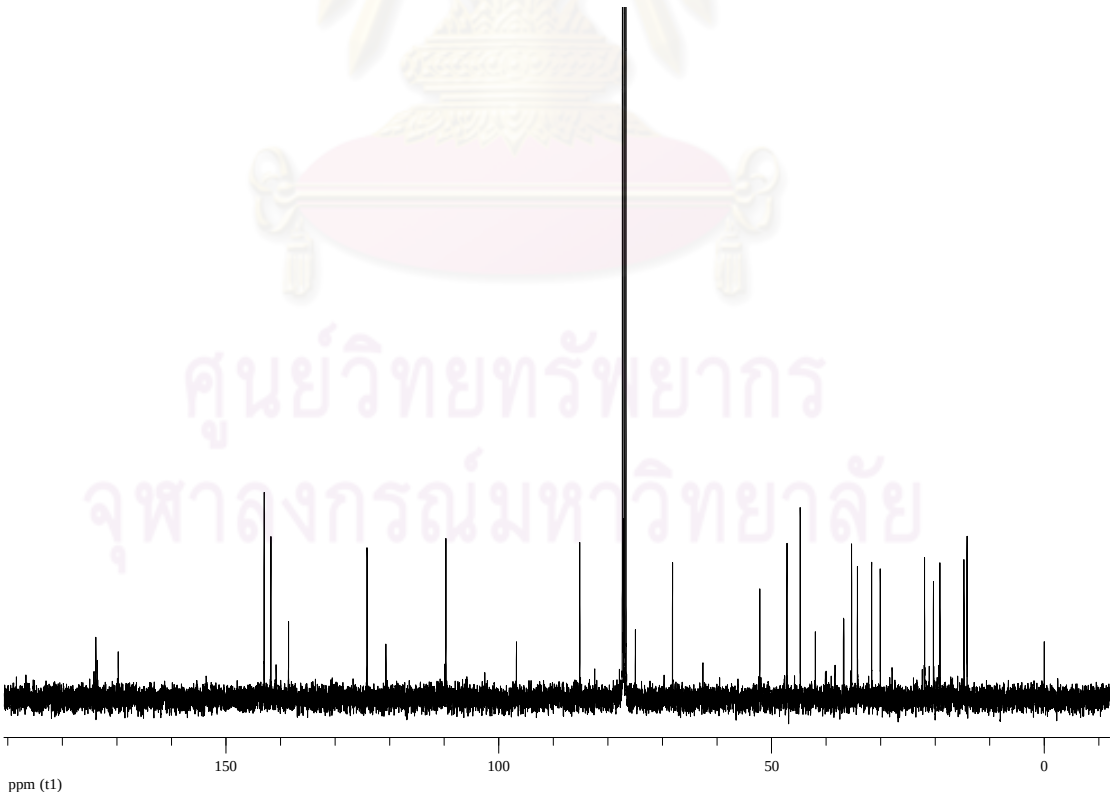

Figure S-57 ^{13}C NMR (100 MHz) spectrum of compound **10** ($CDCl_3$)

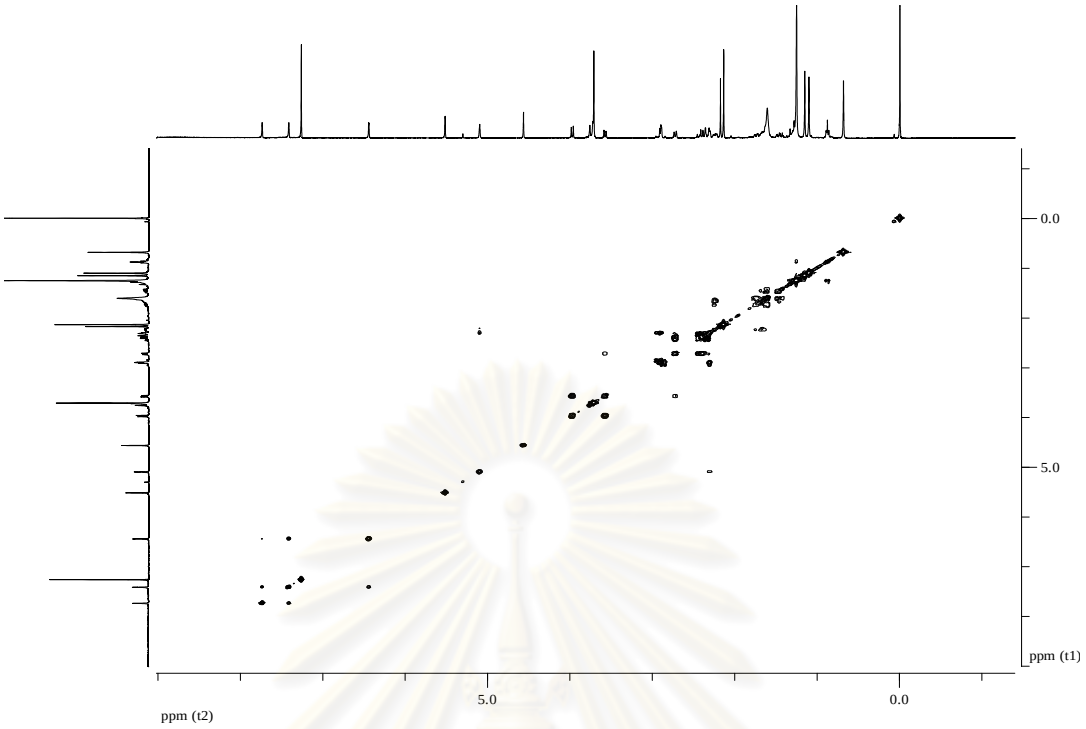

Figure S-58 ^{1}H-^{1}H COSY spectrum of compound **10** ($CDCl_3$)

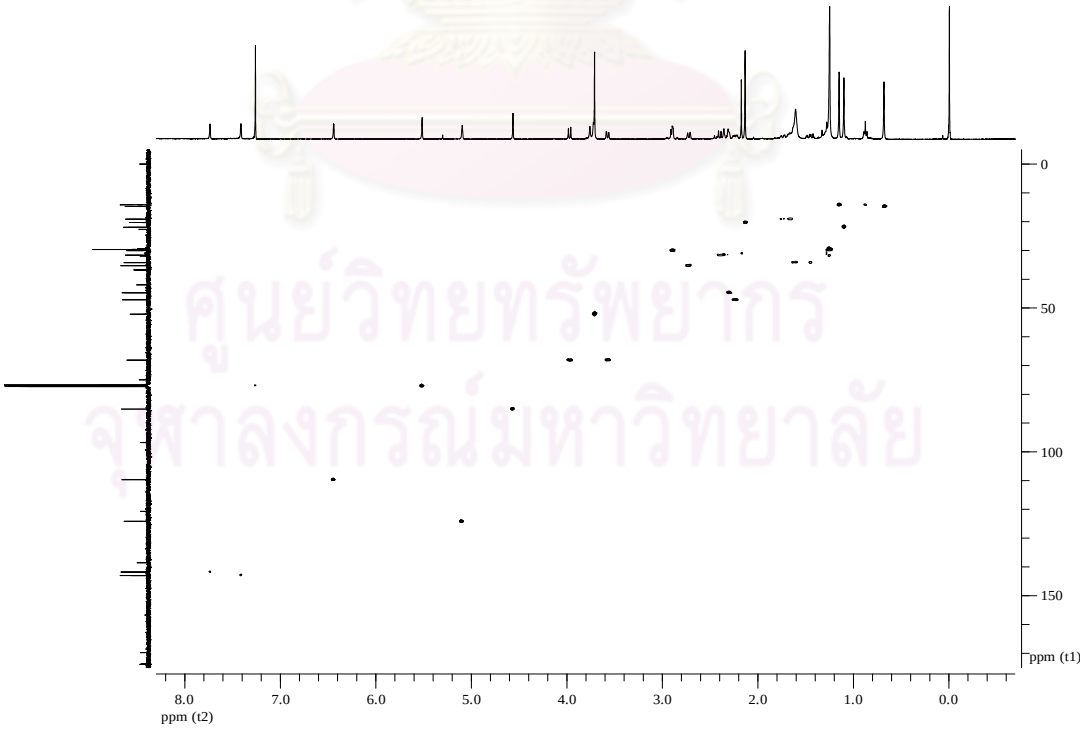

Figure S-59 HSQC spectrum of compound **10** ($CDCl_3$)

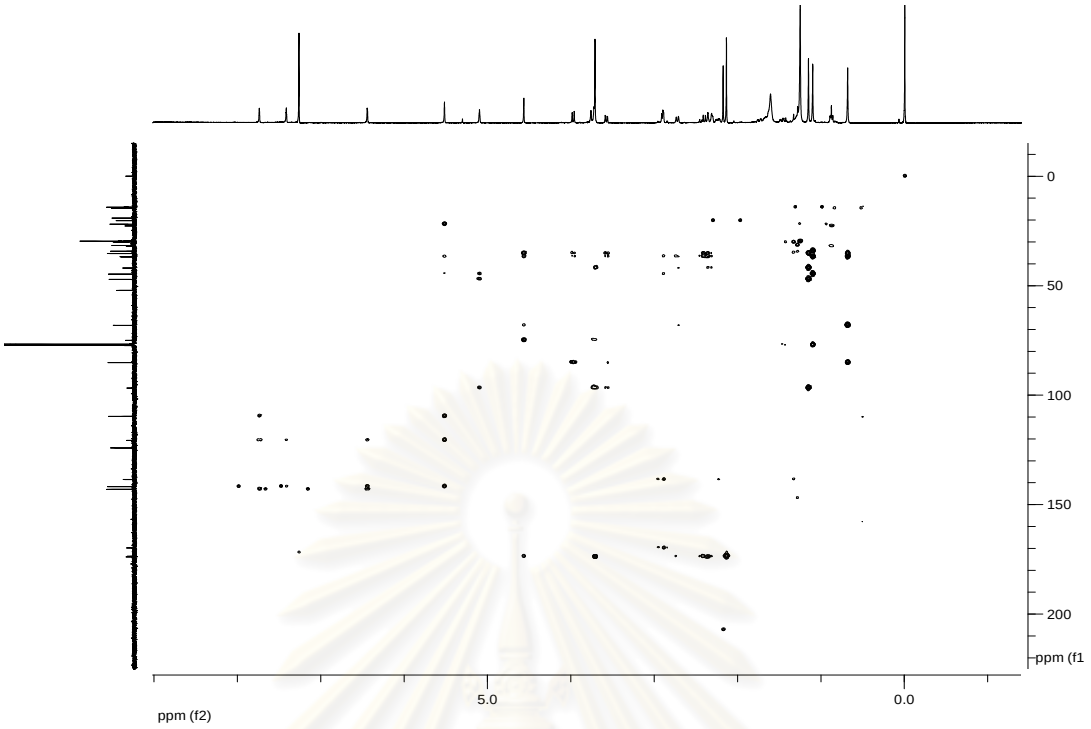

Figure S-60 HMBC spectrum of compound **10** ($CDCl_3$)

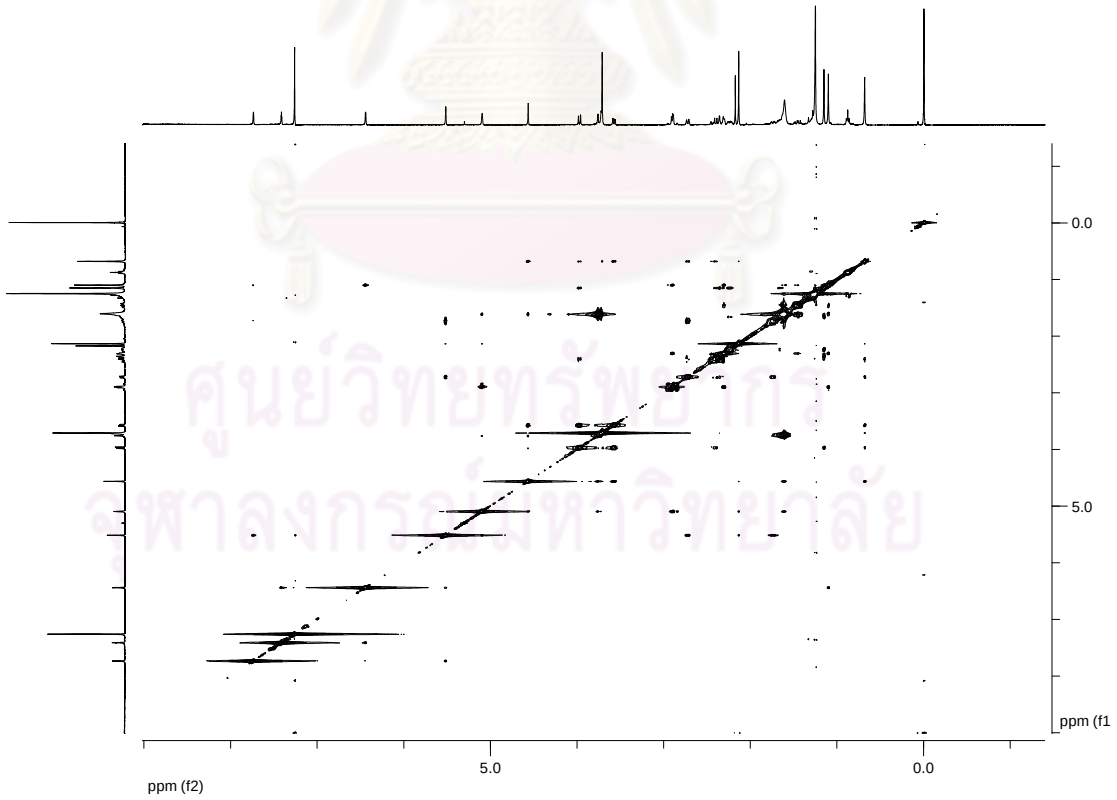

Figure S-61 NOESY spectrum of compound **10** ($CDCl_3$)

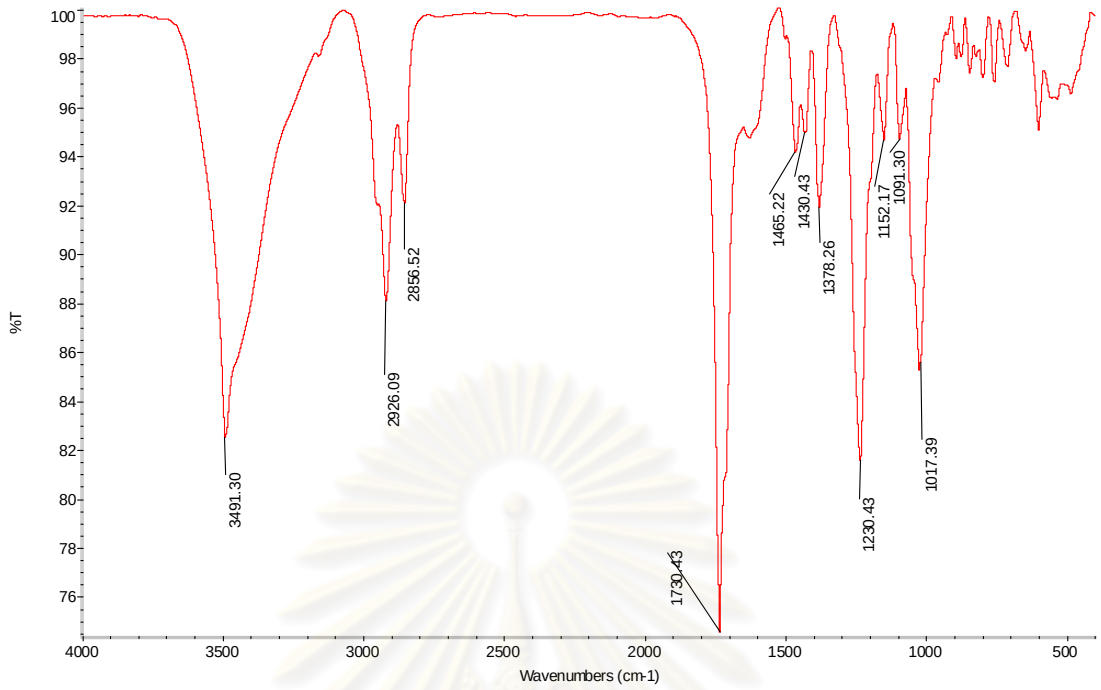

Figure S-62 IR spectrum of compound **10** (KBr)

BIORESOURCES RESEARCH UNIT

High resolution report

		Acquisition Date	12/16/2010 10:04:13 AM
Analysis Name	D:\Data\customer\Warin_1.d		
Method	NaFormate_pos_infusion.m	Operator	Sutichai Ext: 3560
Sample Name	Warin_1	Instrument	micrOTOF Bruker
		Calibrate by	Sodium Formate

Acquisition Parameter

Source Type	ESI	Ion Polarity	Positive	Set Nebulizer	1.0 Bar
Focus	Not active			Set Dry Heater	150 °C
Scan Begin	100 m/z	Set Capillary	4000 V	Set Dry Gas	6.0 l/min
Scan End	1000 m/z	Set End Plate Offset	-500 V	Set Divert Valve	Source

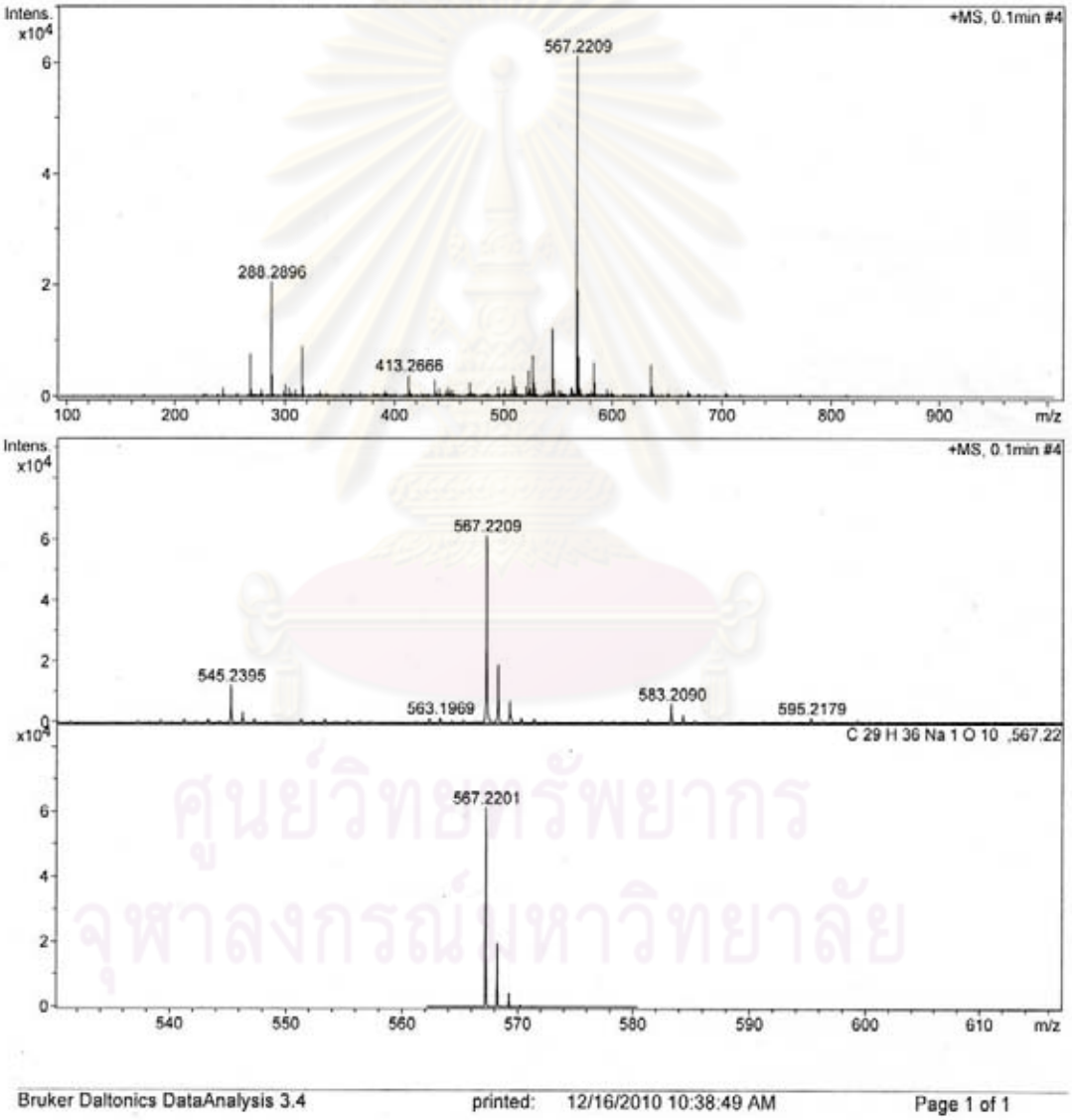

Bruker Daltonics DataAnalysis 3.4 printed: 12/16/2010 10:38:49 AM Page 1 of 1

Figure S-63 HRESIMS Mass spectrum of compound **10**

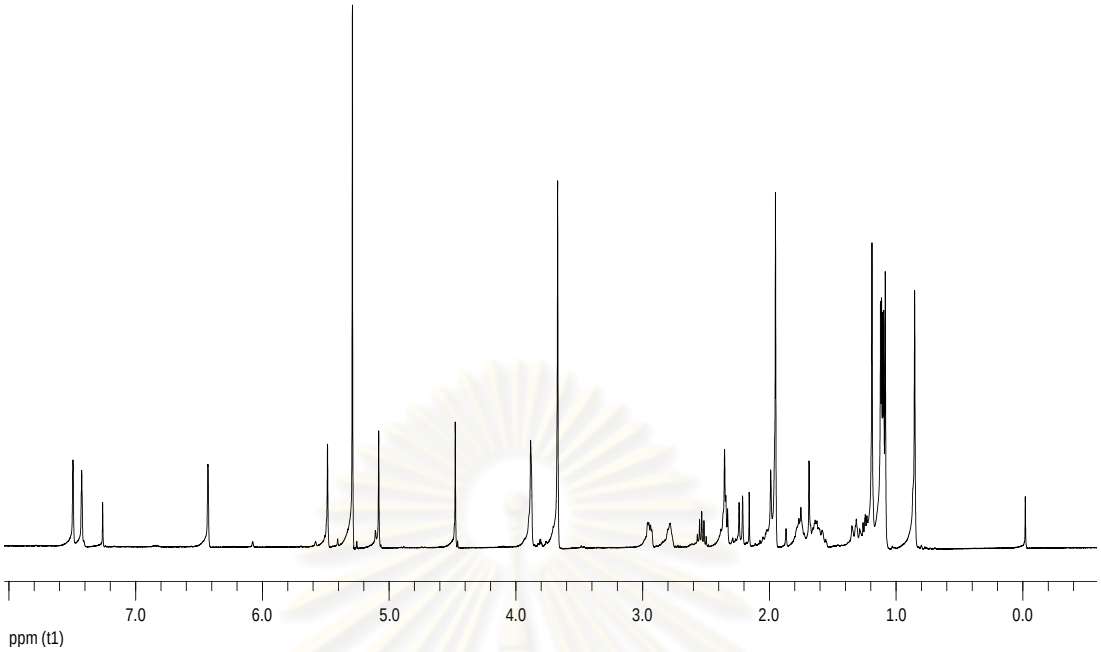

Figure S-64 ^{1}H NMR (400 MHz) spectrum of compound **11** ($CDCl_3$)

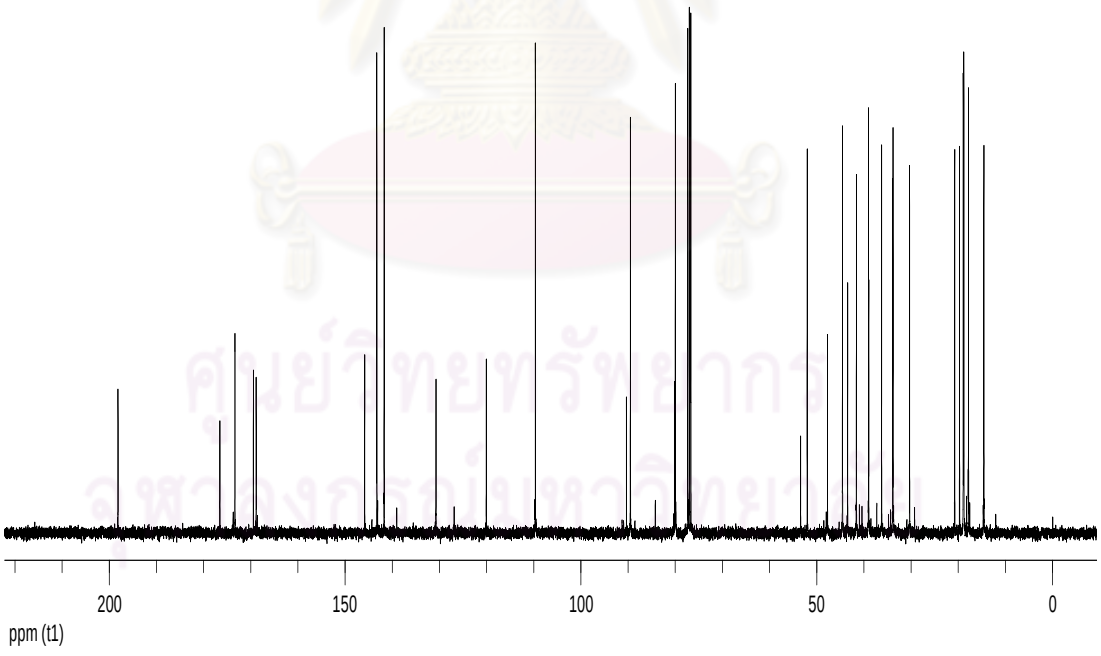

Figure S-65 ^{13}C NMR (100 MHz) spectrum of compound **11** ($CDCl_3$)

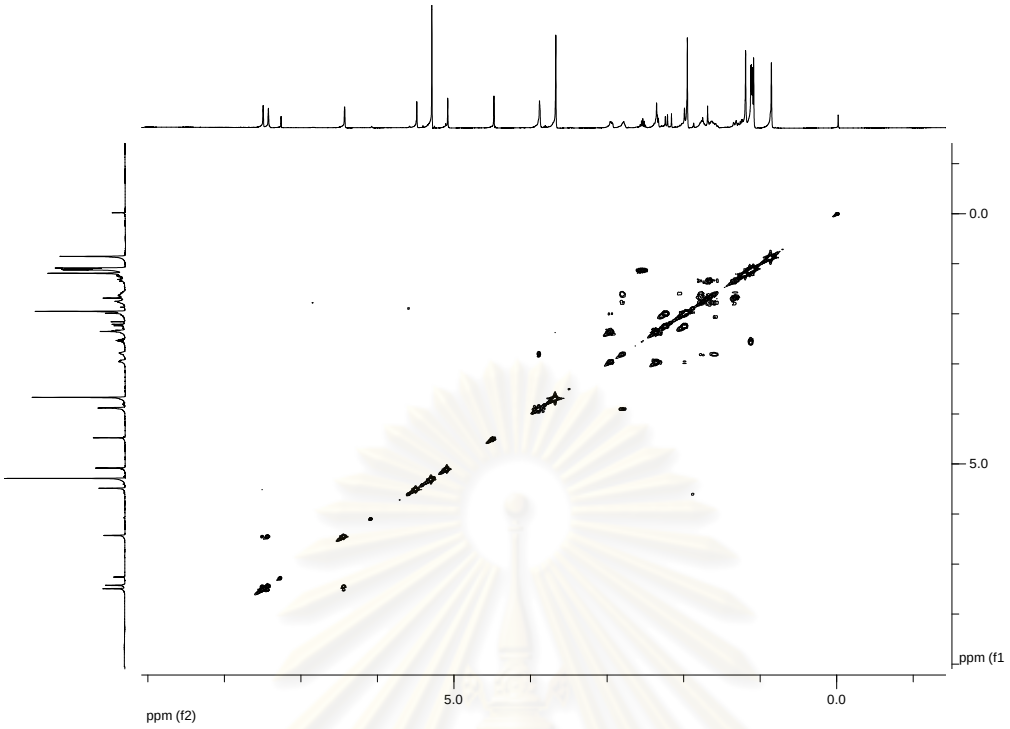

Figure S-66 ^{1}H-^{1}H COSY spectrum of compound **11** ($CDCl_3$)

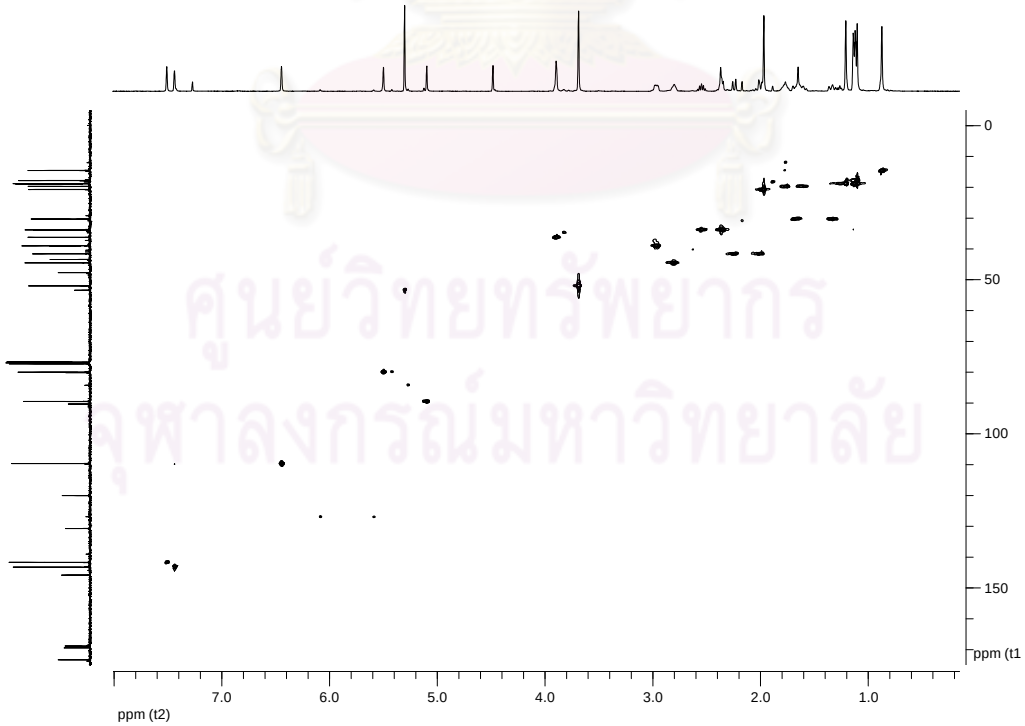

Figure S-67 HSQC spectrum of compound **11** ($CDCl_3$)

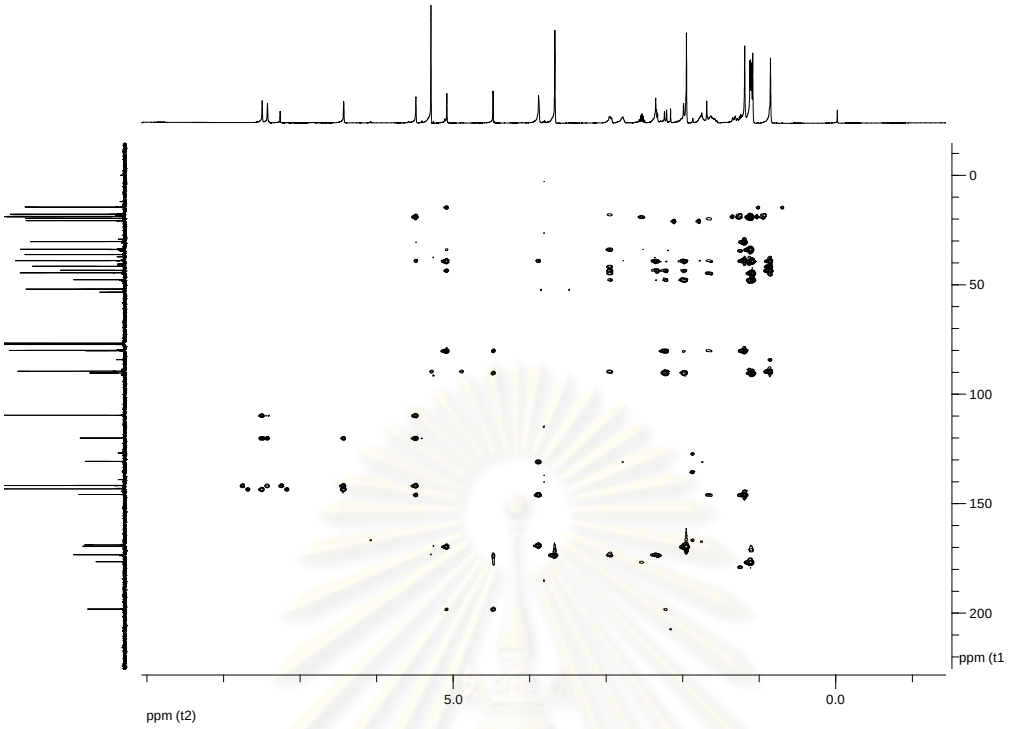

Figure S-68 HMBC spectrum of compound **11** ($CDCl_3$)

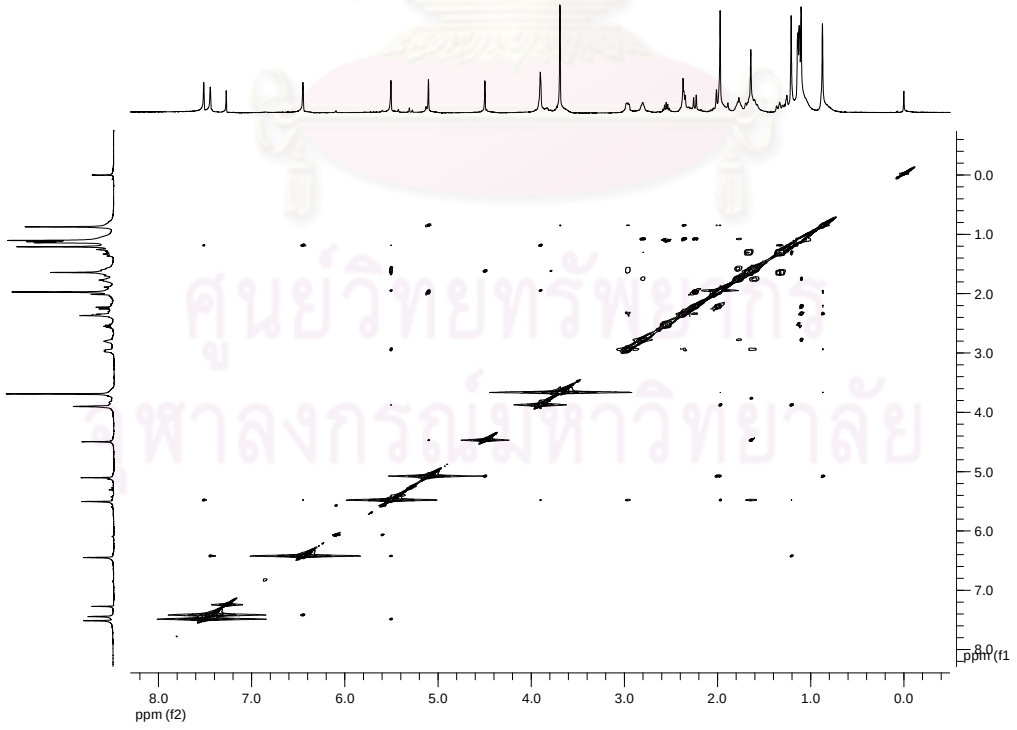

Figure S-69 NOESY spectrum of compound **11** ($CDCl_3$)

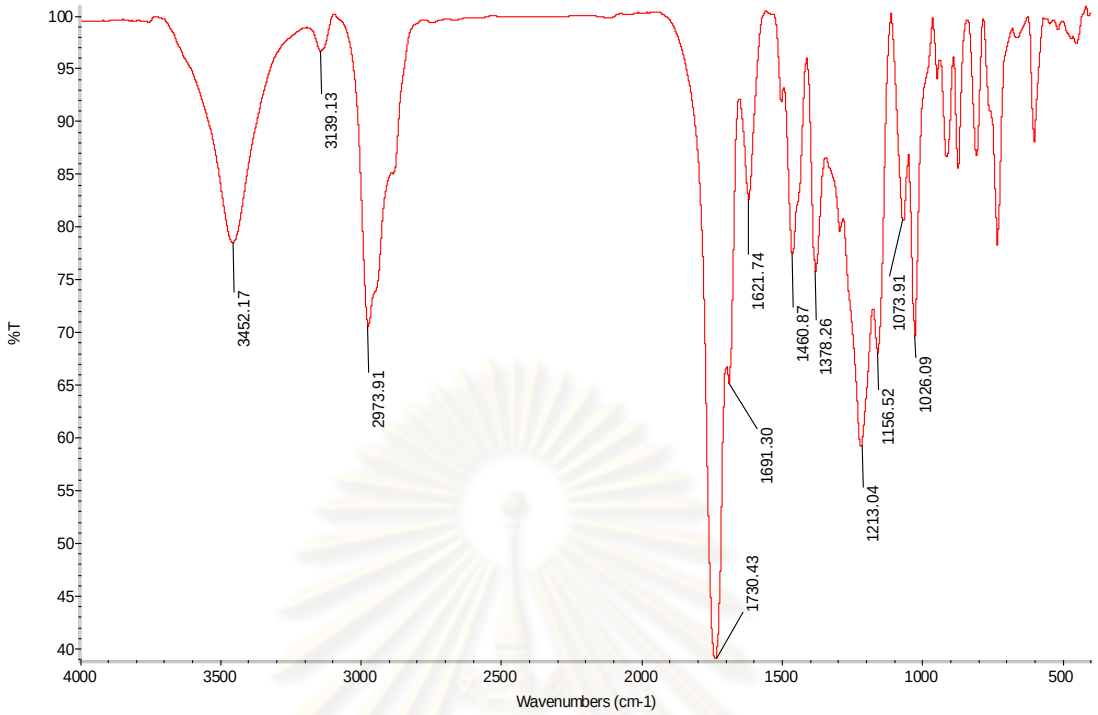

Figure S-70 IR spectrum of compound **11** (KBr)

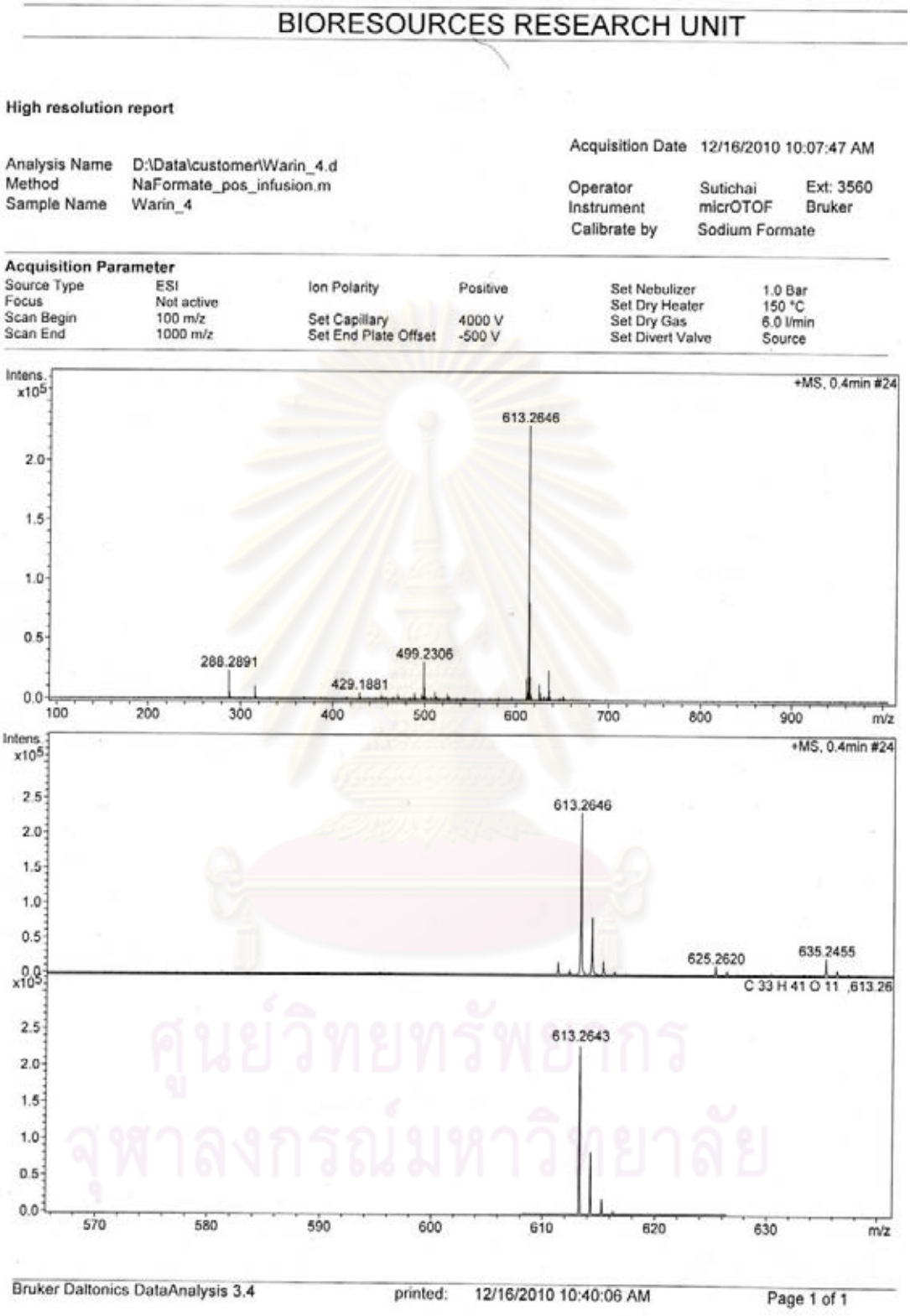

Figure S-71 HRESIMS Mass spectrum of compound **11**

VITAE

Miss Warin Ravangpai was born on October 20, 1986 in Sukhothai, Thailand. He graduated with Bachelor's Degree of science in Chemistry from Faculty of Science, Naresuan University, in 2009. During the time he was studying in the Master Degree in Chemistry program, Faculty of science, Chulalong University

Her present address is 127 Moo 1 Tamton Bantuk, Srichatchanalai Direct, Sukhothai 64130 Tel: 085-1591302